國　立　交　通　大　學

電子工程學系　　電子研究所碩士班

碩士論文

符合 IEEE802.16e 都會區域網路傳輸系統的框同步技術研究

Pilot-Assisted Frame Synchronization Technique for IEEE 802.16e Wireless Metropolitan Area Network

研 究 生：鍾國洋

指導教授：魏哲和　博士

杭學鳴　博士

中 華 民 國 九 十 五 年 六 月

符合 IEEE802.16e 都會區域網路傳輸系統的框同步技術研究

Pilot-Assisted Frame Synchronization Technique for IEEE 802.16e Wireless Metropolitan Area Network

研 究 生:鍾國洋　　Student: Gwo Yung Chung

指導教授:魏哲和 博士　　Advisor: Dr. Che-Ho Wei

杭學鳴 博士　　Dr. Hsueh-Ming Hang

國立交通大學

電子工程學系　電子研究所碩士班

碩士論文

A Thesis

Submitted to Department of Electronics Engineering & Institute of Electronics

College of Electrical and Computer Engineering

National Chiao Tung University

in partial Fulfillment of the Requirements

for the Degree of

Master

in

Computer and Information Science

June 2006

Hsinchu, Taiwan, Republic of China

中 華 民 國 九 十 五 年 六 月

符合 IEEE802.16e 都會區域網路傳輸系統的框同步技術研究

研究生:鍾國洋　　指導教授：魏哲和 博士

杭學鳴 博士

國立交通大學

電子工程學系　電子研究所

摘要

WiMax 主要是由 IEEE 802.16e 的規格來實現，它利用 OFDM 的技術來傳送資料，可把資料傳到 30 哩外，並涵蓋半徑一哩內的範圍。IEEE 802.16e 是 802.16-2004 架構的延伸，支援定點或移動環境的傳輸。

OFDM 的系統性能對時間與頻率的同步非常敏感，不同步的情況會造成系統效能嚴重的衰減。本篇論文針對 IEEE 802.16e 都會區域網路(WiMax)的碼框同步，提出一個低複雜度的演算法，並與 Schmidl & Cox 的方法在複雜度與系統效能上分別在 AWGN 及具有移動性以及靜止的多重路徑環境下做一比較 。電腦模擬結果顯示新的演算法的確是簡單而且有效。

Pilot-Assisted Frame Synchronization Technique for IEEE 802.16e Wireless Metropolitan Area Network

Student：Gow-Yung Chung Advisor：Dr. Che-Ho Wei

Dr. Hsueh-Ming Hang

Department of Electronics Engineering

Institute of Electronics

National Chiao Tung University

ABSTRACT

WiMax is realized by the specification of IEEE 802.16e.It can transmit data over 30 miles and contain the range within 1 mile radius .The transmission system is implemented by OFDM technique. IEEE 802.16e is the extension of 802.16-2004 structure,which supports both fixed position and mobile transmission environments. OFDM system is very sensitive to the timing and frequency errors,the effect of timing and frequency error will degrade the system performance seriously.In this paper,a low-complexity algorithm for the frame synchronization of IEEE 802.16e WiMax is proposed.The proposed method is compared with the method proposed by Schmidl and Cox's in AWGN,mobile,and static mutipath channel，respectively.Simulation results also show that the proposed method can be implemented efficiently with lower

complexity.

致謝

本篇論文能夠得以順利完成，首先致上最真摯的感謝給魏哲和老師。在這兩年的指導中，使我了解到從事研究的處理方法與態度，並在我迷失於研究的路途上，適時指引我一盞明燈，糾正我的研究方向。

另外，我要感謝通訊電子與訊號處理實驗室的師長，提供了良好的研究設備與環境，還有實驗室的諸位伙伴們慷慨大方的幫助之下，克服研究中遭遇的困境與生活上的照顧，尤以陳勇竹、陳宜寬、紀國偉、陳韋霖等同學。學姐唐之璇與學長鐘翼洲的幫忙更是銘記在心。

我要感謝我的好友們，在我心情沮喪時，能夠給予我一股暖流，讓我可以產生勇氣來面對自己。最後，我要感激我的爸媽，感謝他們一直以來的關心，並支持我一路走來完成我的學業，我必須要承認，沒有爸媽就沒有今天的我。

在此，將這篇論文獻給所有給予我幫助的人。

鍾國洋

謹誌於風城交大

2006 / 06

Contents

List of Figures

List of Tables

Chapter 1 Introduction

Orthogonal Frequency Division Multiplexing (OFDM) is a technique that has a high bandwidth efficiency in signaling for high-speed wireless communication system .OFDM is more robust against frequency selective fading by inserting a guard interval in a frame.

OFDM technology has been applied in many digital transmission systems such as digital audio broadcasting(DAB) system , digital video broadcasting terrestrial TV system(DVB-T),wireless local area network(WLAN) and broadband wireless access(BWA)network.

However , an OFDM system is very sensitive to the non-ideal synchronization parameters , such as timing offset,carrier frequency offset,sampling frequency offset.In this thesis,we focus on the issues of timing offset (timing synchronization) estimation.A symbol timing error will both introduce inter carrier interference(ICI) and inter symbol interference(ISI), ISI and ICI effect may dramatically degrade the system performance.Hence,an estimation used to extract a frame timing precisely is necessary,because of a frame timing error results in a timing error in each symbol within the frame.

This thesis is organized as follows.In Chapter 2,we demonstrate the essential elements of an OFDM system.Chapter 3 briefly introduces IEEE 802.16e standard.

In Chapter 4,we review the conventional frame synchronization algorithm [4] and present the proposed method. We also show computer simulation results and comparisons of the performance of synchronization algorithms. Finally ,a conclusion is given in Chapter 5.

Chapter 2 OFDM Overview

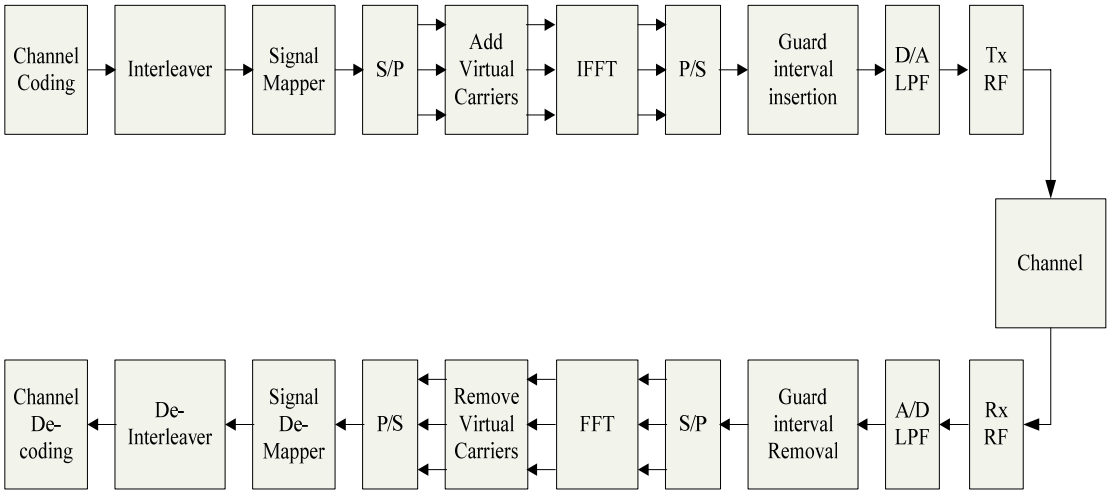

Figure 2 OFDM Transmission System

Multicarrier modulation systems have been employed in military applications since the 1950s.The concept of using parallel data transmission and orthogonal frequency division multiplexing was published in early 1970s.Discrete Fourier transform(DFT) which can be practically implemented with fast Fourier transform (FFT) ,was applied to perform modulation and demodulation in order to eliminate the need of banks of subcarrier oscillator and demodulator. A key improvement to OFDM is adding cyclic prefix in the guard time interval in order to maintain the signal orthogonality over the dispersive channels. Thus,even relatively complex OFDM transmission systems with high data-rates are technically feasible.Now,the OFDM modulation scheme has matured and become a well-established technology.Figure 2 shows a typical OFDM transmission system.

2.1 Principle of OFDM Transmission [1]

For the purpose of enhancing the data transmission rate,the idea of using different frequency band to parallelly transmit data in parallel is presented.In traditional frequency division multiplexing(FDM) systems,the total frequency band is divided into N non-overlapping subcarriers to avoid inter carrier interference(ICI).Because of these spectrum are non-overlapped for FDM system,we can design a filter to demodulate each subcarrier at the receiver side. In this case, it is not efficient in terms of utilization of available spectrum bandwidth. However, the available spectrum bandwidth can be used much more efficiently if the individual subcarriers are allowed to overlap.If the frequency spacing between signal in adjacent bands is Δf ,then the total bandwidth in a FDM system with N sub-carriers needs $2N\Delta f$ or more as illustrated in Figure 2.1-1.But in an OFDM system with N subcarriers,the total bandwidth needed is $(N-1)\Delta f + 2\Delta f = (N+1)\Delta f$, which is more efficient than the conventional FDM system as shown in Figure 2.1-2.

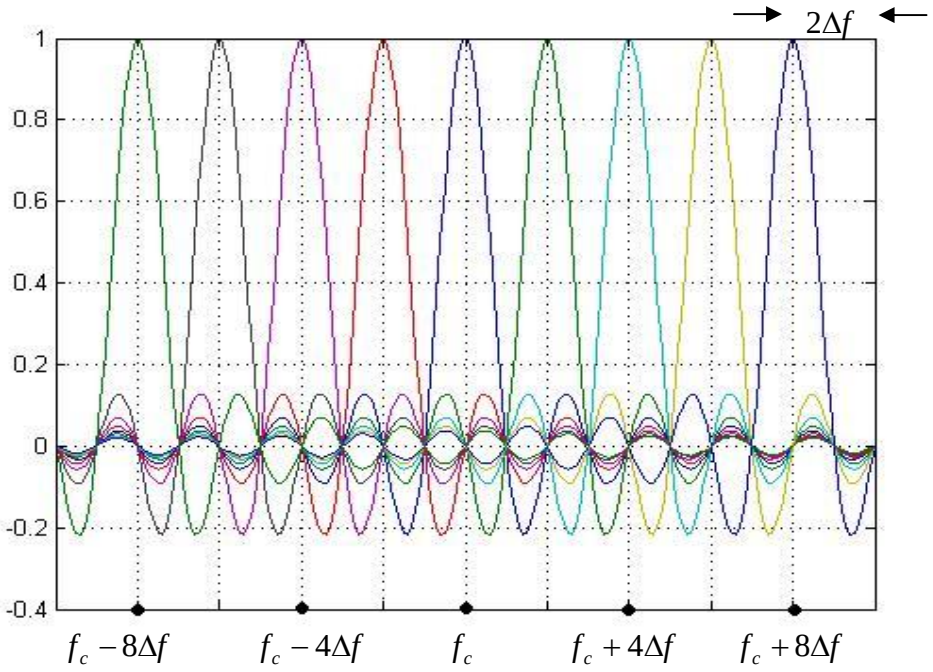

Figure 2.1-1 The spectra of a FDM system

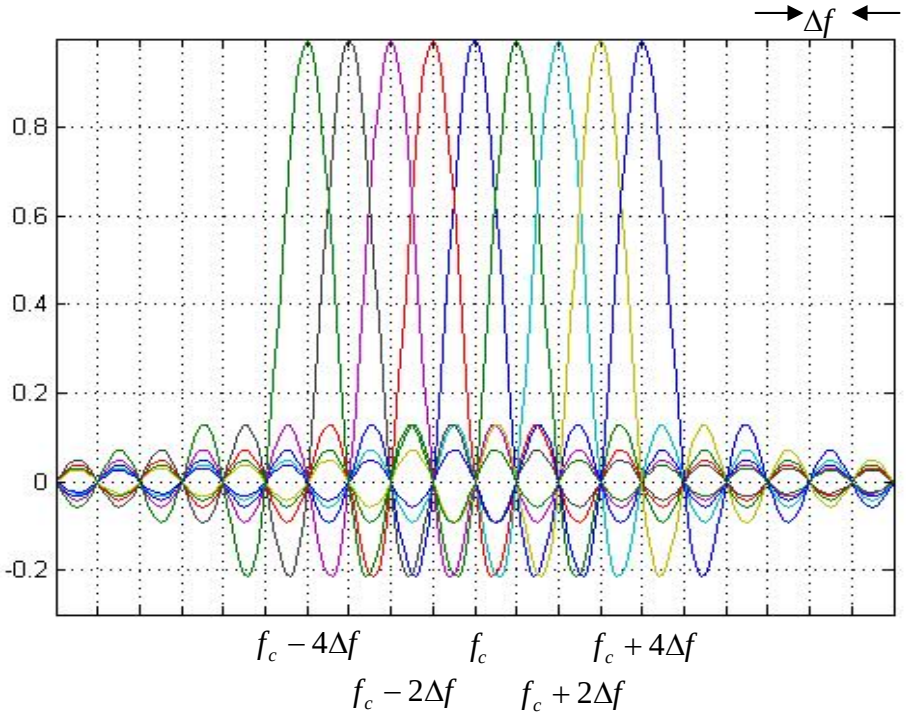

Figure 2.1-2 The spectra of an OFDM system

In the OFDM system,the serial data stream defined as input is rearranged into a sequence $d(k)$ $(k = 0,1,\cdots,N\text{-}1)$ of N QAM symbols at baseband.The time duration between two QAM symbols is T_s (where symbol rate is $f_s = \frac{1}{T_s}$),

At the k-th QAM symbol instant,the complex form of QAM symbol $d(k)$ is represented by an in-phase component $d_I(k)$ and a quadrature-phase component $d_Q(k)$,i.e. $d(k) = d_I(k) + j \cdot d_Q(k)$.A block of N QAM symbols are applied to a serial to parallel converter simultaneously .There are N pairs of balanced modulators which modulate each pair of QAM symbols, respectively . For example , the in-phase and the quadrature-phase components , $d_I(k)$ and $d_Q(k)$, of a QAM symbols are modulated by quadrature carriers , $\cos(2\pi f_k t)$ and $\sin(2\pi f_k t)$, respectively.Notice that the symbol interval of the subcarriers in the parallel system is N times longer than that of the serial system giving that $T = N \cdot T_s$,which corresponds to an N-times lower symbol rate.The sub-carriers frequencies , $f_k = f_c + k \cdot \Delta f$, are spaced apart by $\Delta f = \frac{1}{T}$.

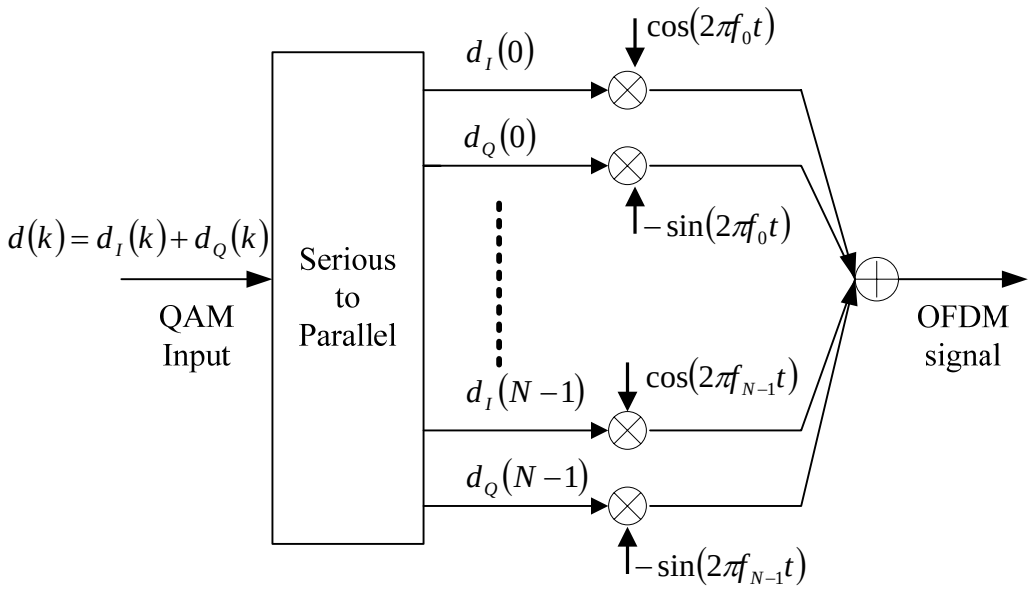

Figure 2.1-3 Conventional OFDM transmitter at passband

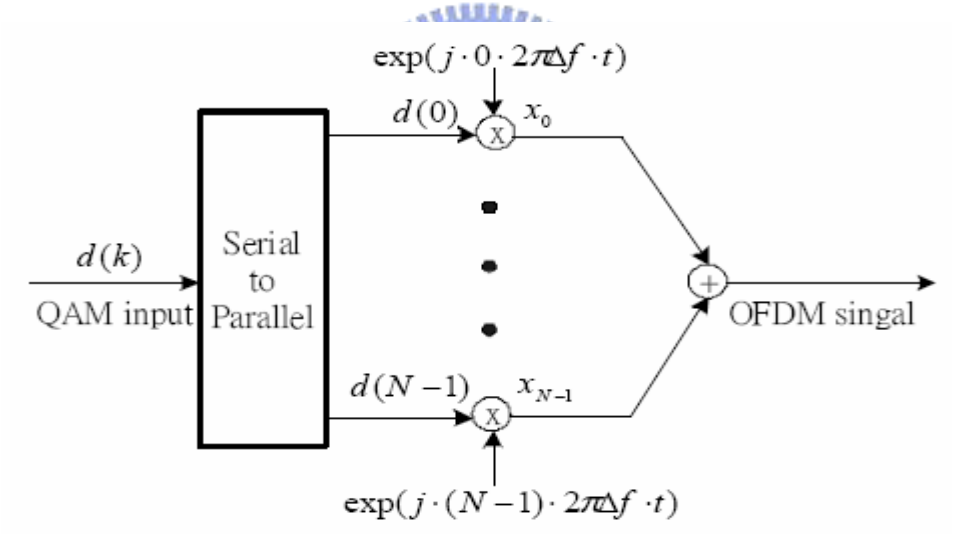

Figure 2.1-4 Conventional equivalent complex baseband OFDM transmitter

Figure 2.1-3 depicts that an OFDM signal is contructed by the summation of modulated carriers, that is , $D_k(t)=d_I(k)\cos(2\pi f_k t)-d_Q(k)\sin(2\pi f_k t)$ with different index k, where $k=0,1,\cdots,N-1$.Thus,we have N QAM symbols at RF,where the k-th QAM symbol at RF is given by ：

$$D_k(t) = d_I(k)\cos(2\pi f_k t) - d_Q(k)\sin(2\pi f_k t)$$

$$= \mathrm{Re}\left\{ d(k) e^{j2\pi k\Delta f t} e^{j2\pi f_c t} \right\} \qquad (2.1\text{-}1)$$

$$= \mathrm{Re}\left\{ x_k(t) e^{j2\pi f_c t} \right\}$$

$x_k(t)$ in (2.1-1) is an eqivalent complex representation for an OFDM signal at baseband $x_k(t)$ is shown in Figure 2.1-4,where the real and imaginary parts correspond to the in-phase and quadrature-phase parts of OFDM signal,which have to be multiplied by a cosine and a sine of the desired carrier frequency ,respectively,to produce the final OFDM signal.By adding the outputs of each subcarrier $x_k(t)$ whose carrier frequency are offset by $\Delta f = \frac{1}{T}$,we obtain the OFDM signal as

$$x(t) = \sum_{k=0}^{N-1} x_k(t) \quad , 0 \le t \le T$$

$$= \sum_{k=0}^{N-1} d(k) e^{j2\pi k\Delta f t} \quad , 0 \le t \le T$$

$$= \sum_{k=0}^{N-1} d(k) \cdot e^{j2\pi k\Delta f t} \cdot u(t) \quad \text{where} \quad u(t) = \begin{cases} 1 & 0 \le t \le T \\ 0 & elsewhere \end{cases} \qquad (2.1\text{-}2)$$

$$= \sum_{k=0}^{N-1} d(k) \cdot g_k(t)$$

where $g_k(t) = e^{j2\pi k\Delta f t} \cdot u(t)$,as shown in Figure 2.1-5.In Figure 2.1-5 , $g_k(t)$ designates the transmitter filter impulse response.

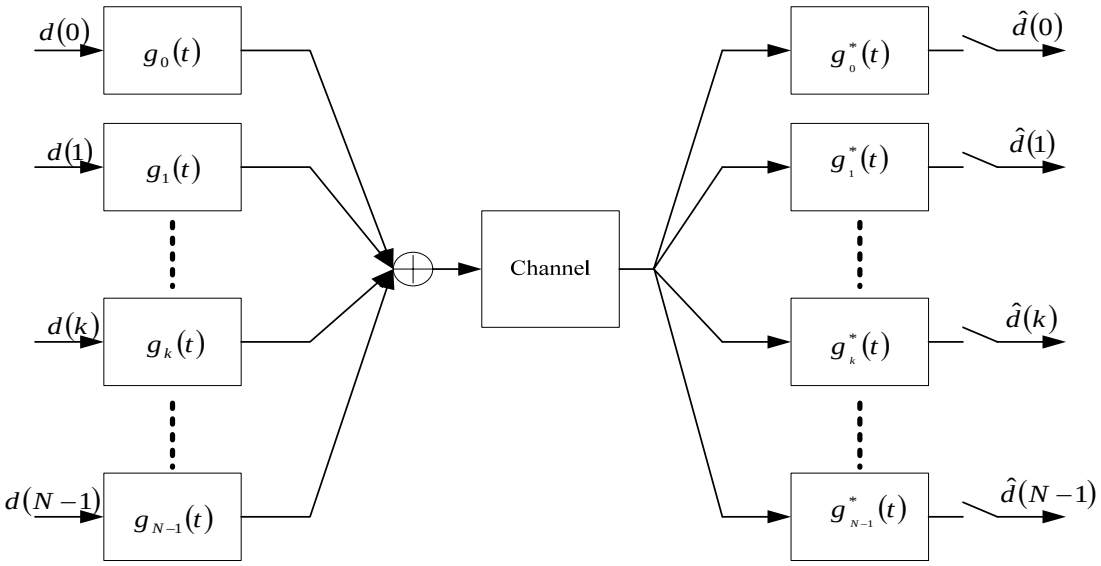

Figure 2.1-5 OFDM transmission model

This set of *N* QAM signals are transmitted simultaneously over the mobile radio channel.At the receiver,the OFDM signal is de-multiplexed using a bank of *N* filters to regenerate the *N* QAM signals.Because of the rectangular pulse shaping,the spectrum of each subcarrier is a sinc function and is formulated as follows：

$$G_k(f) = F\{g_k(t)\} = T\frac{\sin c(\pi T(f-\Delta f))}{\pi T(f-\Delta f)}\exp(j\pi T(f-\Delta f)) \qquad (2.1\text{-}3)$$

Hence,the spectrum of an OFDM signal is constituted by the spectrum of all subcarriers which overlap in the adjacent bands.It is shown in Figure 2.1-2.

It can seen that if the block size *N* is getting larger,we need a larger number of subcarrier modems.The cost for the subcarrier modems is very high and also difficult to implement .Fortunately ,with the help of digital implementation technique and the progress in VLSI technology ,OFDM becomes realizable and popular in recent years.

A discrete-time baseband model of OFDM is needed for digital implementation.It can be shown mathematically that taking the inverse discrete Fourier transform (IDFT) of the original block of *N* QAM symbols .Then transmitting the IDFT coefficients serially is exactly equivalent to the operations required by the OFDM transmitter employing a bank of N transmitted filter.

The total bandwidth of the OFDM system is $B = N \cdot \Delta f$ .The signal can be reconstructed by the complex samples at the time instant $t = n \cdot \frac{T}{N}$ with sampling period $\Delta t_{sampling} = \frac{1}{B} = \frac{T}{N}$ .According to (2.1-2),the samples of the signal waveform can be written as

$$x_n = \sum_{k=0}^{N-1} d(k) \exp\left(j2\pi k \frac{n}{N} \right) \qquad (2.1\text{-}4)$$

This equation is equivalent to IDFT of $d(k)$ and shown in Figure 2.1-6.

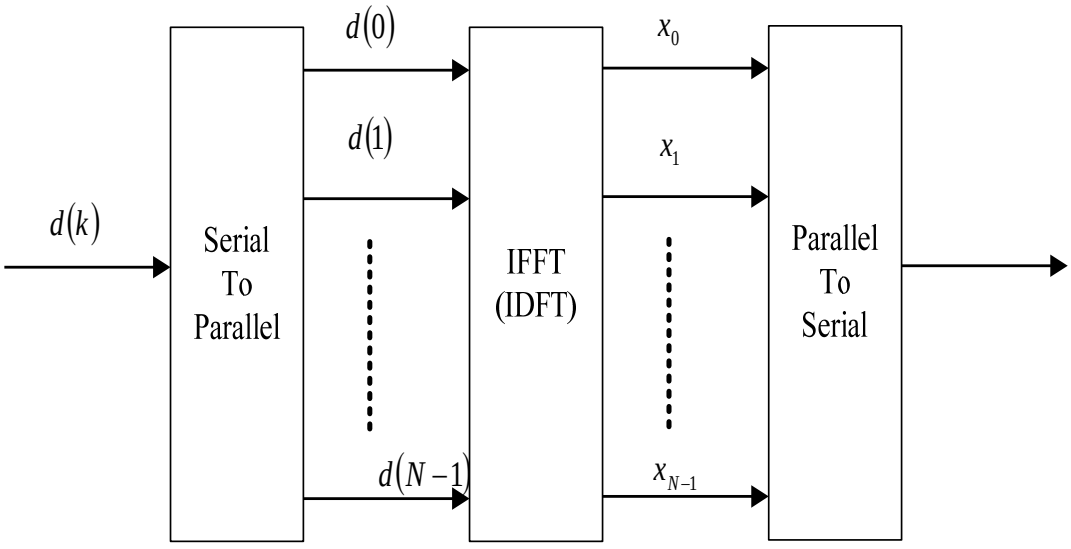

Figure 2.1-6 Implementation of the OFDM transmission system using IFFT

In practice,IDFT can be implemented efficientlly by inverse fast Fourier transform (IFFT) at the transmitter side.The computation complexity of IFFT can be reduced from N^2 to $N \log N$ or less.Since the receiver performs the inverse operation of transmitter,so a discrete Fourier transform (DFT) is needed at the receiver side.DFT also can be implemented efficientlly by fast Fourier transform (FFT).

A bank of subcarrier modems are implemented using the computationally efficient pair of inverse fast Fourier transform and fast Fourier transform (IFFT/FFT).

FFT and IFFT are defined by

$$X_k = \sum_{n=0}^{N-1} x_n \exp\left(-j2\pi k \frac{n}{N}\right) \quad k = 0,1,\cdots,N-1 \qquad (2.1\text{-}5)$$

$$x_n = \sum_{k=0}^{N-1} X_k \exp\left(j2\pi k \frac{n}{N}\right) \quad n = 0,1,\cdots,N-1 \qquad (2.1\text{-}6)$$

2.2 Pilot and Vitual Carriers

In practice,some of subcarriers are allocated to carry already known data and some of subcarriers are allocated to carry nothing in the window before IDFT operation.These subcarriers carrying already known data are named pilots,and subcarriers carrying nothing are named virtual subcarriers.The purpose we exploit the two types of speciall subcarriers will be explained in the following .

There is necessity of dynamic channel estimation before demodulation of received OFDM signal,since the wireless communication channel is time-varying and time-dispersive.Usually,there are two types of arrangement for pilot insertion: Comb-type and Block-type.

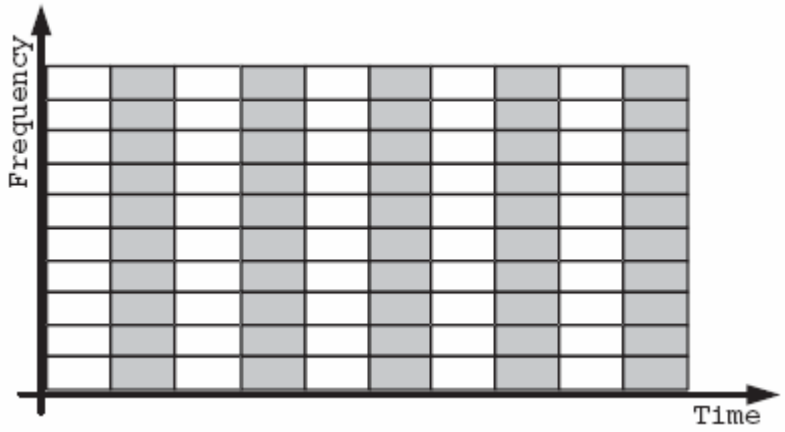

Figure 2.2-1 (a) Block-Type pilot insertion

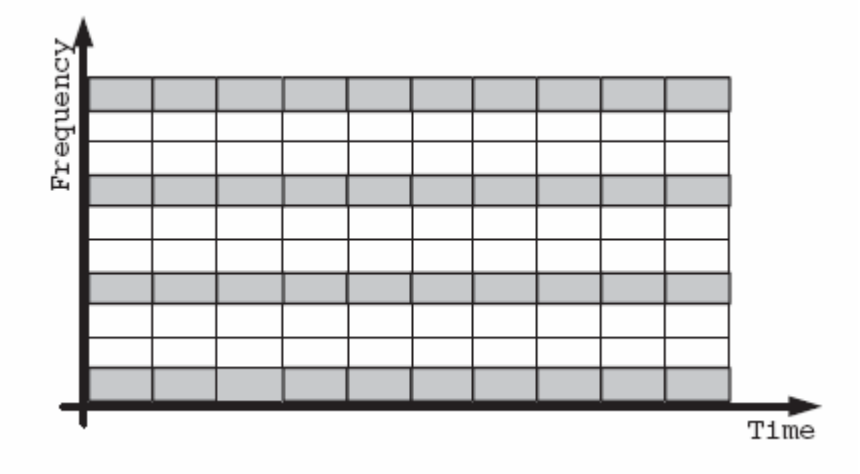

Figure 2.2-1 (b) Comb-Type pilot insertion

For Block-type arrangement,the pilots are inserted into all of the subcarriers of an OFDM symbol called pilot symbol .These pilot symbols are sent peroidiclly among the transmitted OFDM symbols.Because these pilot symbols were sent with a specific period,it is suitable for the following condition ：if the Doppler spread of channel is f_d ,the specificed period Δt_p should be less than the coherent time $\frac{1}{f_d}$,i.e, $\Delta t_p < \frac{1}{f_d}$.

For Comb-Type arrangement,pilots are inserted in some specified subcarriers in each OFDM symbol.These subcarriers carrying pilot informations are called pilot tones.In order to estimate the channel for the subcarriers not carrying pilot information,it needs an efficient interpolation technique.But Comb-type arrangement is more suitable than Block-type arrangement for flat fading channel and fast fading channel,because Comb-type arrangement has pilot informations for each transmitted OFDM symbol.If the delay spread of the channel is $\tau_{\max}$,the spacing between adjacent

pilot tones , Δf_p ,should be less than the coherent bandwidth $\frac{1}{\tau_{\max}}$,i.e. $\Delta f_p < \frac{1}{\tau_{\max}}$.

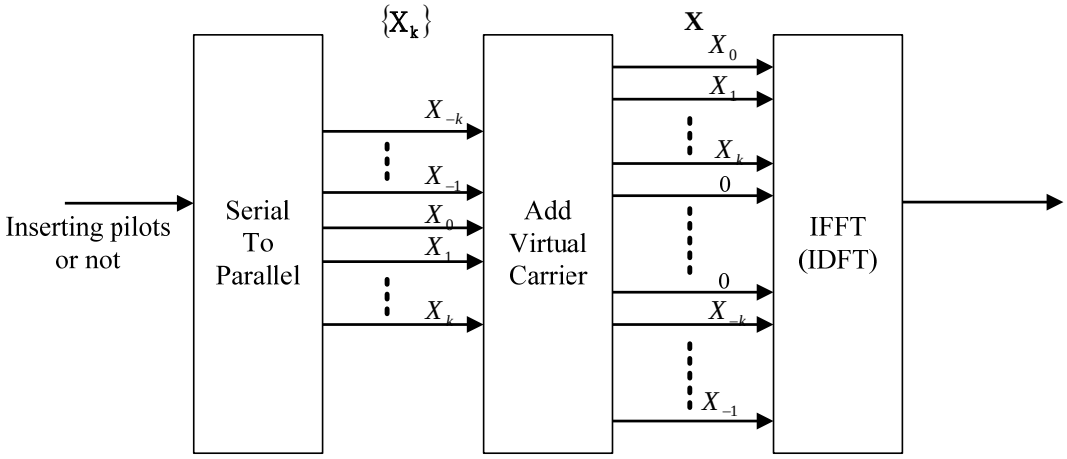

Figure 2.2-2 The modulated sequence are added virtual carriers

Some subcarriers without carying any data information are called virtual subcarriers.The reason for using zero padding is that the spectra of OFDM signals are not strictly bandlimited ,there still exits large out-of-band energy.Adding zeros as a guard band would decrease the energy spread to adjacent frequency bands which are allocated for other wireless communication systems.It also could avoid aliasing.If there are 2K+1 modulation variables,such as $\{X_k\} = \{X_{-k}, \cdots, X_{-1}, X_0, X_1, \cdots, X_k\}$, then $\{X_k\}$ are padded zero as a guard band at the tail of $\{X_k\}$.Since the index of IFFT input is from 0 to N-1,the input X of IFFT becomes

$$\mathbf{X} = \{X_0, X_1, \cdots, X_k, 0, \cdots, 0, X_{-k}, \cdots, X_{-1}\}$$

This process is demonstrated in Figure 2.2-2.

2.3 Cyclic Prefix

Due to the multipath propagation,the OFDM symbol may be interfered by previous OFDM symbol .This phenomenon is called inter symbol interference (ISI).To eliminate the effect of ISI,a guard interval is inserted before the OFDM symbol.This is also one of the reasons and characteristics that OFDM system is robust for multipath fading channel.

Generally,the length of guard interval should be longer than the root-mean-square (RMS) delay spread of the channel so that ISI only damages the information within the guard interval.Figure 2.3-1 shows how the ISI is dealt with by the guard Interval.

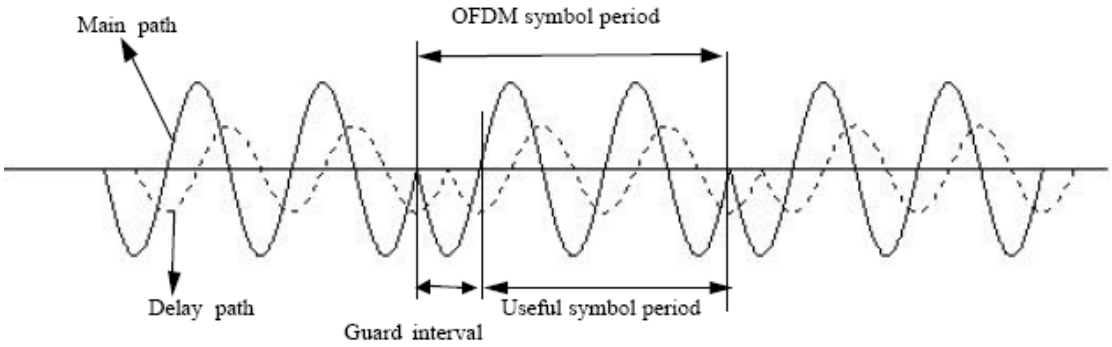

Figure 2.3-1 An example of a subcarrier signal in two-ray multipath channel

The component of guard interval is the duplicate of the last data in an OFDM symbol block,hence it is named Cyclic Prefix (CP).An OFDM frame diagram with CP is plotted in Figure 2.3-2.Since the signal is transmitted over a multipath channel,the

received OFDM siganl may contain the delayed by itself.We would like to demodulate by FFT operation.However,the result of FFT operation could be exact because of the orthogonality among each subcarrier,like the case in Figure 2.3-3 (a).

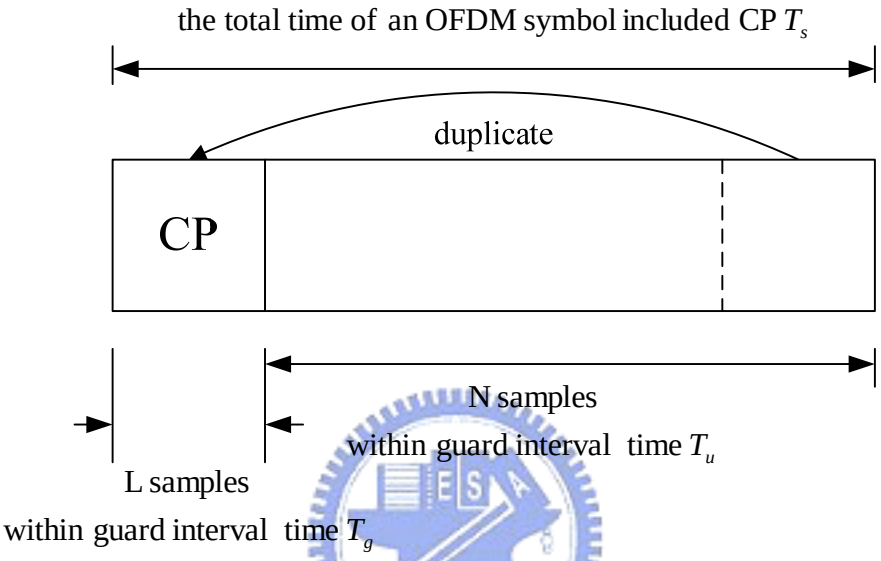

Figure 2.3-2 An OFDM symbol diagram with CP

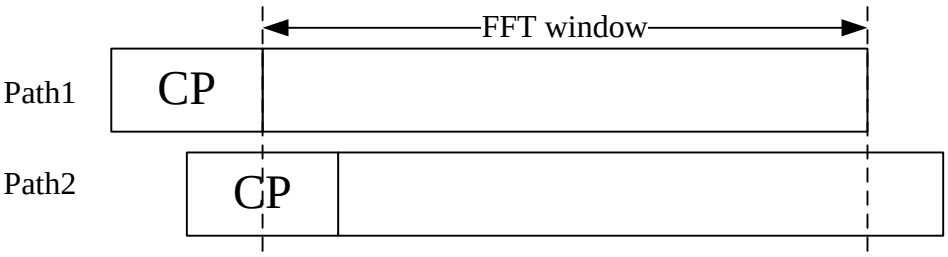

Figure 2.3-3 (a) Two-ray multipath effect without ISI

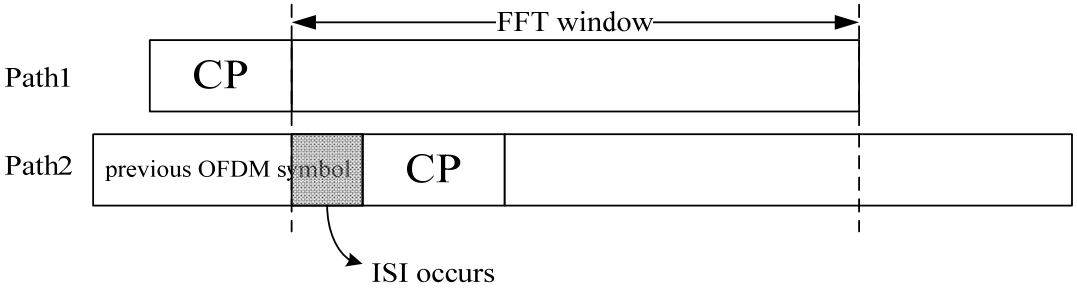

Figure 2.3-3 (b) Two-ray multipath effect with ISI

Noticing that the component of guard interval can not be inserted with zeros.If we insert zeros within guard interval,then system performance will degrade seriously after DFT operation.This is because there will lose orthogonality between zero information and each component of subcarrier.Hence inserting zero information will introduce inter carrier interference (ICI) during the process of DFT.

The case in Figure 2.3-3 (b) shows that ISI and ICI are introduced.

The channel is modeled as a discrete-time time-invariant system with finite-length impulse response,ie. : $\begin{cases} h[n] \neq 0 & , \ 0 \le n \le N_g \\ h[n] = 0 & , \ elsewhere \end{cases}$,

The transmitted OFDM signal is given by

$$x_t[n] = \begin{cases} x_g[n] & , \ 0 \le n < N_g \ \ where \ x_g[n] = x[n+N] \\ x[n] & , N_g \le n \le N + N_g \end{cases} , 0 \le n < N_g$$

and the received OFDM signal without noise is obtained as

$$x_r[n] = \begin{cases} x_g[n] \otimes h[n] & , \ 0 \le n < N_g + N_h \\ x[n] \otimes h[n] & , N_g \le n \le N + N_g + N_h \end{cases}$$

Then

$x_g[n] \otimes h[n]$, $0 \le n < N_g + N_h$ is equal to $x[n] \otimes h[n]$, $N + N_g \le n \le N + N_g + N$

$$x[n] \textcircled{N} h[n] \xrightarrow{\text{FFT}} X_k H_k \qquad (2.3\text{-}1)$$

After removing the cyclic prefix,the linear convolution of the useful transmitted signal and the channel response can be regarded as circular convolution (2.3-1).

The time domain channel effect could be transformed into a multiplicative effect when demodulating by DFT at the receiver..It is shown that only simple channel estimation and equalization is needed.

In summary,the cyclic prefixed guard interval not only preserves the mutual orthogonality between subcarriers but also prevents the ISI between adjacent OFDM symbols.

2.4 Time and Frequency Offset

At receiver side,OFDM sysytem must operate the inverse process of the transmitter side.Hence we have to determine the arrival time of an OFDM symbol's start point in order to capture the most suitable samples in a window for FFT operation.Since timing errors may introduce both inter carrier interference(ICI) and inter symbol interference(ISI),the OFDM system that has synchronization problem may dramatically degrade the system performance. Timing offset is defined in Figure 2.4-1 (a) & (b).

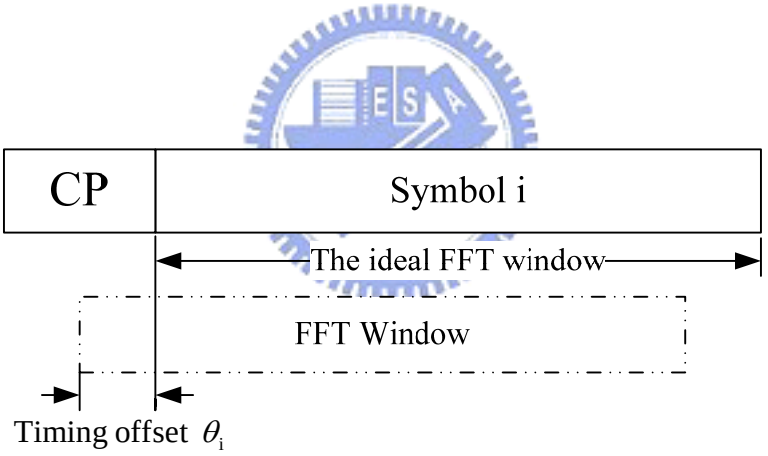

Figure 2.4-1 (a) Timing offset inside CP

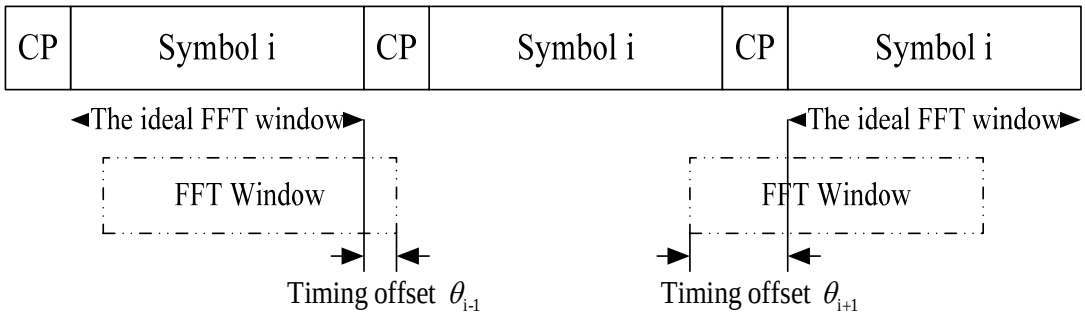

Figure 2.4-1 (b) Timing offset outside CP

In discrete-time baseband model,timing offset can be modeled as an integral delay θ,so the received signal $y(n)$ can be easily expressed as $x(n-\theta)$.If θ is less than the CP length as shown in Figure 2.4-1 (a),the received signal is then given by $y(n)=x[(n-\theta)_N]$.Because of the circular shift property of DFT,the received signal after DFT , Y_k , in frequency domain is given by

$$Y_k = X_k \exp\left(\frac{2\pi\theta}{N}\right) \qquad (2.4\text{-}1)$$

It can be easily explained as the follows. The constellation is a phase rotation if timing offset is less than the CP length , as illustrated in Figure 2.4-3.However,if timing offset exceeds the CP length as shown in Figure 2.4-1 (b),then ISI and ICI occur and the system performance degrades seriously , as shown in Figure 2.4-4.

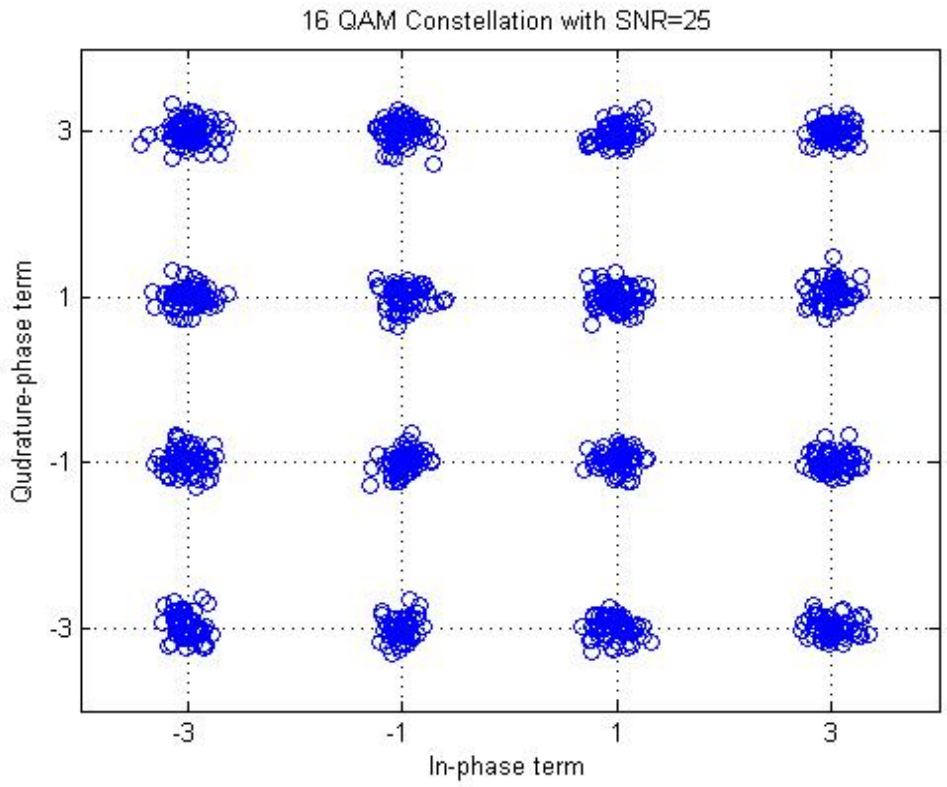

Figure 2.4-2 16 QAM constellation with SNR=25

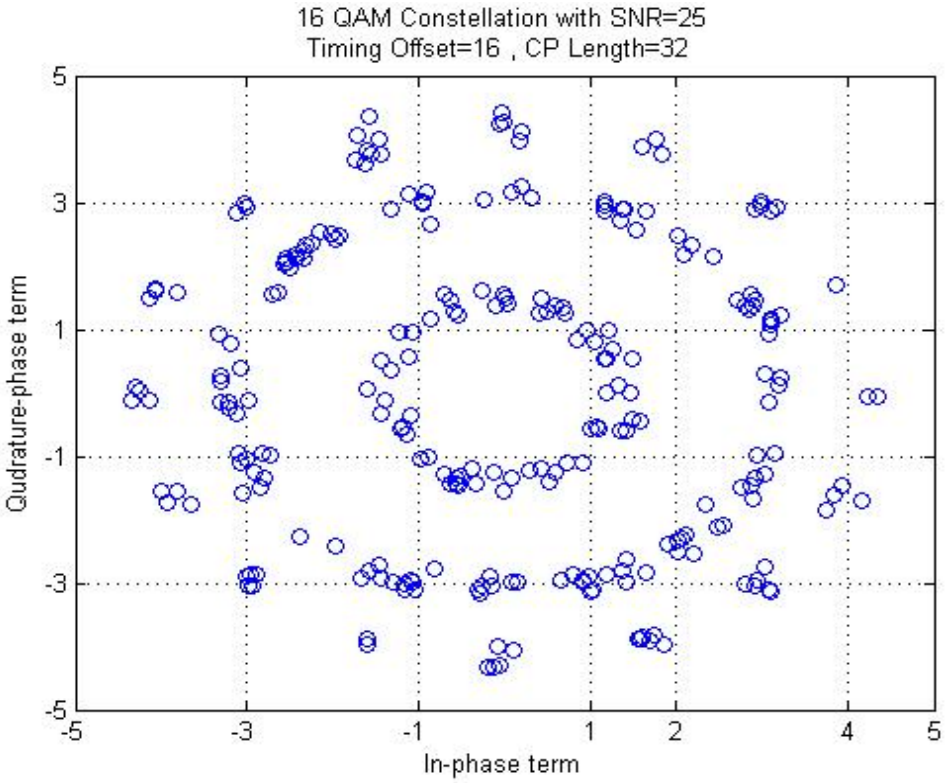

Figure 2.4-3 Timing offset is less than CP

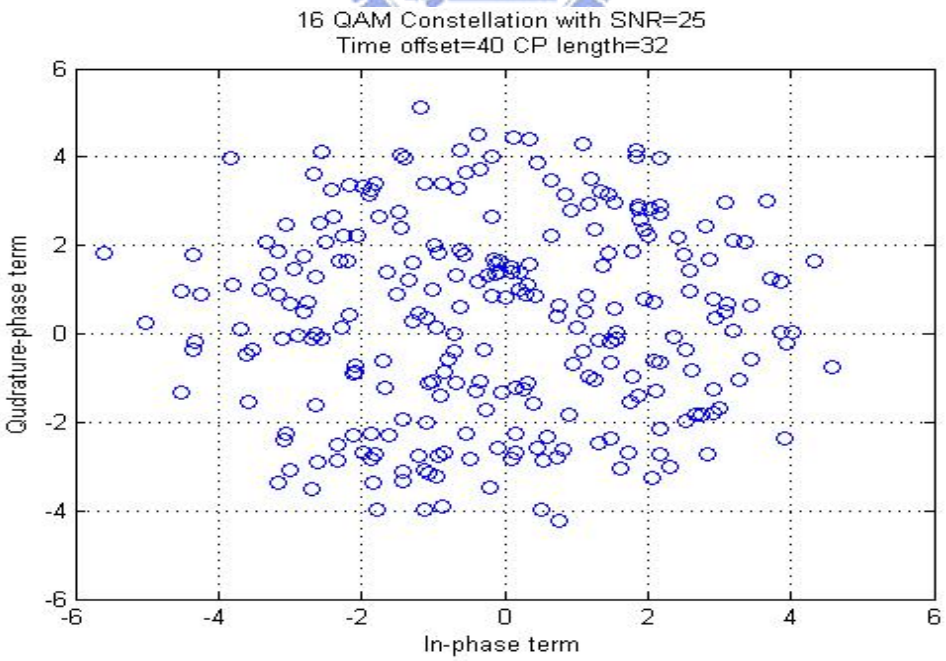

Figure 2.4-4 Timing offset is larger than CP

The frequency difference of the oscilators in transmitter and receiver will result in the frequency offset,which leads to ICI caused by the loss of orthogonality between subcarriers , as shown in Figure 2.4-5.

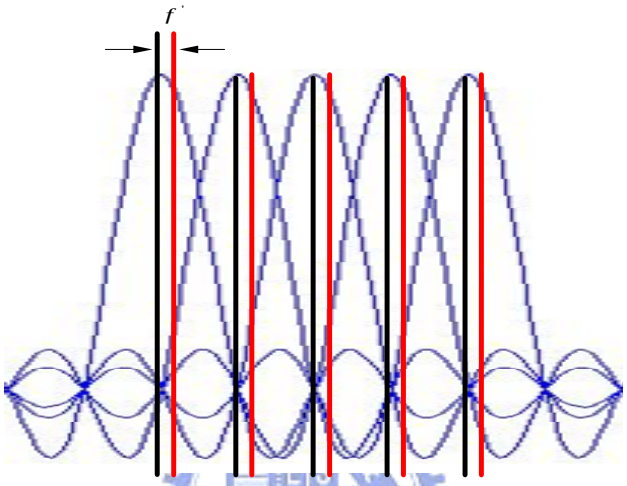

Figure 2.4-5 Sampling OFDM siganl with a frequency offset or not

The solid black lines in Figure 2.4-5 show the perfect synchronized position in frequency domain.Sampling at these positions of solid black lines will not introduce ICI and can maintain orthogonality with each subcarrier.If there is frequency offset illustrated by solid red lines,then an offset f' occurs when comparing with the solid black lines.In the descrete-time baseband model,the effect of frequency offset between two oscillators in the transmitter and receiver can be modelled as $\exp\left(j\frac{2\pi k\varepsilon}{N}\right)$,where ε is the ratio of the real frequency offset to the intercarrier spacing,i.e. $\varepsilon = \frac{f'}{\Delta f}$.The received siganl with frequency offset is investigated by [3]

and can be represented as

$$y_n = \frac{1}{N}\sum_{k=-K}^{K} X_k \exp\left(j\frac{2\pi n(k+\varepsilon)}{N}\right) = x_n \exp\left(j\frac{2\pi n\varepsilon}{N}\right), n = 0,\cdots,N-1, N \geq 2K+1$$

(2.4-2)

where the channel effect and the noise term are ignored.

After the DFT operation,we have

$$Y_k = X_k \frac{(\sin(\pi\varepsilon))}{N\sin\left(\pi\varepsilon/N\right)}\exp\left(j\pi\varepsilon(N-1)/N\right) + I_k, \text{(2.4.3)}$$

where

$$I_k = \sum_{\substack{l=-K \\ l\neq k}}^{K} X_l \left\{\frac{\sin(\pi\varepsilon)}{(N\sin(\pi(l-k+\varepsilon)/N))}\right\}\exp\left(j\pi\varepsilon(N-1)/N\right)\exp\left(-j\pi(l-k)/N\right) \quad .$$

From (2.4.3),we can see that X_k experiences an amplitude reduction and phase shift.

I_k is the ICI term caused by frequency offset.

It can be seen in Figure 2.4-6 and 2.4-7 that the constellation is only rotated by a small angele under small frequency offset,but the constellation is distored and can not be distinguished when there is a larger frequency offset.

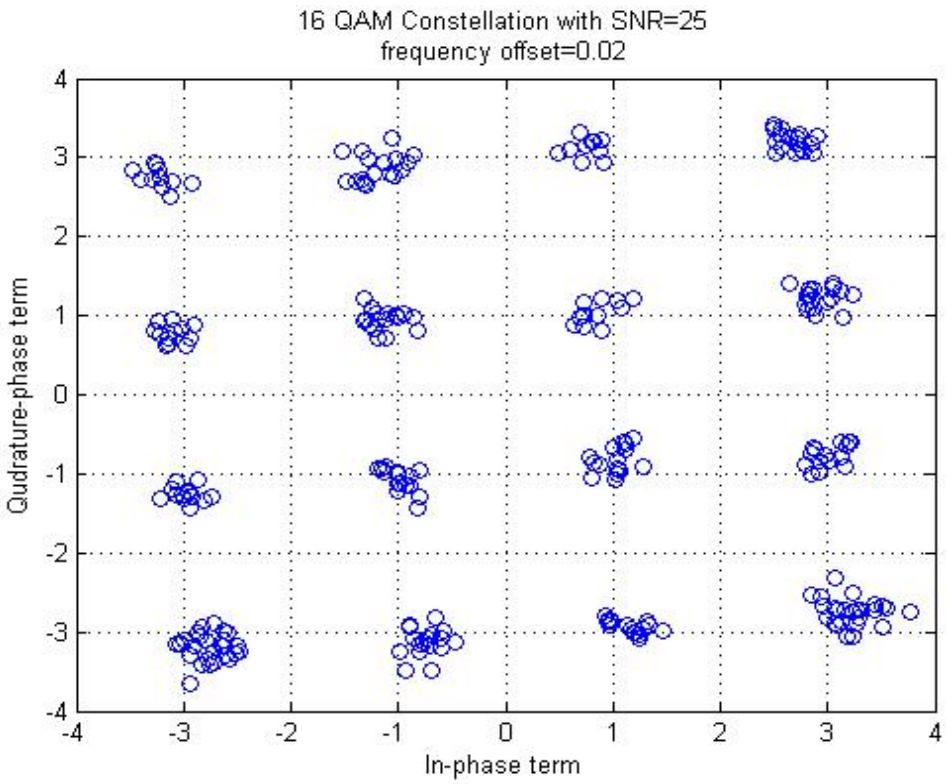

Figure 2.4-6 The contellation is influenced by a small frequency offset

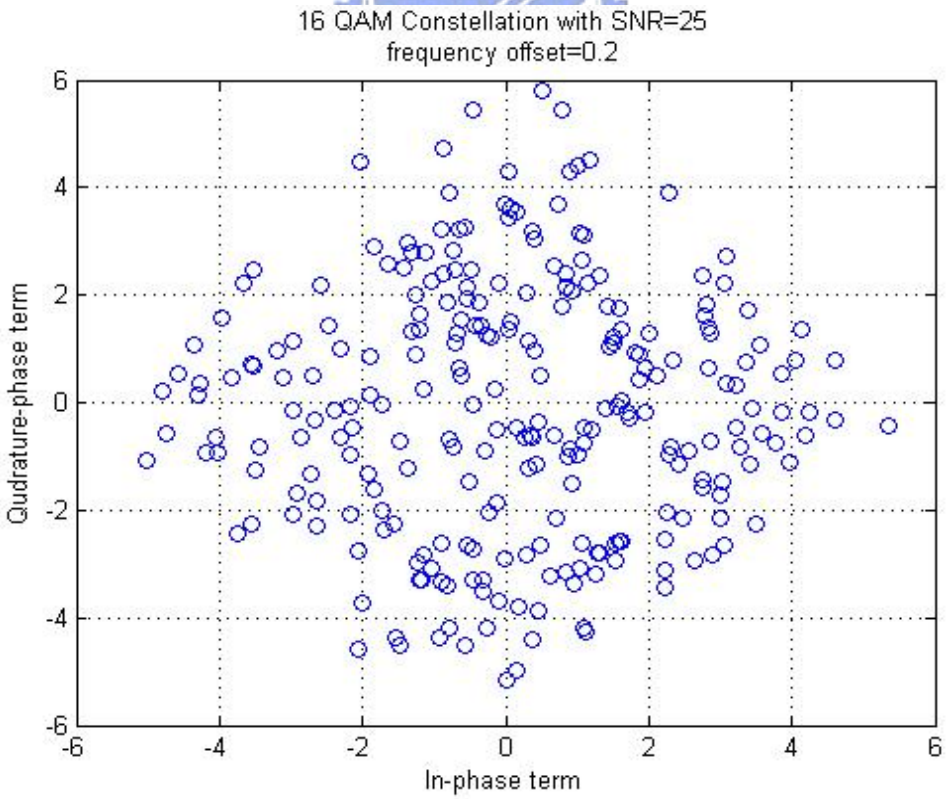

Figure 2.4-7 The contellation is influenced by a lager frequency offset

Chapter 3

IEEE 802.16e WiMax

Worldwide Interoperability for Microwave Access(WiMax) is the common name associated to IEEE 802.16a/d/e standards.

These standards are issued by the IEEE 802.16 subgroup that originally covered the Wireless Local Loop technologies with radio spectrum from 10 to 66 GHz.

According to the different locations of subscriber station (SS) and to avoid the interference from the other base station on SS,the modulation and coding schemes may be adjusted individually to each subscriber station (SS) on a burst-by-burst basis, as illustrated by Figure 3.

For downlink(DL) transmission,multiple SSs can associate the same downlink burst; and for uplink(UL) transmission,SS transmits in an given time slot with a specific burst.

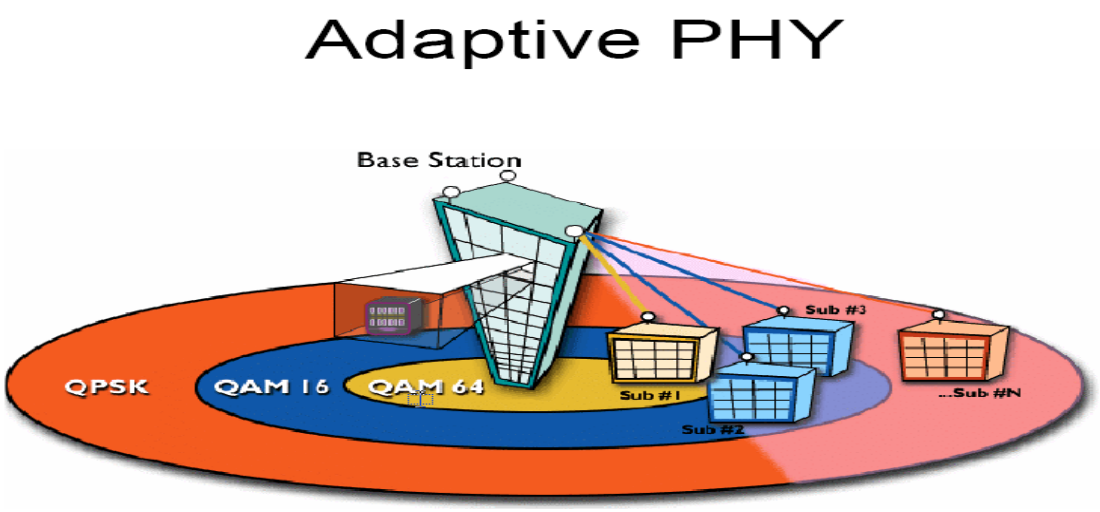

Figure 3 Adaptive PHY

3.1 IEEE 802.16

IEEE 802.16 standard is for Line-of-Sight (LOS) applications utilizing 10-66 Ghz spectrum. Although this spectral range has a severe atmospheric attenuation, it is suitable for connections in the operator network between two nodes with high amounts of bandwidth because many base stations are deployed at elevated positions from the ground. This is not suitable for residential settings because of the Non-Line-of-Sight (NLOS) characteristics caused by rooftops or trees.

IEEE 802.16a is an amendment for NLOS utilizing 2-11Ghz,which is good for Point-to-Multipoint(PMP) and home application.Orthogonal Frequency Division Multiplexing(OFDM) is adopted for transmission.

IEEE 802.16-2004 revises and replaces 802.16,802.16a,and 802.16REVd. This is the completion of the essential fixed wireless standard.Some operators are already interested in integrating this with the Cellular backhaul.After some political debates,it was decided to support not mobile but fixed wireless and nomadic communications.Nomadicity is this: Users are attached to the network.After a session completes,they can move to a different network.But the session should be re-established (possibly including the authentication) from scratch; ; it does not have a hand-off mechanism.

IEEE 802.16e is a MAC/PHY enhancement for supporting truly mobile

communications at vehicular speeds.This supports a full hand-off.A user’s session is maintained when he moves around.

3.2 OFDM PHY Specification

3.2.1 Time and Frequency Description of OFDM

The WirelessMAN-OFDM PHY is based on OFDM modulation and designed for NLOS operation in the frequency bands below 11 GHz.

The transmitter energy increases with the length of the guard interval while the receiver energy remains the same (the cyclic extension is discarded).Thus there is a

$$10\log\left(1-\frac{T_g}{T_g+T_b}\right)\Big/\log(10)$$ dB loss in $\frac{E_b}{N_0}$.

On initialization,an SS should search all possible values of CP until it finds the CP being used by the BS.The SS shall use the same CP on the uplink. Once a specific CP duration has been selected by the BS for operation on the downlink, it should not be changed.Changing the CP would force all the SSs to resynchronize to the BS.

Figure 3.2-1 illustrates the time structure of OFDM symbol ,while Figure 3.2-2 gives a frequency description of OFDM signals.

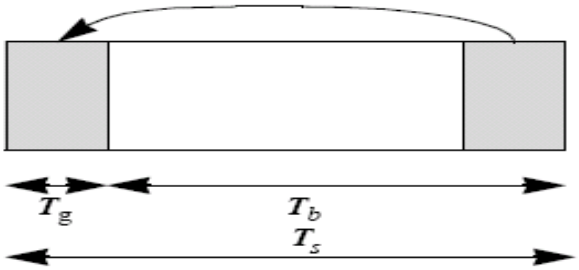

Figure 3.2.1-1 OFDM symbol time structure

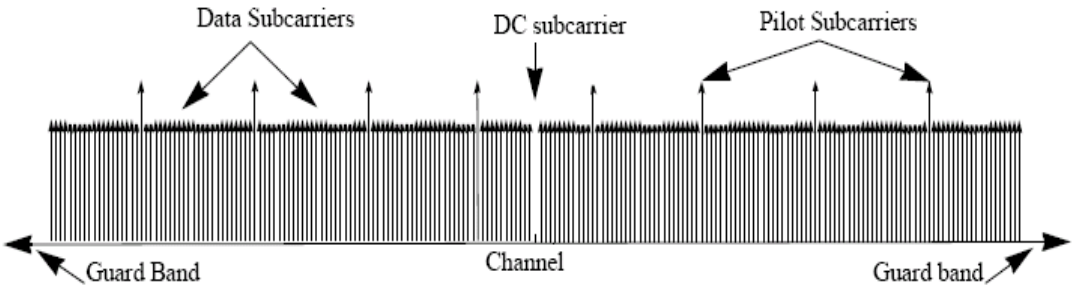

Figure 3.2.1-2 OFDM frequency description

Data sub-carriers：For data transmission.

Pilot- subcarriers：For various estimation purposes.

Null- subcarriers： No transmission at all, for guard bands, non-active subcarriers and the DC subcarrier.

3.2.2 Parameter Setting

(a) Primitive parameter definitions：

– BW ： This is the nominal channel bandwidth.

– N_{used} ： Number of used subcarriers.

– n ：Sampling factor. This parameter, in conjunction with BW and N_{used} determines the subcarrier spacing, and the useful symbol time.

– G ： This is the ratio of CP time to “useful” time.

(b) Derived parameter definitions ：

– N_{FFT} ：Smallest power of two greater than N_{used}.

– Sampling Frequency： $F_s = floor\left(n \cdot BW / 8000\right) \times 8000$

– Subcarrier spacing ： $\Delta f = F_s / N_{FFT}$

– Useful symbol time： $T_b = 1/\Delta f$

– CP Time： $T_g = G \cdot T_b$

– OFDM Symbol Time： $T_s = T_b + T_g$

– Sampling time： T_b / N_{FFT}

(c) Table 3.2.2-1 gives the OFDM Symbol parameters

Parameter	Value
N_{used} / N_{FFT}	**200/256**
G	1/4 ， 1/8 ， 1/16 ， 1/32
Frequency offset indices of pilot carriers	–88,–63,–38,–13,13,38,63,88
Frequency offset indices of guard subcarriers	–128,–127...,–101 (numbers：28) +101,+102,...,127 (numbers：27)
n	For channel bandwidths that are a multiple of {1.75 MHz then n = 8/7 1.5 MHz then n = 86/75 1.25 MHz then n = 144/125 2.75 MHz then n = 316/275 2.0 MHz then n = 57/50 otherwise specified then n = 8/7}

Table 3.2.2-1 OFDM symbol parameters

3.2.3 Randomization of Data

A Pseudo Random Binary Sequence(PRBS) generator is shown in Figure 3.2.3-1

Data randomization is performed on each burst of data on the downlink and uplink.The randomization is performed on each allocation (downlink or uplink),which means that for each allocation of a data block (subchannels on the frequency domain and OFDM symbols on the time domain) the randomizer shall be used independently.If the amount of data to transmit does not fit exactly the amount of data allocated,padding of 0xFF (“1” only) shall be added to the end of the transmission block for the unused integer bytes. For RS-CC and CC encoded data,,padding will be added to the end of the transmission block, up to the amount of data allocated minus one byte,which shall be reserved for the introduction of a 0x00 tail byte by the FEC.

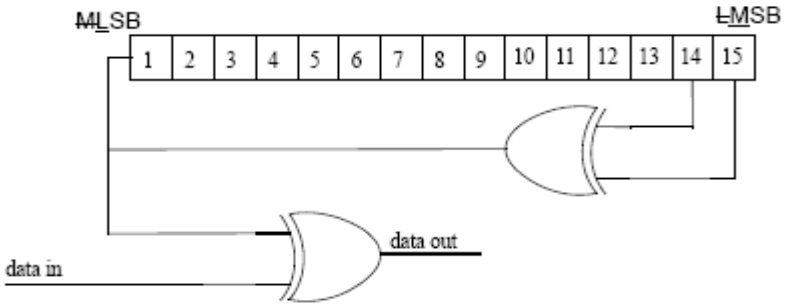

Figure 3.2.3-1 PRBS generator for data randomization

On the downlink, the randomizer shall be re-initialized at the start of each frame with the sequence: 1 0 0 1 0 1 0 1 0 0 0 0 0 0 0 0. The randomizer shall not be reset at the start of burst #1. At the start of subsequent bursts,the randomizer shall be initialized with the vector shown in Figure 3.2.3-2.

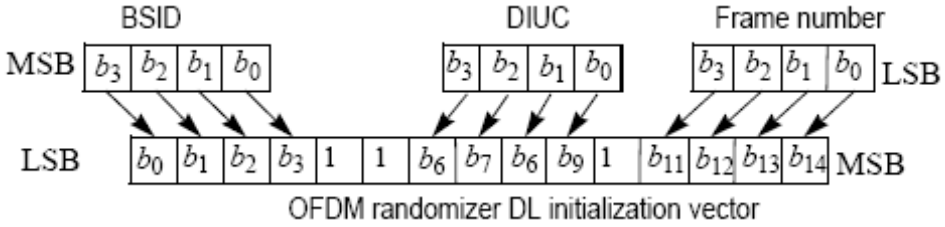

Figure 3.2.3-2 OFDM randomizer downlink initialization vector for burst #2...N

On the uplink,the randomizer is initialized with the vector shown in Figure 3.2.3-3.The frame number used for initialization is that of the frame in which the UL map that specifies the uplink burst was transmitted.

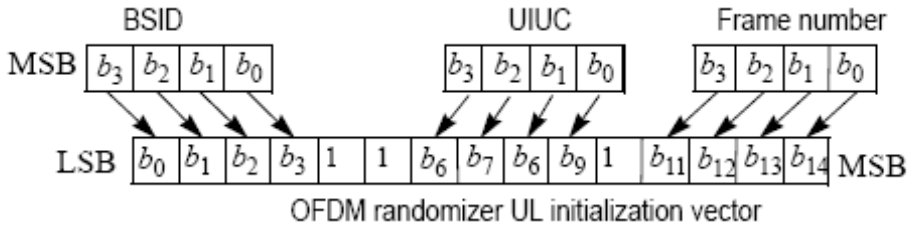

Figure 3.2.3-3 OFDM randomizer uplink initialization vector

3.2.4 FEC

A Forward Error-Correction code(FEC),consisting of the concatenation of a Reed–Solomon outer code and a rate-compatible convolutional inner code, shall be supported on both uplink and downlink. Support of Block Turbo Code(BTC) and Convolutional Turbo Code (CTC) is optional.

The most robust burst profile shall always be used as the coding mode when requesting access to the network and in the FCH burst.The encoding is performed by first passing the data in block format through the RS encoder and then passing it through a zero-terminating convolutional encoder.

The Reed–Solomon encoding shall be derived from a systematic RS (N = 255, K = 239, T = 8) code.Puncturing patterns and serialization order that shall be used to realize different code rates are defined in Table 3.2.4-2. In the table,“1” means a transmitted bit and “0” denotes a removed bit, whereas X and Y are in reference to Figure 3.2.4-1.

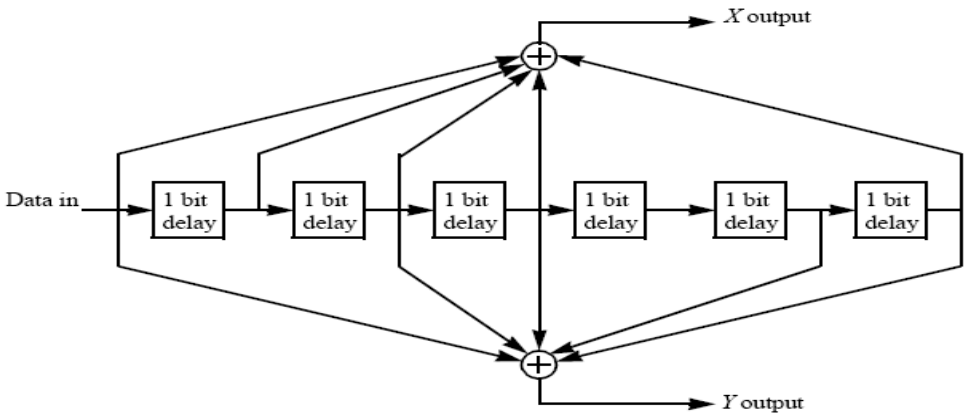

Figure 3.2.4-1 Convolutional encoder of rate 1/2

	Code rates			
Rate	1/2	2/3	3/4	5/6
d_{free}	10	6	5	4
X	1	10	101	10101
Y	1	11	110	11010
XY	X_1Y_1	$X_1Y_1Y_2$	$X_1Y_1Y_2X_3$	$X_1Y_1Y_2X_3Y_4X_5$

Table 3.2.4-2 The inner convolutional code with puncturing configuration

Table 3.2-4-3 gives the block sizes and the code rates used for the different modulations and code rates. As 64-QAM is optional for license-exempt bands, the codes for this modulation shall only be implemented if the modulation is implemented.

Modulation	Uncoded block size (bytes)	Coded block size (bytes)	Overall coding rate	RS code	CC code rate
BPSK	12	24	1/2	(12,12,0)	1/2
QPSK	24	48	1/2	(32,24,4)	2/3
QPSK	36	48	3/4	(40,36,2)	5/6
16-QAM	48	96	1/2	(64,48,8)	2/3
16-QAM	72	96	3/4	(80,72,4)	5/6
64-QAM	96	144	2/3	(108,96,6)	3/4
64-QAM	108	144	3/4	(120,108,6)	5/6

Table 3.2.4-3 Mandatory channel coding per modulation

When subchannelization is applied, the FEC shall bypass the RS encoder and use the Overall Coding Rate as indicated in Table 3.2.4-3 as CC Code Rate.The Uncoded Block Size and Coded Block size may be computed by multiplying the values listed in Table 3.2.4-3 by the number of allocated subchannels divided by 16. In the case of BPSK modulation,the RS encoder should be bypassed.

3.2-5 Interleaving

All encoded data bits shall be interleaved by a block interleaver with a block size corresponding to the number of coded bits per the allocated subchannels per OFDM symbol,*N*cbps.Table 3.2-5-1 gives the block size of the Bit Interleaver.

	Default (16 subchannels)	**8 subchannels**	**4 subchannels**	**2 subchannels**	**1 subchannel**
	N_{cbps}				
BPSK	192	96	48	24	12
QPSK	384	192	96	48	24
16-QAM	768	384	192	96	48
64-QAM	1152	576	288	144	72

Table 3.2.5-1 Block sizes of the Bit Interleaver

3.2.6 Modulation

After bit interleaving,the data bits are entered serially to the constellation mapper.BPSK,Gray-mapped QPSK,16-QAM,and 64-QAM as shown in Figure 3.2-6-1 shall be supported,whereas the support of 64-QAM is optional for license-exempt bands.The constellations (as shown in Figure 3.2-6-1) shall be normalized by multiplying the constellation point with the indicated factor *c* to achieve equal average power.For each modulation, *b0* denotes the least significant bit (LSB).

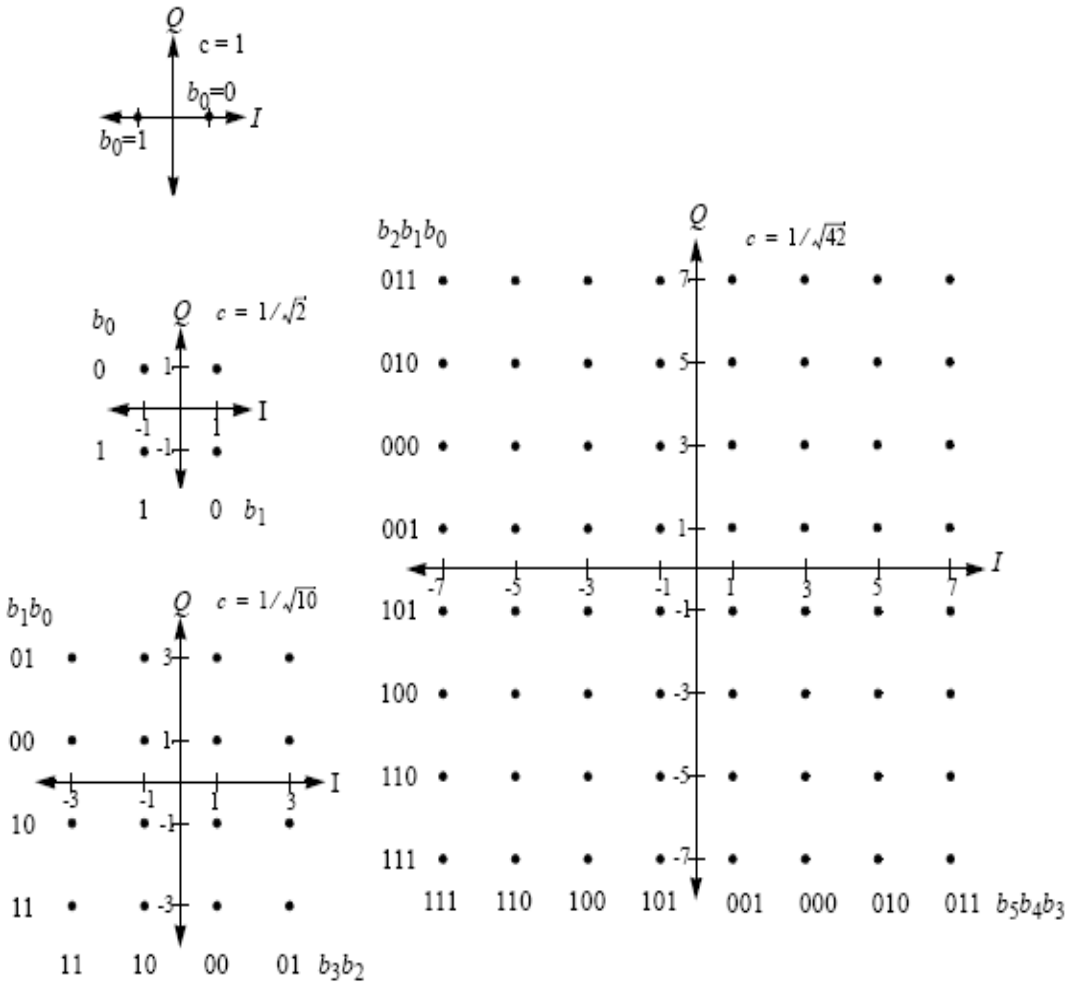

Figure 3.2.6-1 BPSK, QPSK,16-QAM,and 64-QAM constellations

The constellation-mapped data shall be subsequently modulated onto all allocated data subcarriers in order of increasing frequency offset index.The first symbol out of the data constellation mapping shall be modulated onto the allocated subcarrier with the lowest frequency offset index.

3.2.7 Pilot Modulation

Pilot subcarriers shall be inserted into each data burst in order to constitute the symbol and they shall be modulated according to their carrier location within the OFDM symbol. The PRBS generator depicted hereafter shall be used to produce a sequence, w_k .The polynomial for the PRBS generator shall be $X^{11} + X^9 + 1$.

The value of the pilot modulation for OFDM symbol k is derived from w_k. On the downlink ,the index k represents the symbol index relative to the beginning of the downlink subframe. For bursts contained in the STC zone when the FCH-STC is present,index *k* represents the symbol index relative to the beginning of the STC zone. In the DL Subchannelization Zone,the index *k* represents the symbol index relative to the beginning of the burst.On the uplink ,the index k represents the symbol index relative to the beginning of the burst.On both uplink and downlink,the first symbol of the preamble is denoted by k=0.The initialization sequences that shall be used on the downlink and uplink are shown in Figure 3.2-7-1.On the downlink,this shall result in the sequence 11111111111000000000110… where the 3rd 1, i.e.,w_2 =1,shall be used in the first OFDM downlink symbol following the frame preamble.For each pilot (indicated by frequency offset index),the BPSK modulation shall be derived as follows

DL: $c_{-88} = c_{-38} = c_{63} = c_{88} = 1 - 2w_k$ and $c_{-63} = c_{-13} = c_{13} = c_{38} = 1 - 2\overline{w}_k$

UL: $c_{-88} = c_{-38} = c_{13} = c_{38} = c_{63} = c_{88} = 1 - 2w_k$ and $c_{-63} = c_{-13} = 1 - 2\overline{w}_k$

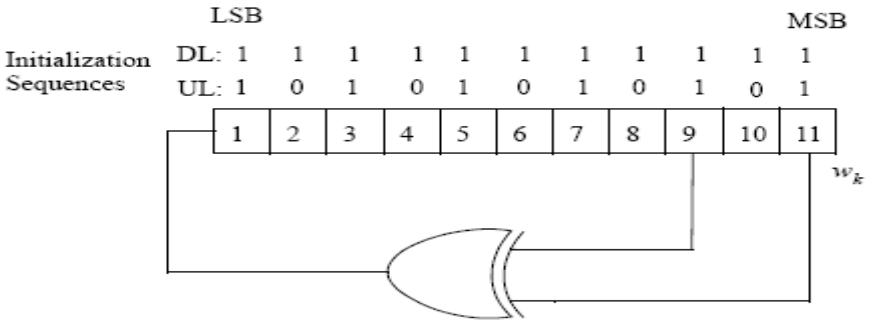

Figure 3.2.7-1 PRBS for pilot modulation

3.2.8 Preamble structure

The first preamble in the downlink PHY PDU,as well as the initial ranging preamble,consists of two consecutive OFDM symbols.The first OFDM symbol uses only subcarriers the indices of which are a multiple of 4.As a result, the time domain waveform of the first symbol consists of four repetitions of 64-sample fragment,preceded by a CP.The second OFDM symbol utilizes only even subcarriers,resulting in time domain structure composed of two repetitions of a 128-sample fragment,preceded by a CP.The time domain structure is exemplified in Figure 3.2-12.This combination of the two OFDM symbols is referred to as the long preamble.

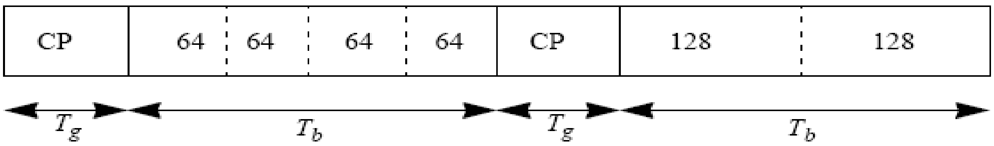

Figure 3.2.8-1 Downlink and network entry preamble structure

The frequency domain sequences for all full-bandwidth preambles are derived from the sequence：

PALL(-100:100) = {1-j, 1-j, -1-j, 1+j, 1-j, 1-j, -1+j, 1-j, 1-j, 1-j, 1+j, -1-j, 1+j, 1+j, -1-j, 1+j, -1-j, -1-j, 1-j, -1+j, 1-j, 1-j, -1-j, 1+j, 1-j, 1-j, -1+j, 1-j, 1-j, 1-j, 1+j, -1-j, 1+j, 1+j, -1-j, 1+j, -1-j, -1-j, 1-j, -1+j, 1-j, 1-j, -1-j, 1+j, 1-j, 1-j, -1+j, 1-j, 1-j, 1-j, 1+j, -1-j, 1+j, 1+j, -1-j, 1+j, -1-j, -1-j, 1-j, -1+j, 1+j, 1+j, 1-j, -1+j, 1+j, 1+j, -1-j, 1+j, 1+j, 1+j, -1+j, 1-j, -1+j, -1+j, 1-j, -1+j, 1-j, 1-j,1+j, -1-j, -1-j, -1-j, -1+j, 1-j, -1-j, -1-j, 1+j, -1-j, -1-j, -1-j, 1-j, -1+j, 1-j, 1-j, -1+j, 1-j, -1+j,-1+j, -1-j, 1+j, 0, -1-j, 1+j, -1+j, -1+j, -1-j, 1+j, 1+j, 1+j, -1-j, 1+j, 1-j, 1-j, 1-j, -1+j, -1+j, -1+j, -1+j, 1-j, -1-j, -1-j, -1+j, 1-j, 1+j, 1+j, -1+j, 1-j, 1-j, 1-j, -1+j, 1-j, -1-j, -1-j, -1-j, 1+j,1+j, 1+j, 1+j, -1-j, -1+j, -1+j, 1+j, -1-j, 1-j, 1-j, 1+j, -1-j, -1-j, -1-j, 1+j, -1-j, -1+j, -1+j, -1+j, 1-j, 1-j, 1-j, 1-j, -1+j, 1+j, 1+j, -1-j, 1+j, -1+j, -1+j, -1-j, 1+j, 1+j, 1+j, -1-j, 1+j, 1-j, 1-j, 1-j, -1+j, -1+j, -1+j, -1+j, 1-j, -1-j, -1-j, 1-j, -1+j, -1-j, -1-j, 1-j, -1+j, -1+j, -1+j, 1-j, -1+j,1+j, 1+j, 1+j, -1-j,

-1-j, -1-j, -1-j, 1+j, 1-j, 1-j}

The frequency domain sequence for the 4 times 64 sequence P_{4x64} is defined by：

$$P_{4\times64}(k)=\begin{cases}\sqrt{2}\cdot\sqrt{2}\cdot conj\left(P_{ALL}(k)\right) & k_{\mathrm{mod}\,4}=0\\ 0 & k_{\mathrm{mod}\,4}\neq 0\end{cases}$$

the factor of $\sqrt{2}$ equates the Root-Mean-Square (RMS) power with that of the data section.The additional factor of $\sqrt{2}$ is related to the 3 dB boost.

The frequency domain sequence for the 2 times 128 sequence P_{EVEN} is defined by：

$$P_{EVEN}(k)=\begin{cases}\sqrt{2}\cdot conj\left(P_{ALL}(k)\right) & k_{\mathrm{mod}\,2}=0\\ 0 & k_{\mathrm{mod}\,2}\neq 0\end{cases}$$

In P_{EVEN} ,the factor of $\sqrt{2}$ is related to the 3 dB boost.

In the uplink,when the entire 16 subchannels are used,the data preamble,as shown in Figure 3.2.8-2 ,consists of one OFDM symbol utilizing only even subcarriers.The time domain waveform consists of two 128 samples preceded by a CP. The subcarrier values shall be set according to the sequence P_{EVEN}. This preamble is referred to as the short preamble. This preamble shall be used as burst preamble on the downlink bursts when indicated in the DL-MAP_IE.

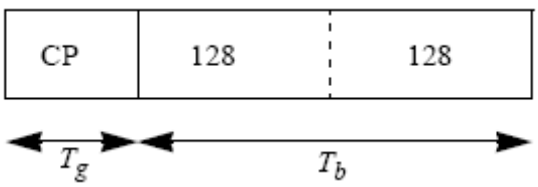

Figure 3.2.8-2 P_{EVEN} time domain structure

3.2.9 Frame Structure

A frame consists of a downlink subframe and an uplink subframe.

(a) Time-Division Duplex(TDD) Frame structure

Figure 3.2.9-1 illustrates an example of OFDM frame structure with TDD.

Downlink

- A downlink subframe consists of only one downlink PHY PDU.
- A downlink PHY PDU starts with a long preamble,which is used for PHY synchronization.
- The FCH burst is one OFDM symbol long and is transmitted using BPSK rate 1/2 with the mandatory coding scheme.
- Each downlink burst consists of an integer number of OFDM symbols,carrying MAC messages,i.e., MAC PDUs.

Uplink

- A uplink subframe consists of contention intervals scheduled for initial ranging and bandwidth request purposes and one or multiple uplink PHY PDUs,each transmitted from a different SS.
- An uplink PHY burst,consists of an integer number of OFDM symbols,carrying MAC messages,i.e., MAC PDUs.

In each TDD frame (see Figure 3.2.9-1),the Tx transition gap(TTG) and Rx transition gap (RTG) shall be inserted between the downlink and uplink subframe and at the end of each frame,respectively,to allow the BS to turn around.

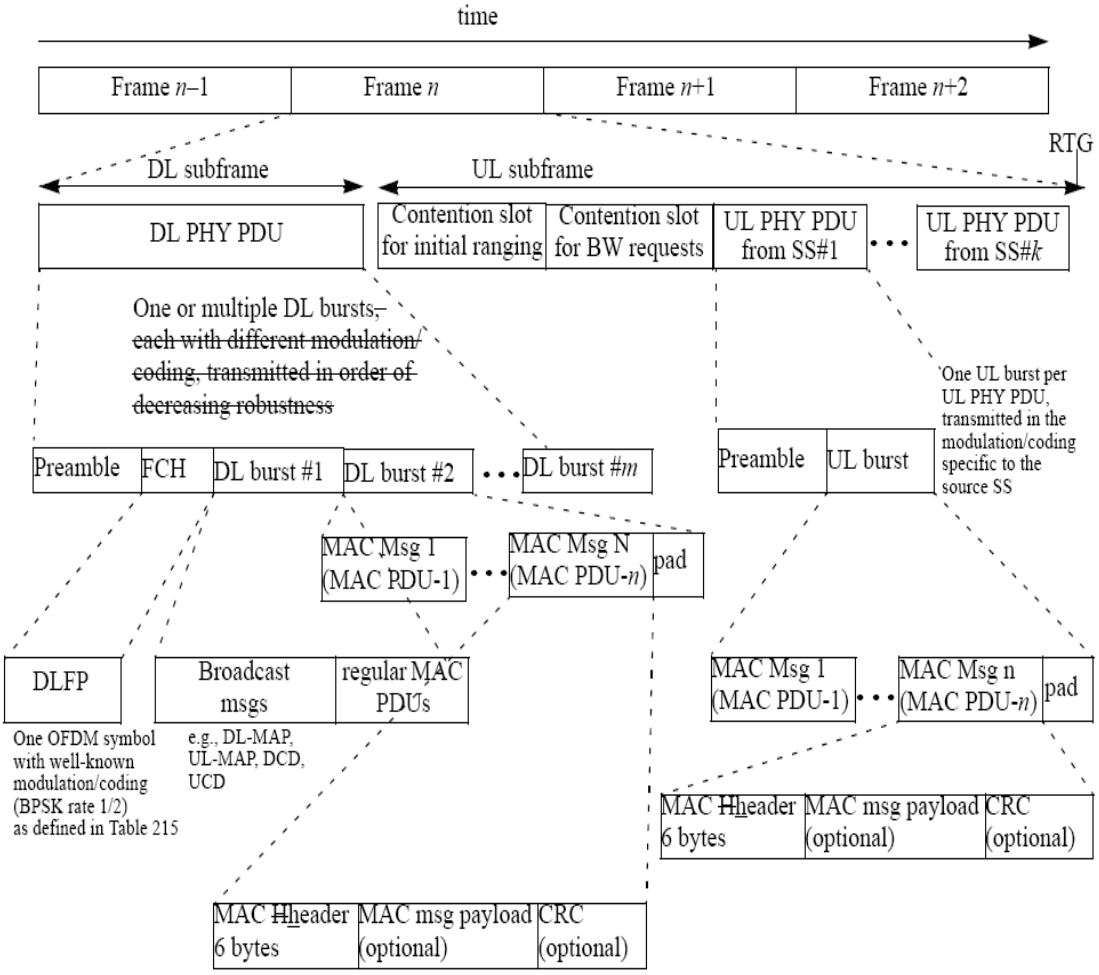

Figure 3.2.9-1 example of OFDM frame structure with TDD

- **Frequency-Division Duplex (FDD) Frame structure**

Basically,the frame structure of FDD is same with the frame structure of TDD.

Figure 3.2.9-2 illustrates downlink and uplink frame structure of an OFDM system.

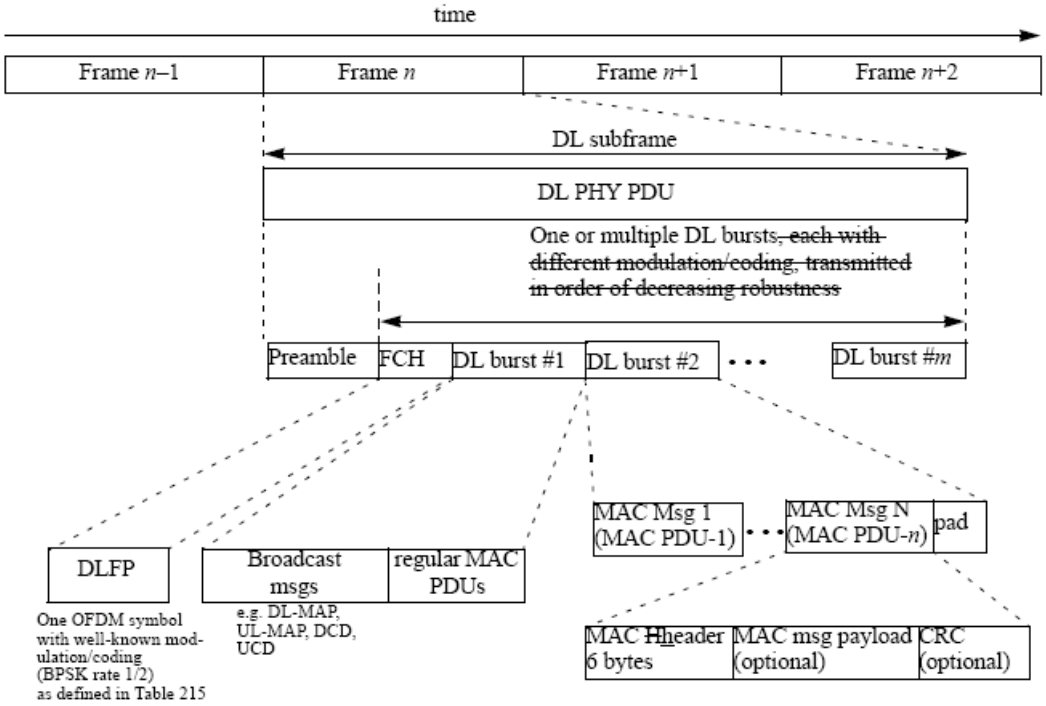

Figure 3.2.9-2 (a) OFDM frame structure with FDD for downlink subframe

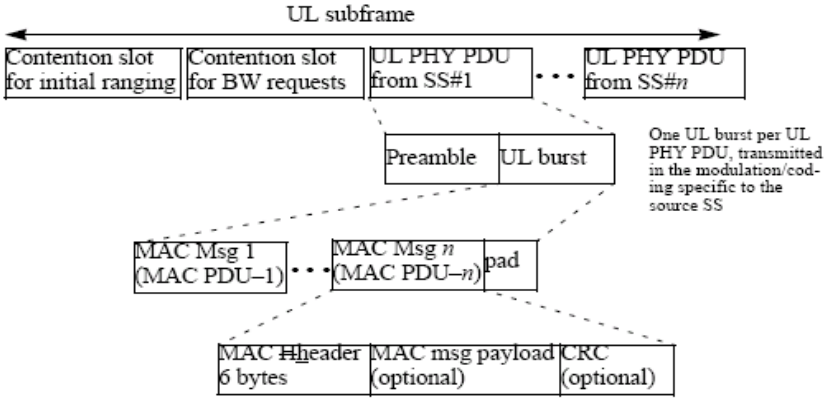

Figure 3.2.9-2 (b) OFDM frame structure with FDD for uplink subframe

3.3 Simulation Parameter

Table 3.3-1 are the simulation parameters used for each simulation in our study (Chapter 4).

Parameter	Value
Used subcarrier(N_{used})	200
IFFT/FFT size (N)	256
CP length(L)	32
Bandwidth(BW)	10MHz(n=57/50)
Sampling Frequency(F_s)	11.392MHz
Useful symbol time(T_b)	22.472 μ sec
CP time(T_g)	2.809 μ sec($G = 1/4$)
OFDM symbol time($T_s = T_b + T_g$)	25.281 μ sec
Modulation	QPSK

Table 3.3-1 Simulation Parameters

3.4 Channel Model

There is not a formal channel model issured for 802.16e.In this thesis we still simulate in SUI channel but make some modifications for Doppler frequency such that it is suitable for mobile channel.

SUI channel is proposed by Stanford University and has 3 terrain types:

(a) Terrain Type A：The maximum path loss category；hilly terrain with moderate-to-heavy tree density.

(b) Terrain Type B：The intermediate path loss category.

(c) Terrain Type C：The minimum path loss category；mostly flat terrain with light tree densities.

Channel Model	Terrain	Delay Spread rms (μ sec)
SUI 1	C	0.111
SUI 2	C	0.202
SUI 3	B	0.264
SUI 4	B	1.257
SUI 5	A	2.842
SUI 6	A	5.240

Table 3.4-1 Terrain type for different SUI channel and with its delay spread

SUI3(10MHz)	Tap power(dB)	Delay samples
Tap1	0	0
Tap2	-5	6
Tap3	-10	12

Table 3.4-2 SUI 3 channel model for BW=10 MHz

SUI2(10MHz)	Tap power(dB)	Delay samples
Tap1	0	0
Tap2	-12	5
Tap3	-15	13

Table 3.4-3 SUI 2 channel model for BW=10 MHz

Table 3.4-1 illustrates the terrain type for different SUI channels ,while Table 3.4-2 illustrates the SUI3 channel for BW=10MHz.

SUI channel model is used for statistic environment,so it is not suit for mobile environment.For NLOS (Non-Line-Of -Sight) transmission,the operating frequency band is between 2~11GHZ.

If relative velocity between transmitter and receiver is v=120 km/hr,we can calculate the Doppler frequency under different operating frequency band.

For example：

f_c ：the carrier frequency 2 GHz

c ：velocity of light(3×10^8 m/s)

α ：the angle between propagation path and direction of vehicle which is plotting in Figure 3.4-1

the definition of Doppler frequency(f_d) is

$$f_d = \frac{v \cdot f_c}{c}\cos(\alpha)$$
$$= \frac{100}{3}\cdot\frac{2\cdot10^9}{3\cdot10^8}\cos(\alpha)$$
$$=222.22\cdot\cos(\alpha) \text{ Hz}$$

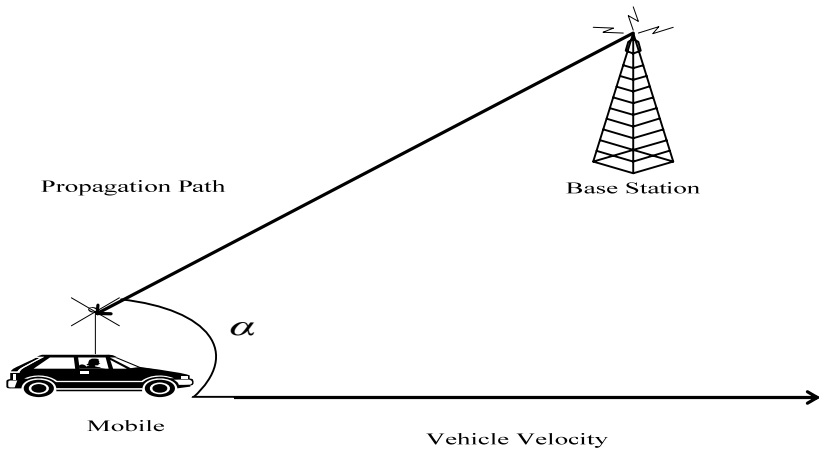

Figure 3.4-1 the angle between propagation path and direction of vehicle

Hence,for the worst case that is $\alpha = 0$,then f_d =222.22Hz.

Next we substitute the Doppler frequency from the each path of original SUI3 or SUI2 channel model for simulation under mobile channel condition.

Chapter 4 Frame Synchronization

In the transmitter,QAM signals are converted into parallel and fed to each port of IFFT.To add the CP within guard interval in front of an OFDM symbol,the copy of latter part of OFDM symbol is added to the symbol as a prefix and converted into serial form for transmission.In the receiving end,received OFDM signal is converted into parallel form and fed to FFT.Since signal is transmitted over a multipath fading channel,the received signal is distorted by multipath delayed signals.A guard interval is often used to reduce the effect of multipath delay spread ,so that the received signal is distorted by the preceding symbol only within the guard interval.To demodulate the OFDM symbol correctly,the ideal frame timing is at the end of the guard interval; otherwise,it should be started at the timing that the signal is not disturbed by the preceding symbol.Figure 4 illustrates process of frame synchronization .Our goal is to estimate the start timing of a frame by timing estimator for a frame.

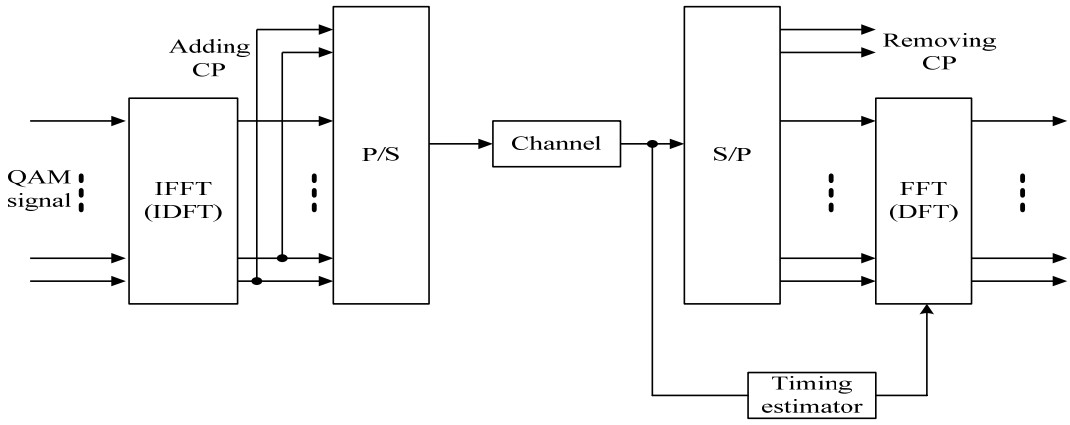

Figure 4　OFDM system with timing synchronization

4.1 Overview of Schmidl & Cox Frame Synchronization Scheme[4]

The downlink preamble structure specified in 802.16e is shown in Figure 4.1-1 which consists of two parts,referred as short preamble and long preamble.The short preamble consists of four repeated 64-sample blocks,and the long preamble consists of two repeated 128-sample blocks.In order to avoid inter symbol interference (ISI), cyclic prefix (CP) is added ,respectively ,in front of short preamble and long preamble.

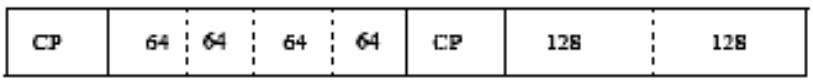

Figure 4.1-1 The downlink preamble structure specified in 802.16e

One of the famous estimation methods that exploit the characteristic of preamble for frame synchronization was proposed by Schmidl & Cox[4].This is mainly used to estimate the start position of training symbol by using the two repeated 128-sample blocks.In [4], a timing metric $M(k)$ is defined as (4.1-3).

$$P(k)=\sum_{m=0}^{D-1} r^{*}(k+m)\,r(k+m+D) \qquad (4.1\text{-}1)$$

$$R(k)=\sum_{m=0}^{D-1} \left|r(k+m+D)\right|^{2} \qquad (4.1\text{-}2)$$

$$M(k)=\frac{|P(k)|^2}{(R(k))^2} \qquad (4.1\text{-}3)$$

where k is a time index

$r(k)$ is the received signal at k-th sample in time domain

D is the length of the half long preamble ,*D=128*

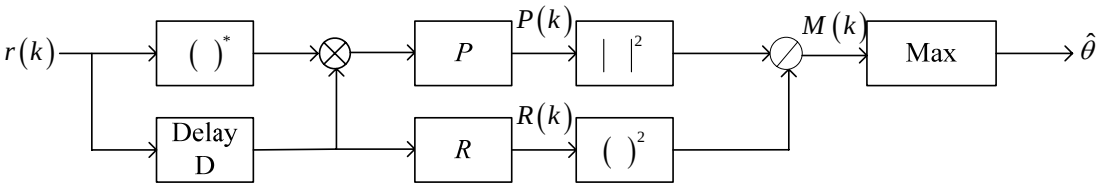

Figure 4.1-2 Block diagram of estimator by [4]

From (4.1-1),we can imagine that a sliding window of $2D$ samples slides along the received signals in time .This window slides as the estimator looks for the start position of the first 128-sample block, as shown in Figure 4.1-3.

Eq.(4.1-2) defines the received energy of the second 128-sample block.

Both (4.1-1) and (4.1-2) can be implemented with the iterative formula such as

$$P(k+1)=P(k)+\left[r^*(k+D)r(k+2\cdot D)\right]-\left[r^*(k)r(k+D)\right] \qquad (4.1\text{-}4)$$

$$R(k+1)=R(k)+\left|r(k+2\cdot D)\right|^2-\left|r(k+D)\right|^2 \qquad (4.1\text{-}5)$$

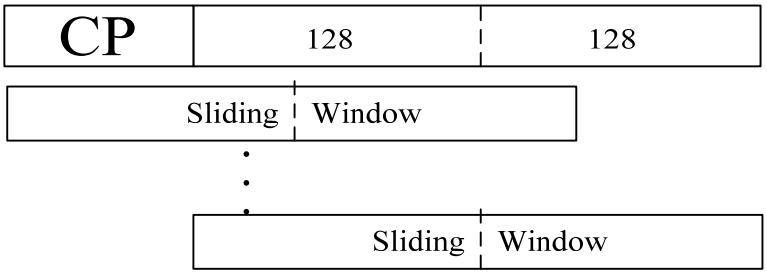

Figure 4.1-3 A sliding window slides to the different position in time domain for searching the first 128-sample block

Noting that, a short preamble can also be regarded as a preamble with two identical halves in time domain.The transmitted long preamble signal is received as a consecutive sequence and calculated by (4.1-1) & (4.1-2).From Figure 4.1-3,if channel is non-time-dispersive,then CP is not damaged.Thus,when the first point of the sliding window is within the interval of CP,then the first half of sliding window is identical to the second half, until the first point of the sliding window is outside the interval of CP.

Hence,this gives the result that the timing metric will reach to a plateau which starts at the first point of CP and ends at the last point of CP.This plateau has a length equal to the length of guard interval in AWGN channel,as shown in the Figure 4.1-4 when SNR is very high,i.e. the noise term is neglected.

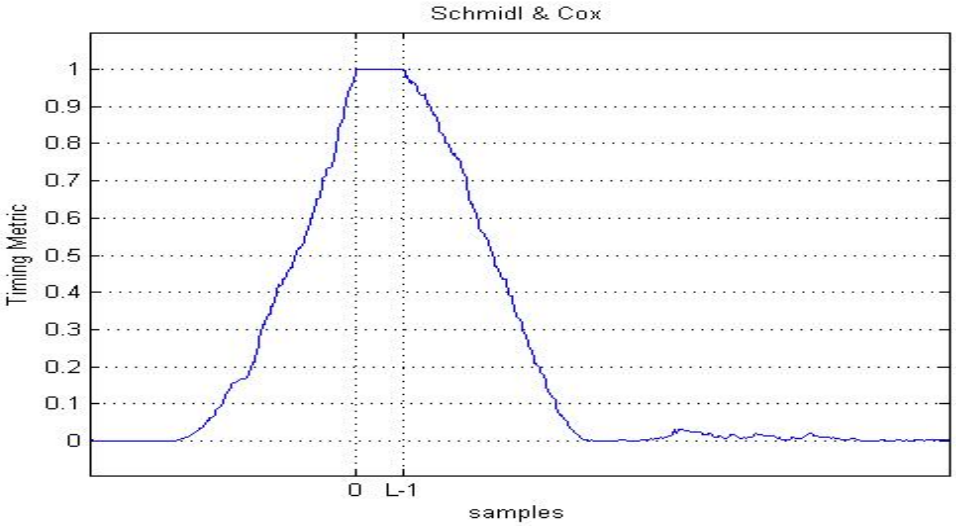

Figure 4.1-4 The timing metric has the length of plateau is L

If there is ISI effect which distorts OFDM signal in the front part of guard interval,then the plateau length is equal to the length of guard interval minus the length of the channel impulse response.Because we take the undistorted signal $r(k)$ within guard interval to calculate the correlation with the delay signal $r(k+D)$ over a summation range with its size equal to D ,the result of $P(k)$ is a large value,until $r(k)$ is outside of guard interval and not all of $r(k)$ is equal to $r(k+D)$ in the sliding window.The way to extract the estimated position proposed by [4] is to find the maximum values of timing metric.

The appearance of plateau leads some uncertainty when we want to confirm the accurate FFT window .The extracted timing gives larger mean and variance for performance even when the average of two 90% are taken.

In the following simulations ,for the simulation frame structure ,there is no

transition gap in time between two transmitted frames and the first symbol of a frame is the long preamble.

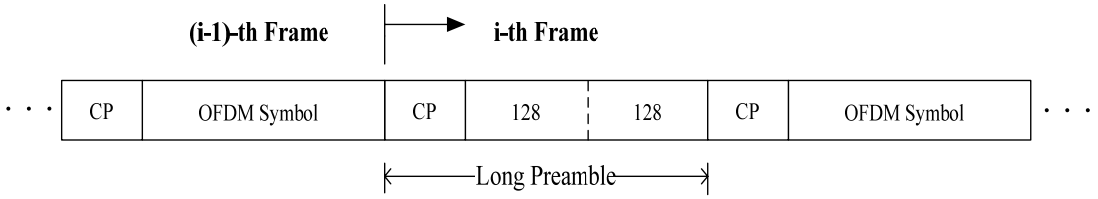

Figure 4.1-5 The simulation frame structure

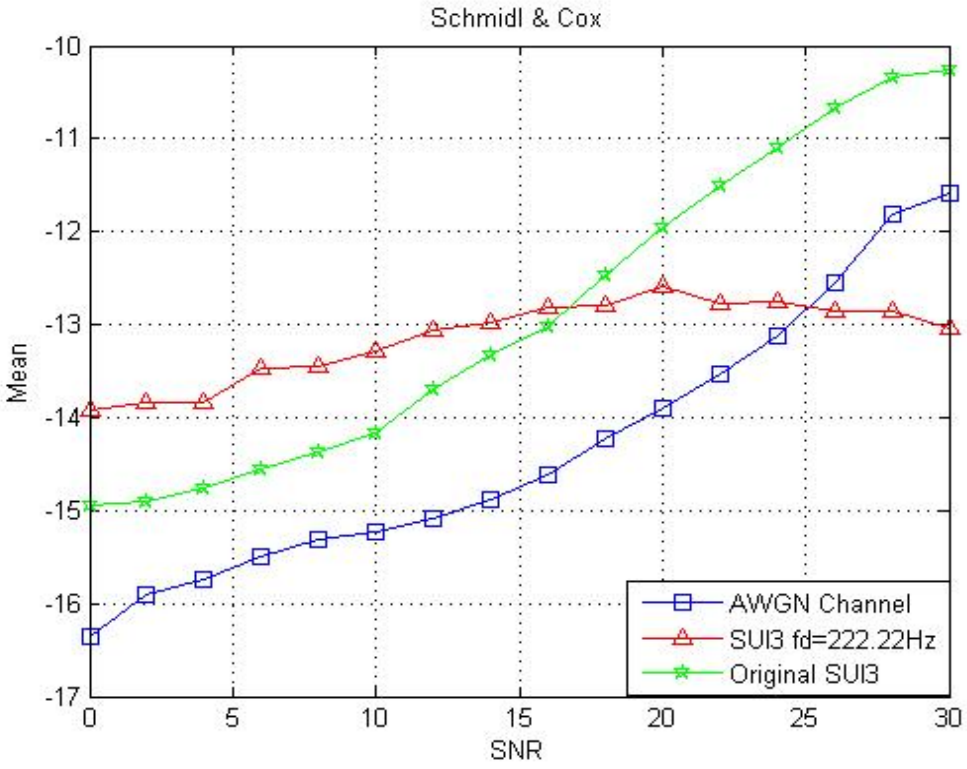

Figure 4.1-6 Mean values in different channel condition

In Figure 4.1-5,mean is defined as ：

$$Mean = \frac{\sum_i \left(\hat{\theta}_i - \theta_i \right)}{\mathrm{N_F}}$$

where θ_i ：the real start position at i-th frame

$\hat{\theta}_i$ ：the estimated position by [4] at i-th frame

$\mathrm{N_F}$ ：the total numbers of frames

If mean is a negative number, it indicates that the estimated start position is too early extracted.For a perfect estimation,we prefer the mean value approximately equal to zero or approximates to a tolerance error in estimation.A tolerance error is that we would like the mean to be negative and the absolute value of mean not to exceed the length of guard interval minus the length of channel impulse response.The mean value in Figure 4.1-5 indicates that although the method of [4] can avoid the ISI effect,it is still not very precise.

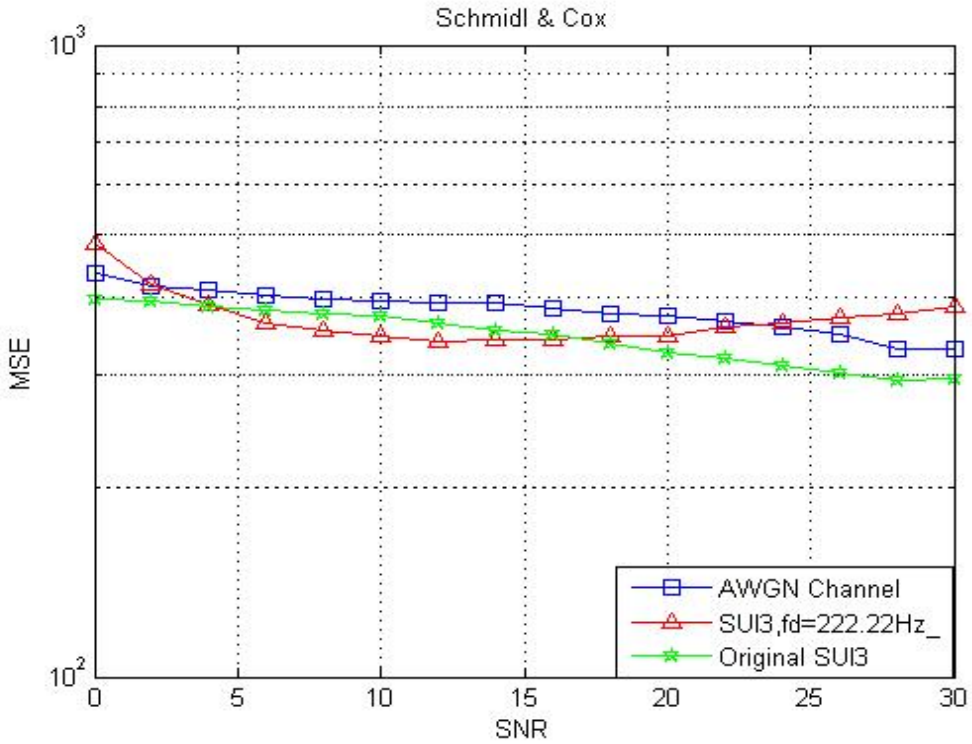

Figure 4.1-7 MSE values in different channel condition

In Figure 4.1-6,MSE(Mean Square Error) is defined as

$$MSE = \frac{\sum_i \left(\hat{\theta}_i - \theta_i\right)^2}{\mathrm{N_F}}$$

where θ_i ：the real start position at i-th frame

$\hat{\theta}_i$ ：the estimated position by [4] at i-th frame

$\mathrm{N_F}$ ：the total numbers of frames

The MSE is still quite large indicates that this is not a precise estimation,but this method still can work at very low signal-to-noise ratio (SNR).

In our proposed method ,the definition of Mean and MSE are the same.

4.2 Proposed Method for Frame Synchronization

Now we consider the transmitted signals as a consecutive sequence as depicted in Figure 4.2-1 (a).Because of the property of multipath fading channel, the received signal $r(k)$ is given by

$$r(k)=\sum_{m=0}^{M} x(k-m)h(k,m)+n(k) \quad k=0,1,\cdots,N+L-1 \qquad (4.2\text{-}1)$$

where $x(k)$ is the complex lowpass representation of the transmitted OFDM signal, $n(k)$ is the zero mean Gaussian noise, $h(k,m)$ is the Rayleigh fading process for the different path with index m corresponding to the delayed transmitted signal $x(k-m)$ as illustrated in Figure 4.2-1 (b).

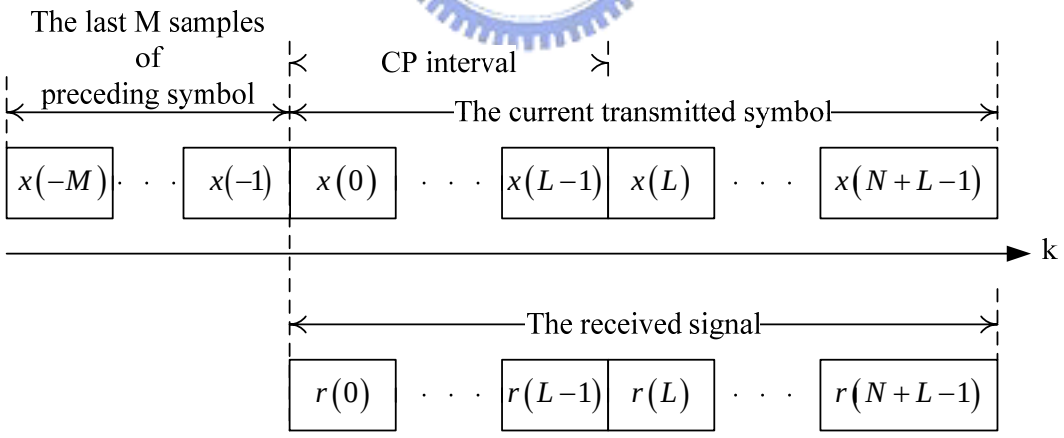

Figure 4.2-1 (a) The relation between transmitted sequence over M+1 path channel and received signal

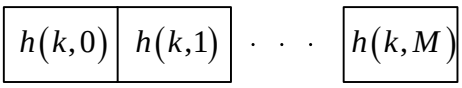

(b) The multipath fading channel impulse reponse

We assume that the maximum delay spread does not exceed the guard interval,i.e. $M \le L$.

We spread out the summation in (4.2-1),the received signal without noise term is given as

$$r(k) = x(k)h(k,0) + x(k-1)h(k,1) + \cdots + x(k-M)h(k,M) \quad (4.2\text{-}2)$$

where $k = 0,1,\cdots, N+L-1$

If the channel is ideal, $r(k)$ should be equal to $x(k)$.But in multipath fading channel, $x(k)$ is influenced by the fading effect and corrupted by the last M fading delay signals.Thus,there are M samples within CP corrupted by the preceding OFDM symbol , called ISI , as shown in Figure 4.2-2.

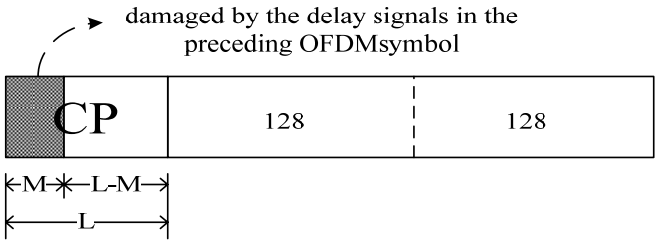

Figure 4.2-2 M samples within CP are damaged by the preceding OFDM symbol

Next ,we define $u(k)$ as $u(k) = r(k) - r(k+D)$

where $r(k+D)$ is a delayed version of $r(k)$.

$$
\begin{aligned}
&u(k) \\
&= r(k) - r(k+D) \\
&= \sum_{m=0}^{M} \left(x(k-m)h(k,m) - x(k+D-m)h(k+D,m) \right) + n(k) - n(k+D)
\end{aligned}
\tag{4.2-3}
$$

According to the structure of long preamble consisting of two repeat sample blocks and CP, we obtain

$$x(k) = x(k+D) \quad k = 0, \cdots, L+D-1 \tag{4.2-4}$$

For one delay path with index m in (4.2-3),if $m \le k \le L+D-1+m$,then

$$x(k-m) = x(k+D-m). \tag{4.2-5}$$

If we take account of all paths with different index m ,while $M \le k \le L+D-1$,then

$$x(k-m) = x(k+D-m) \tag{4.2-6}$$

Now (4.2-3) becomes

$$
\begin{aligned}
&u(k) = r(k) - r(k+D) \\
&= \begin{cases}
\sum_{m=0}^{M} \left(x(k-m)h(k,m) - x(k+D-m)h(k+D,m) \right) + n_{sub}(k) & \textit{elsewhere} \\
\sum_{m=0}^{M} x(k-m)\left(h(k,m) - h(k+N,m) \right) + n_{sub}(k) & M \le k \le L+D-1
\end{cases}
\end{aligned}
$$

where $n_{sub}(k) = n(k) - n(k+N)$ (4.2-7)

In (4.2-7),when the maximum Doppler frequency is assumed to be small compared with the symbol rate,i.e. the channel is slow fading,the value of $h(k,m) - h(k+D,m)$ can be approximated as zero. Furthermore,when

signal-to-noise power ratio (SNR) is high,the average value of $n_{sub}(k)$ is approximated as zero in average. Therefore, the difference between $r(k)$ and $r(k+D)$ is approximated as zero within the interval $M \le k \le L+D-1$.

From the above description,we define a new timing metric

$$\begin{aligned} M_{diff}(k) &= -\sum_{i=k-L'+1}^{k} \left|u(i)\right|^2 \\ &= -\sum_{i=k-L'+1}^{k} \left|r(i)-r(i+D)\right|^2 \end{aligned} \qquad (4.2\text{-}8)$$

where $D \le L' \le L+D-M$ and

L' is the length of summation window in (4.2-8).

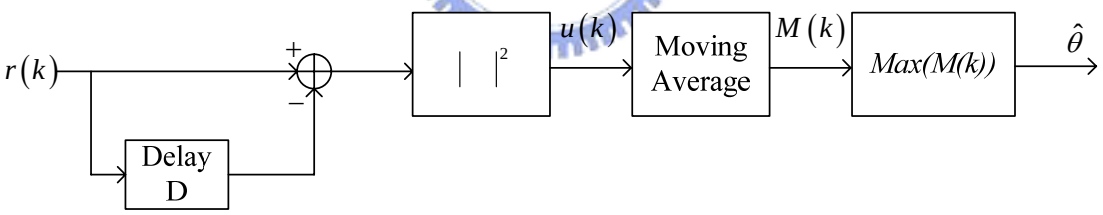

Figure 4.2-3 proposed timing estimator

If $r(k)$ is not similar to $r(k+D)$,then $\left|r(k)-r(k+D)\right|^2$ is a large positive number. Therefore,the result of (4.2-8) is a small negative value if all components of $r(k)$ in the summation window is not similar to $r(k+D)$.Otherwise ,if $r(k)$ is similar to $r(k+D)$ for all components in the summation window,the result of (4.2-8) gives a maximum value and very close to zero.The maximum value will locate at the

boundary of two repeated sample blocks as plotted in Figure 4.2-4.

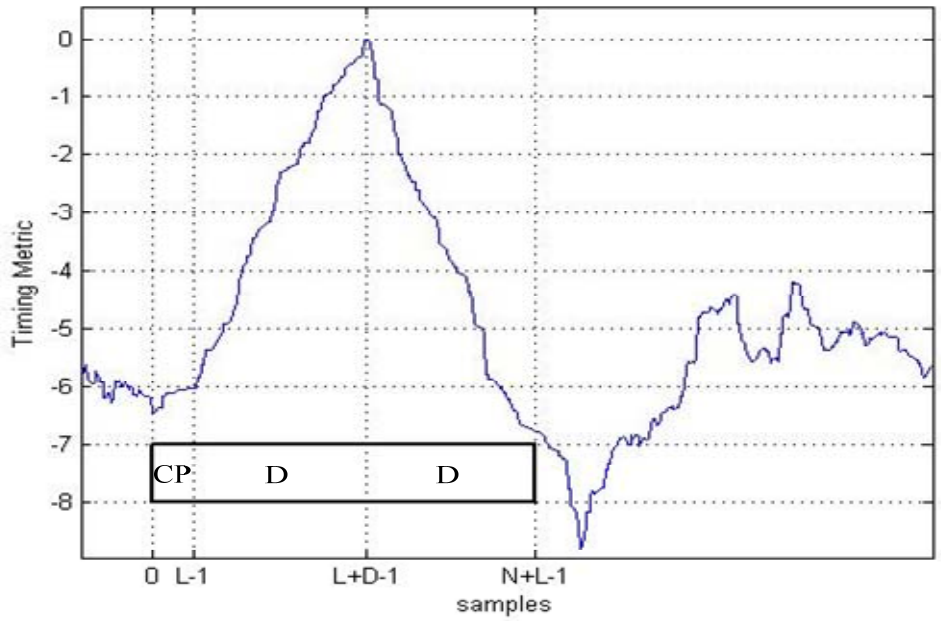

Figure 4.2-4 timing metric of perfect channel without noise term, $M=0$, $L'=L+D$ and normalized by L'

For the case $M\neq 0$,i.e.under multipath fading,we select the summation size L' such that $L'\leq L+D-M$. Figure 4.3-5 illustrates that in the interval $L+D-d\leq k\leq L+D-1$,the timing metric will reach a plateau near the boundary of two repeated sample blocks.Since, within the summation window of (4.2-8) with summation window length L',all the elements $r(k)$ are similar to $r(k+D)$,until index k is outside the boundary $L+D-1, r(k)$ is not similar to $r(k+D)$,and the timing metric decreases from the plateau as shown in Figure 4.2-6. According to Figure 4.3-5,the length of plateau is $d=L+D-M-L'+1$.

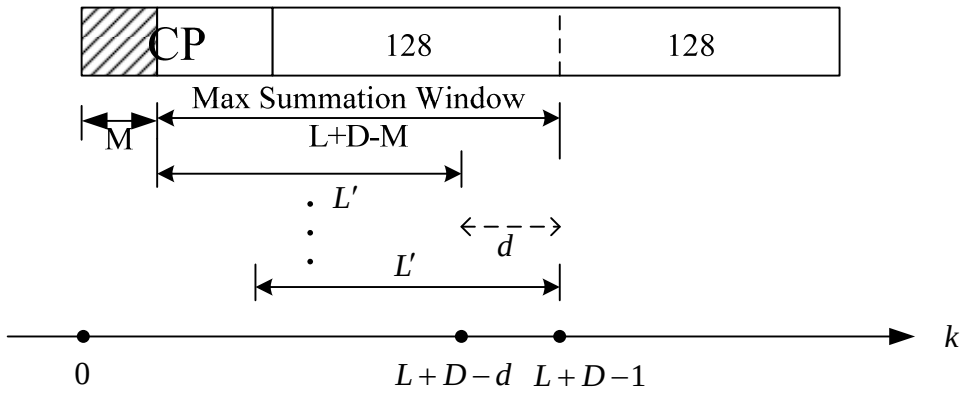

Figure 4.2-5 $r(k)-r(k+D)$ approximates to zero within summation window of (4.2-8) ,with summation window length L'

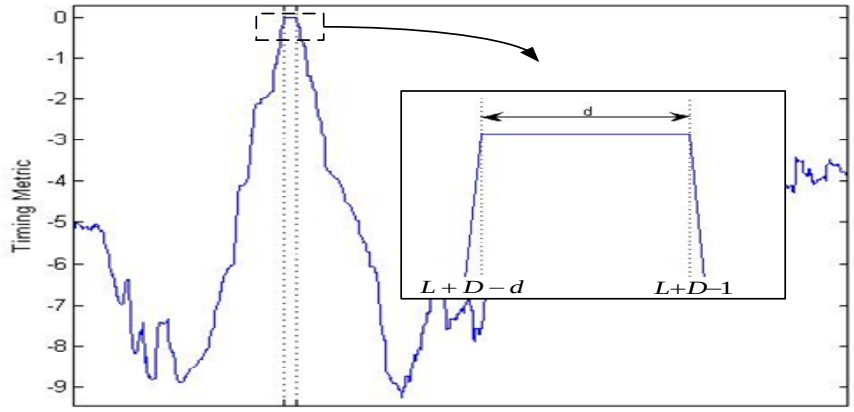

Figure 4.2-6 timing metric reach a plateau in the interval $L'-1 \le k \le L+D-1$ (M=0)

Now we consider the condition that the signal is transmitted over a multipath fading channel,like the case in the Figure 4.2-2 which has ISI terms within the guard interval.In order to avoid the ISI effect, L' should be chosen smaller than $L+D-M$ and longer than D. This is because we would like to avoid exploiting the signal which is disturbed by the delayed signals and to calculate the summation of amplitude difference over L' samples. As L' is getting smaller than $L+D-M$,

not only the plateau becomes wider (d gets larger),but also the maximum peak value is estimated earlier,i.e. the first point of DFT window is more likely located at the initial transition edge of the channel impulse response,as shown in Figure 4.3-6(a).Since this plateau has the same effect compared with the plateau in previous section, that will make some uncertainty in extracting the estimated start position of a frame such that there may be larger MSE or mean value,but much less influence caused by ISI effect, as shown in Figure 4.2-6(a)&(b).Hence, choosing L' properly will reduce the uncertainty in extracting the estimated start position.

4.3 Simulation and Performance Evaluation

In the following simulations ,there is no transition gap in time between two transmitted frames and the first symbol of a frame is the long preamble.

4.3.1 AWGN Channel

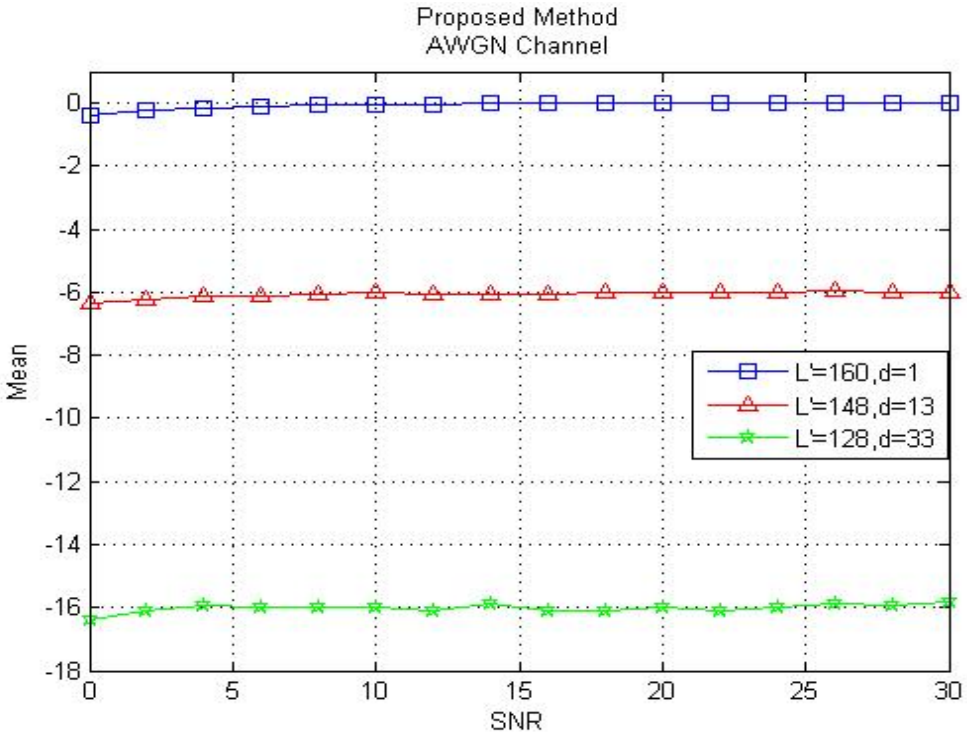

Figure 4.3.1-1(a) Mean in AWGN channel for the case($L'=160, d=1$)、($L'=148, d=13$)、($L'=128, d=33$)

In Figure 4.3.1-1 (a),for the AWGN channel,there is no ISI term.Thus we can imagine that the boundary of channel impulse response locates at the prior sample of the first point of CP. While L' is getting smaller,the first point of DFT window is more likely locating at the boundary of channel impulse response.

It can be seen that,for the two cases ($L'=148, d=13$) & ($L'=128, d=33$),with

d the length of plateau, the result of mean value will locate at the middle position of plateau which are at the position -6 and -16 for each SNR,respectively.

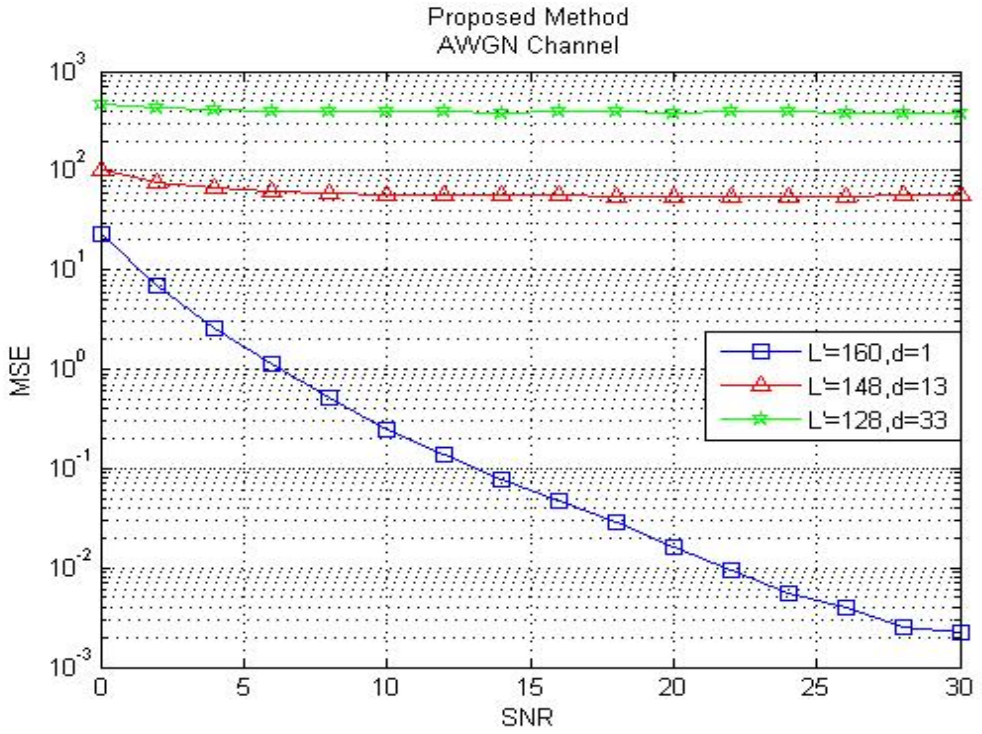

Figure 4.3.1-1 (b) MSE in AWGN channel for the case($L'=160, d=1$)、($L'=148, d=13$)、($L'=128, d=33$)

In Figure 4.3.1-1(b),for the case ($L'=160, d=1$),the plateau is narrower as a point,hence the case($L'=160, d=1$) has little uncertainty for estimating the start position.

4.3.2 Mobile SUI3 Channel Environment

Here,we just show several representative cases of mobile channel in Figure 4.3.2-1 (a),(b).

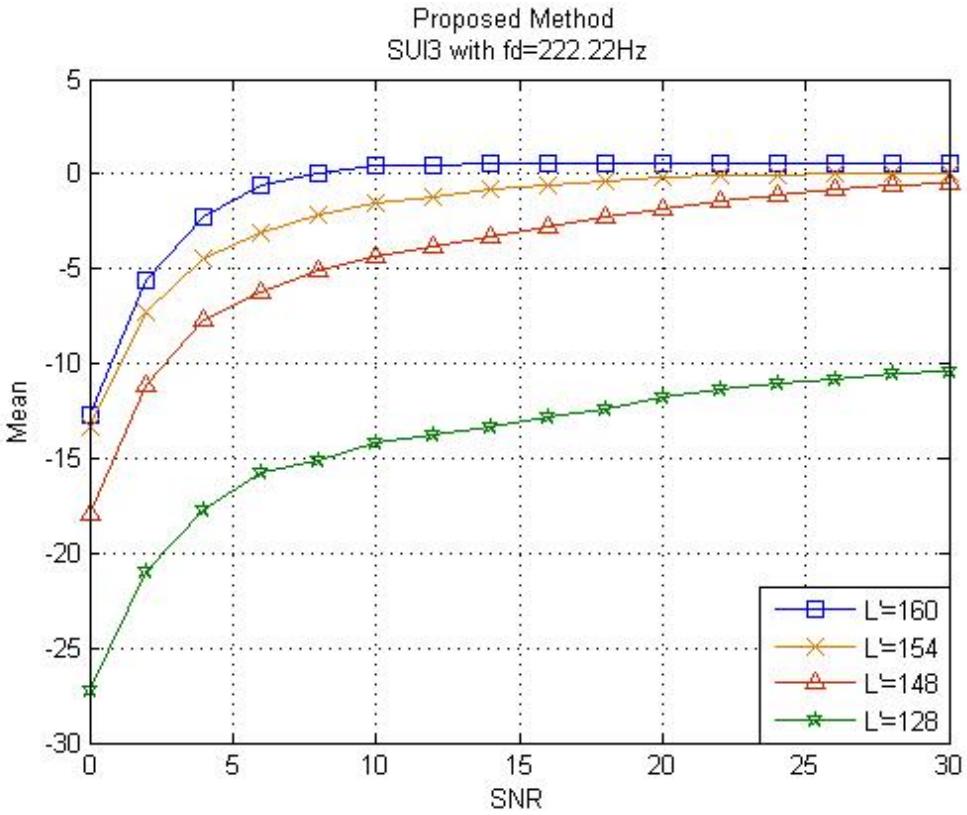

Figure 4.3.2-1 (a) Mean in SUI3 channel with $f_d = 222.22Hz$ for the case $(L' = 160, d = 1)$、$(L' = 154, d = 1)$、$(L' = 148, d = 1)$、$(L' = 128, d = 21)$

For a mobile SUI3 channel,the length of channel impulse response M is 12 as illustrated in Table 3.4-2. According to the above discussion, L' should be chosen under the limit $D \le L' \le L + D - M$ $(128 \le L' \le 148)$. In Figure 4.3.2-1 (a),the mean value of the estimation in case with $L' = 160, d = 1$ is a positive number when SNR becomes larger than 10 dB. But the mean value of the estimation in case with

$L'=148, d=1$ is always a negative number and is closer to zero while SNR becomes larger.

It can be seen that case with $L'=154, d=1$, has a better performance since the mean value is closer to zero than the case with $L'=148, d=1$ and always a negative value while SNR bellow 22 dB.For the case, $L'=154, d=1$,the corresponding channel length *M* is 6.

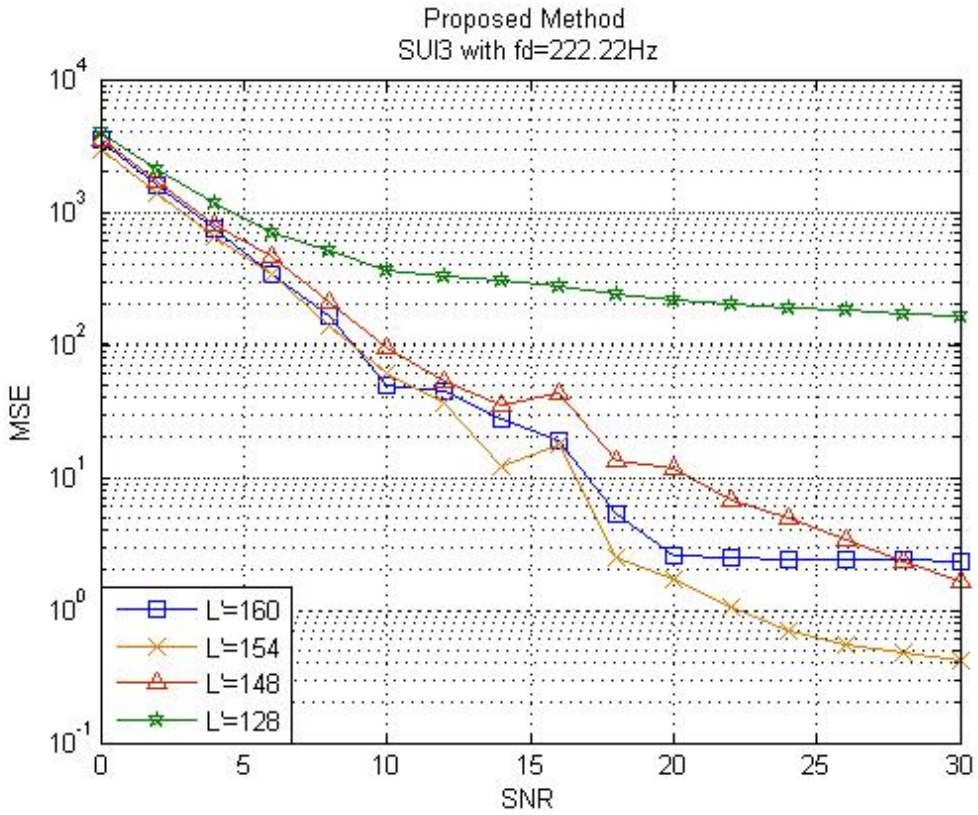

Figure 4.3.2-1 (b) MSE in SUI3 channel with $f_d = 222.22Hz$ for the case $(L'=160, d=1),(L'=154, d=1),(L'=148, d=1)\&(L'=128, d=21)$

Theoretically, the proposed method should has the best performance for the case $L'=148, d=1$, in SUI3 channel model where *M*=12.But the case $L'=154, d=1$, which corresponds to the channel length *M*=6 has the best performance compared with the other cases and also has the smallest MSE for all of possible values of L' from the simulation results.This is because SUI3 channel has 3 main paths ,and the tap power of the last path (which has the longest delay spread) is too small that the proposed method for the case, $L'=148, d=1$ can not distinguish,until SNR is high enough and start to has a better performance than the case , $L'=160, d=1$.

4.3.3 Static SUI3 Channel

Figure 4.3.3-1 (a) & (b) are the simulation results under static SUI3 channel model.When SNR is lower than 10 dB,the performance is similar as the performance in AWGN channel.In other words,if SNR is higher than 10 dB and then the advantage of the proposed method start appear.

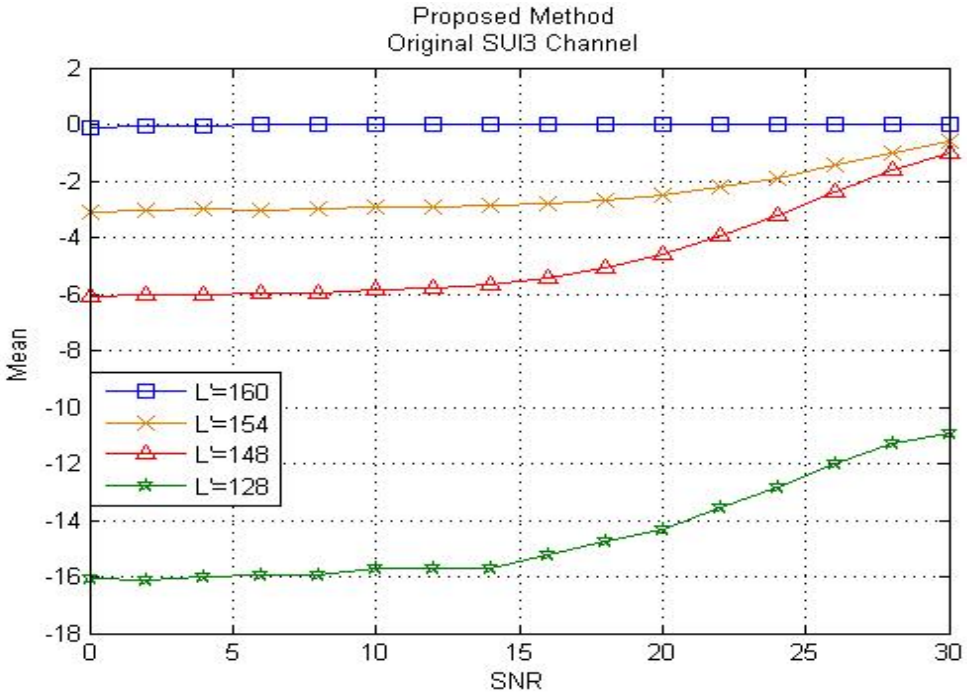

Figure 4.3.3-1 (a) Mean in static SUI3 channel for the case $(L'=160, d=1),(L'=154, d=1),(L'=148, d=1)\&(L'=128, d=21)$

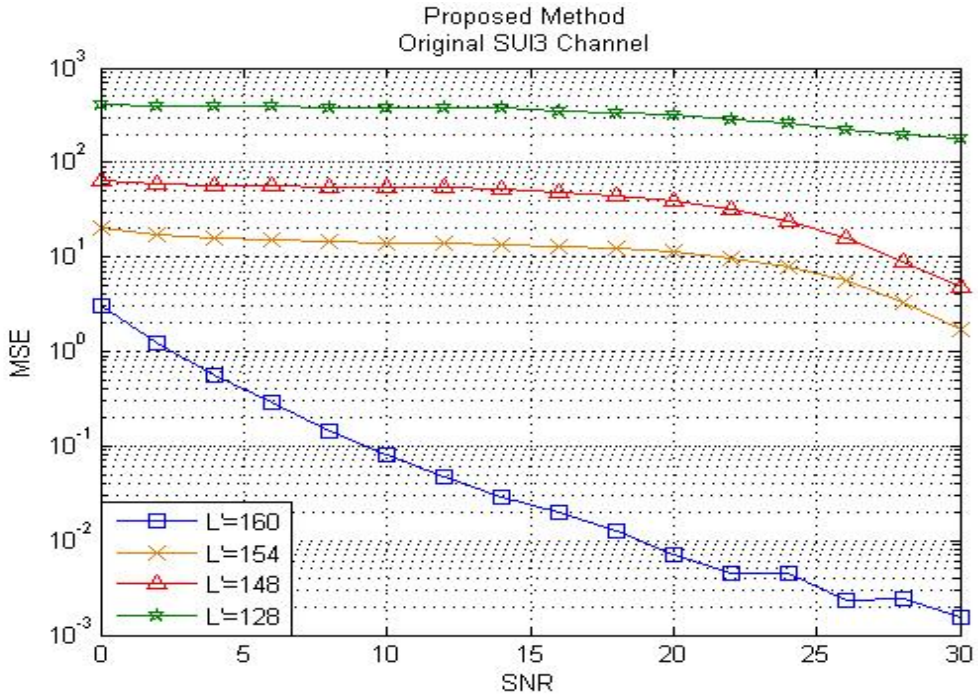

Figure 4.3.3-1 (b) MSE in static SUI3 channel for the case $(L'=160, d=1),(L'=154, d=1),(L'=148, d=1)\&(L'=128, d=21)$

4.4 Comparison

Figure 4.4-1 (a)&(b), Figure 4.4-2 (a)&(b), Figure 4.4-3(a)&(b) are the performance comparison between the method of Schmidl & Cox [4] and proposed method in different channel.When SNR is high,our proposed method is always better than that of Schmidl & Cox for choosing L' properly.

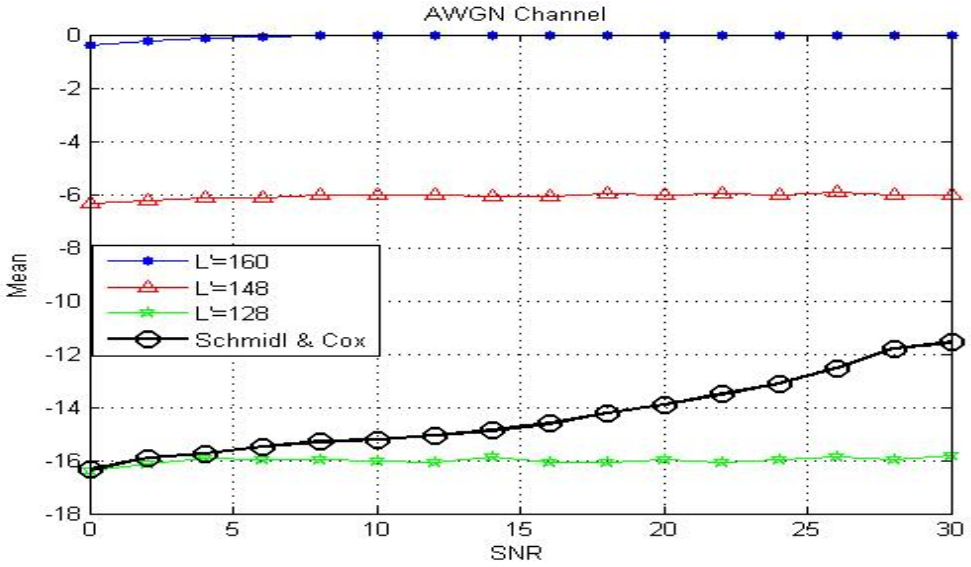

Figure 4.4-1(a) Mean comparison in AWGN channel

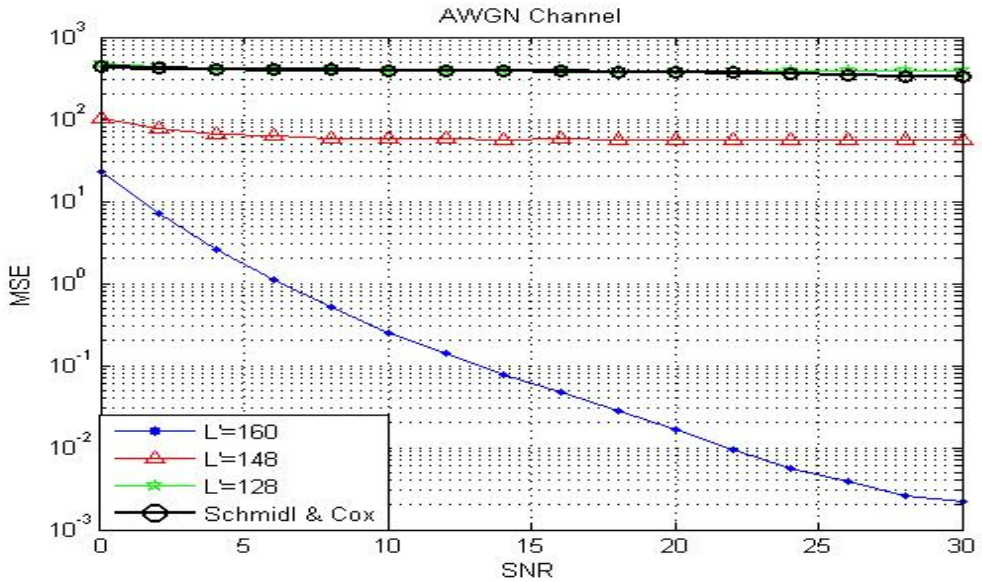

Figure 4.4-1(a) MSE comparison in AWGN channel

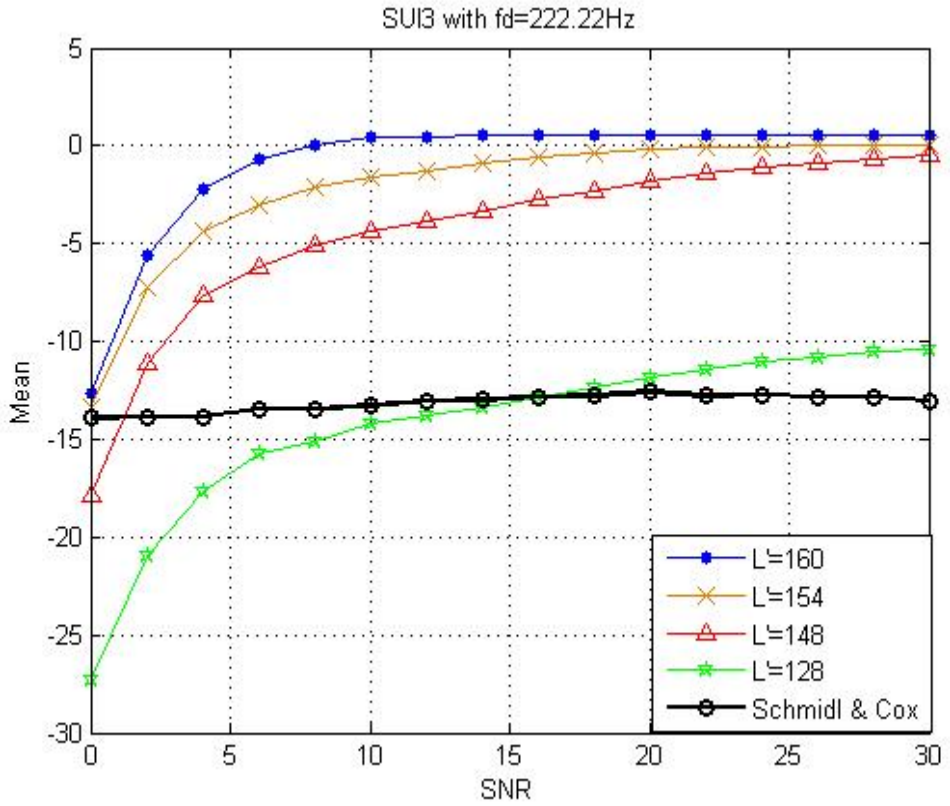

Figure 4.4-2(a) Mean comparison in mobile SUI3 with f_d=222.22Hz

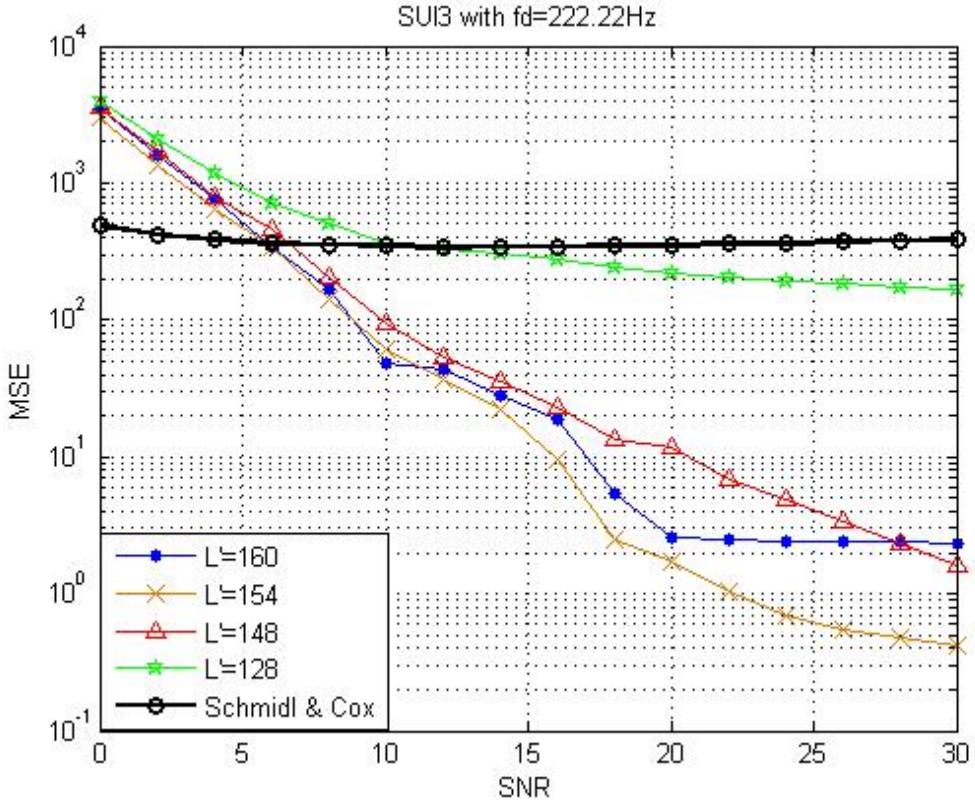

Figure 4.4-2(b) MSE comparison in mobile SUI3 with f_d=222.22Hz

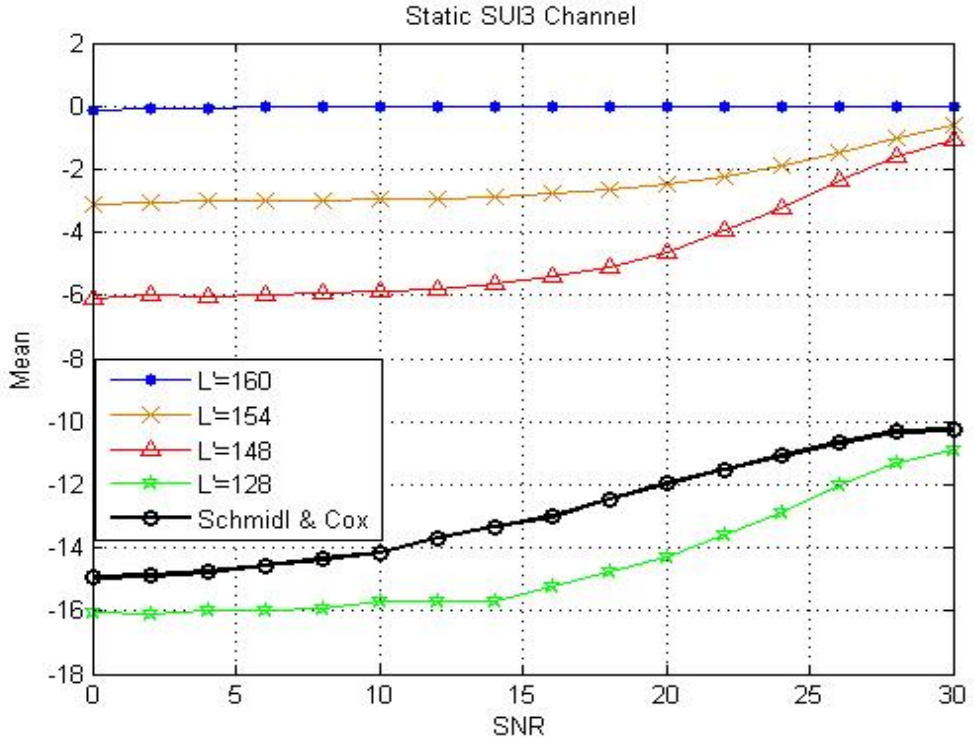

Figure 4.4-3 (a) Mean comparison in static SUI3 Channel

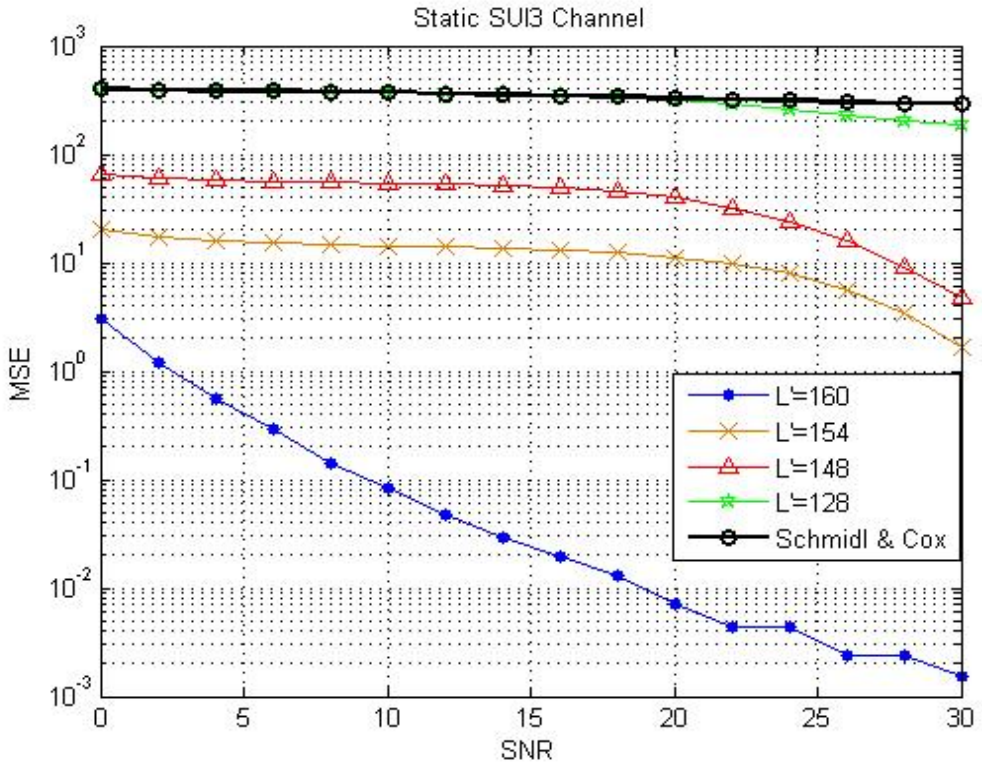

Figure 4.4-3 (b) MSE comparison in static SUI3 Channel

Considering the complexity in implementation ,respectively ,the estimator in Schmidl & Cox method needs a multiplication operator ,a complex square Operator,a square operator and a division operator,but the estimator of our proposed method only needs an addition operator and a complex square operator.Thus the complexity of proposed method is much less than that of Schmidl & Cox method.Thus the proposed Method is better than [4] whatever in terms of both performance and complexity.

In the following,we will discuss how to properly choose L' for the proposed method so that it can always work well in different environment.

For AWGN channel and there ISI terms among the CP, L' to be chosen to be 160 has for the best performance,because timing metric has no uncertainty caused by the plateau.

For Mobile SUI 3 with f_d=222.22Hz, L' is chosen to be 154 for the best performance.The corresponding length of the channel response M is 6.However the real length of channel impulse response M is 12,so we chose L' equal to 160. In this case ,the performance is compatible to that of L'=154.

For static SUI 3,when SNR is low,the simulation result is similar to that in AWGN channel.However, if SNR is high enough,the advantage of the proposed method starts to appear. If L' is chosen to be 160 , the performance is still compatible to the case

with L' =154.

In the next sub-section 4.4.1 & 4.4.2,the following simulations show the performance comparison between the method of Schmidl & Cox [4] and proposed method in downlink and uplink mode ,respectively. In downlink or uplink mode, simulations also show the performance when received side under the condition that has velocities, which are 120 km/hr ,60 km/hr and 30 km/hr ,respectively .The different velocities,120 km/hr ,60 km/hr and 30 km/hr correspond to Doppler frequencies which are 222.22Hz,111.11Hz and 55.55Hz ,respectively. In additional to the channel model SUI-3,we introduce the channel model SUI-2 in the next subsection.

4.4.1 Preamble Structure in Downlink Mode

In the several previous section ,Figure 4.1-1 had shown the downlink preamble. Hence,the frame structure in downlink mode in our simulation is specified as Figure 4.4.1-1.

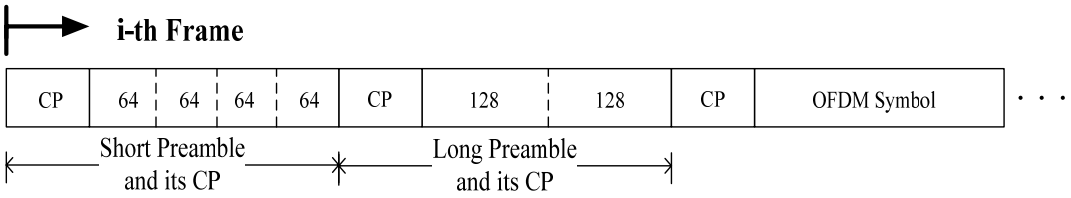

Figure 4.4.1-1 The simulation frame structure in the downlink mode

Under multipath fading channel, the CP of long preamble is damaged by delayed short preamble. The SUI-3 channel has more serious ISI effect than SUI-2 channel.

Figure 4.4.1-2 (a)&(b), 4.4.1-3 (a)&(b), 4.4.1-4 (a)&(b) show the performance when received side has the different velocities 120,60 and 30 km/hr and under SUI-2 channel.

Figure 4.4.1-5 (a)&(b), 4.4.1-6 (a)&(b), 4.4.1-7 (a)&(b) show the performance when received side has the different velocities 120,60 and 30 km/hr, and under SUI-3 channel.

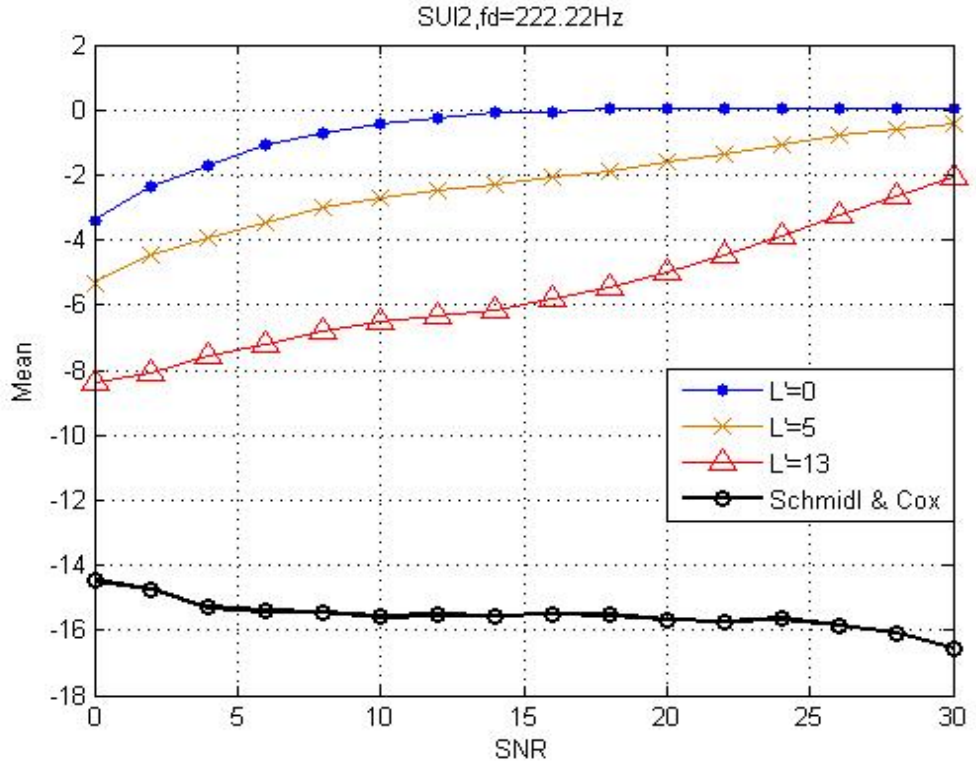

Figure 4.4.1-2 (a) Mean comparison in mobile SUI2 with f_d=222.22Hz in downlink mode

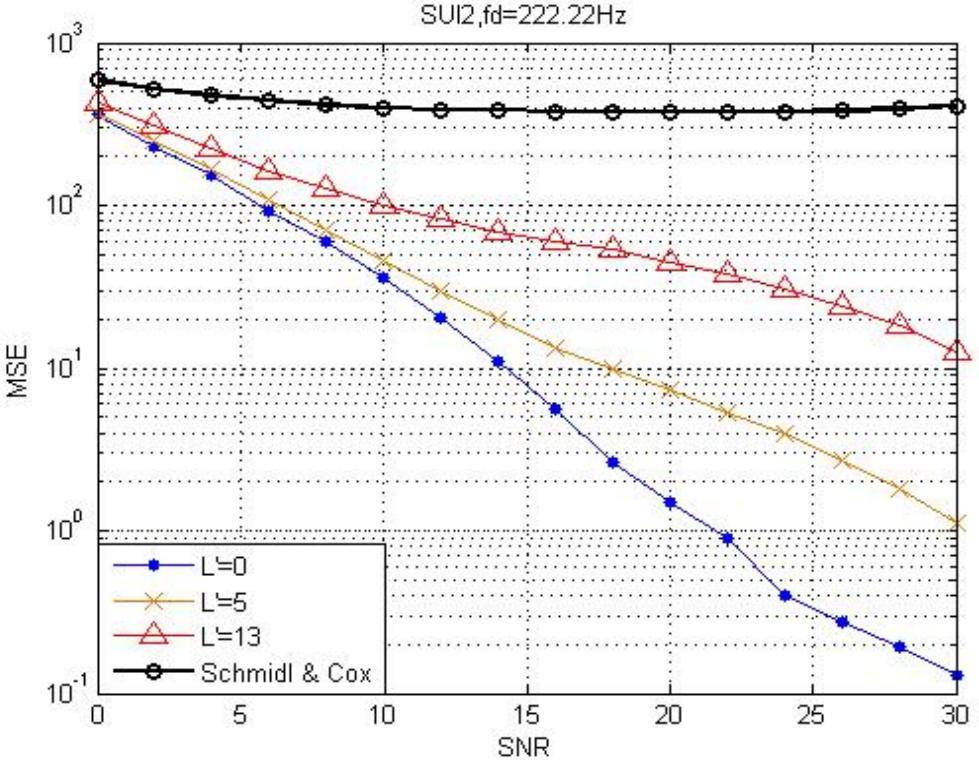

Figure 4.4.1-2 (b) MSE comparison in mobile SUI2 with f_d=222.22Hz in downlink mode

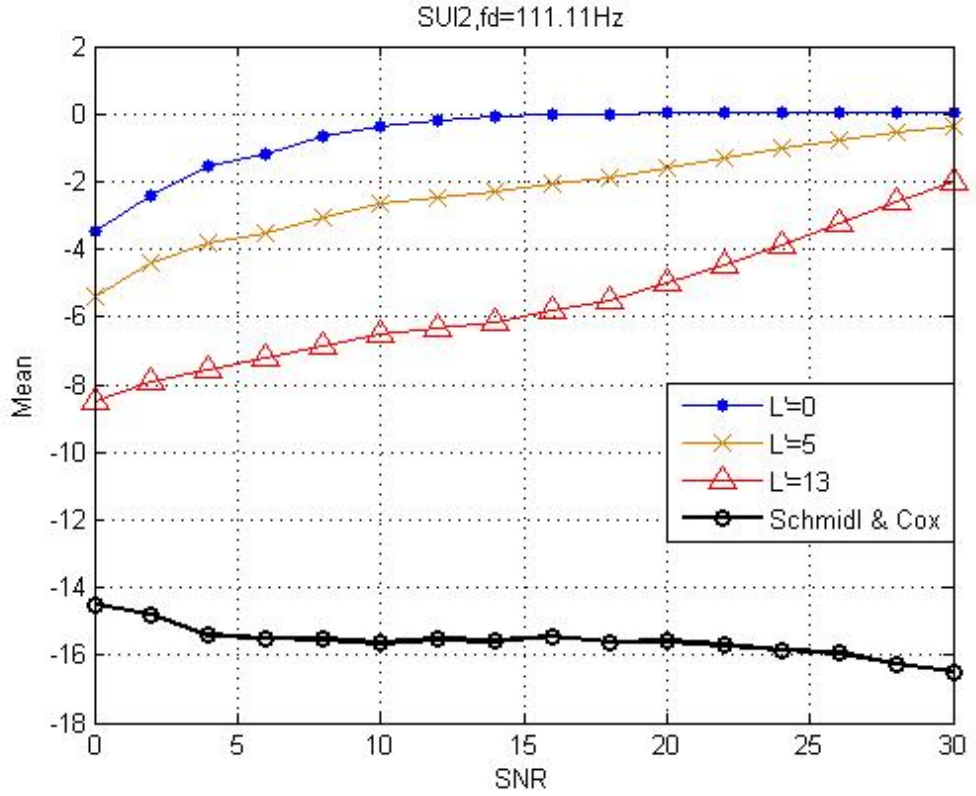

Figure 4.4.1-3 (a) Mean comparison in mobile SUI2 with f_d=111.11Hz in downlink mode

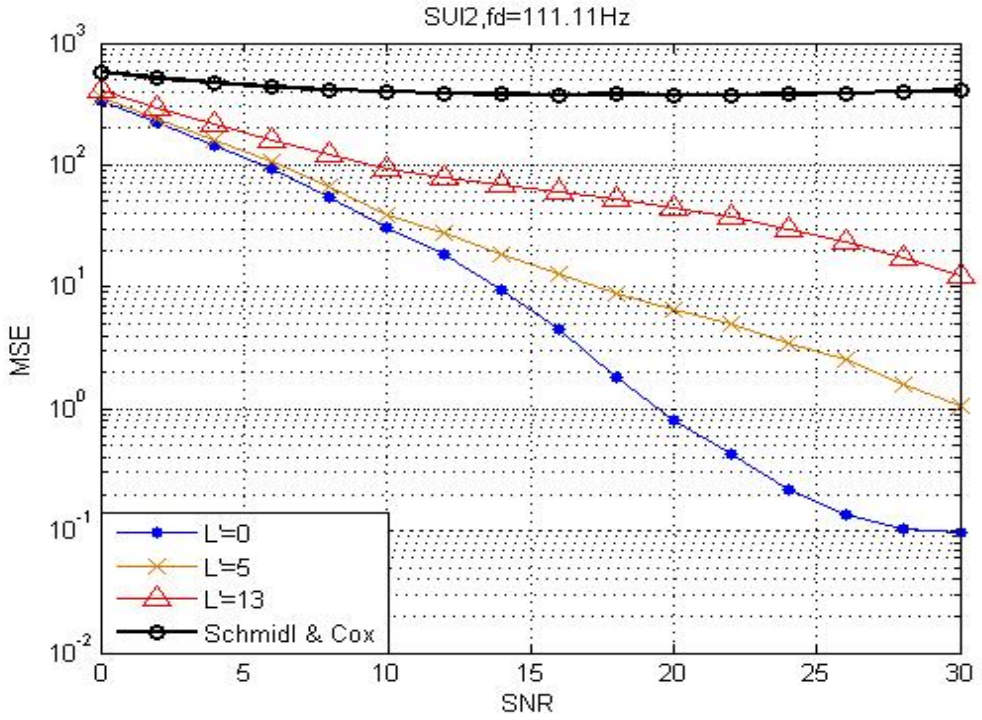

Figure 4.4.1-3 (b) MSE comparison in mobile SUI2 with f_d=111.11Hz in downlink mode

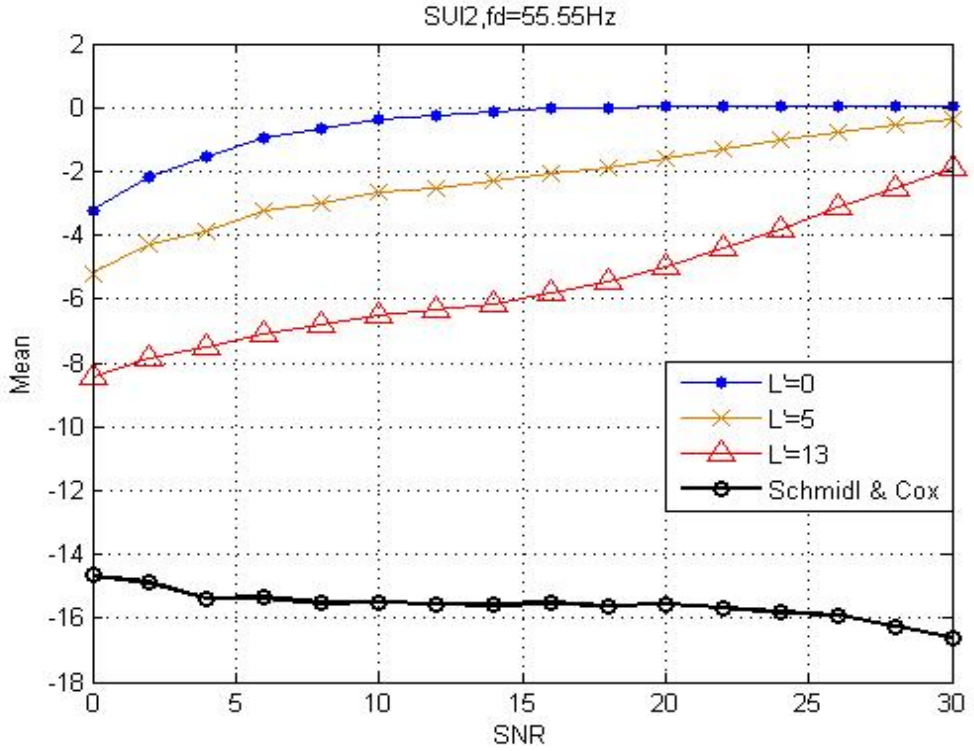

Figure 4.4.1-4 (a) Mean comparison in mobile SUI2 with f_d=55.55Hz in downlink mode

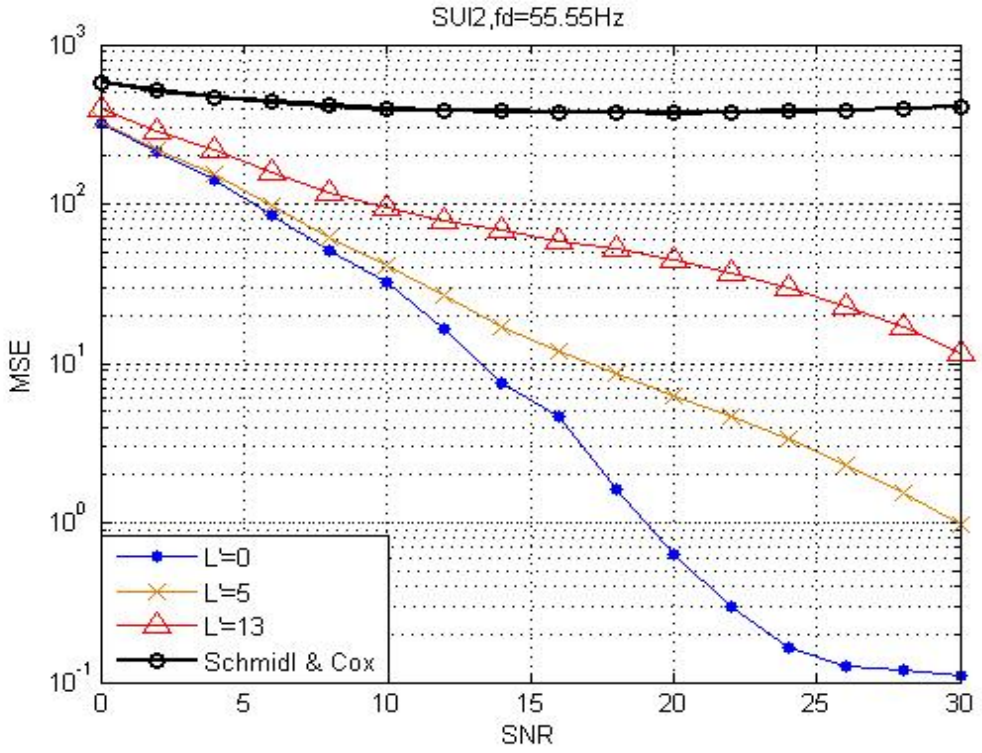

Figure 4.4.1-4 (b) MSE comparison in mobile SUI2 with f_d=55.55Hz in downlink mode

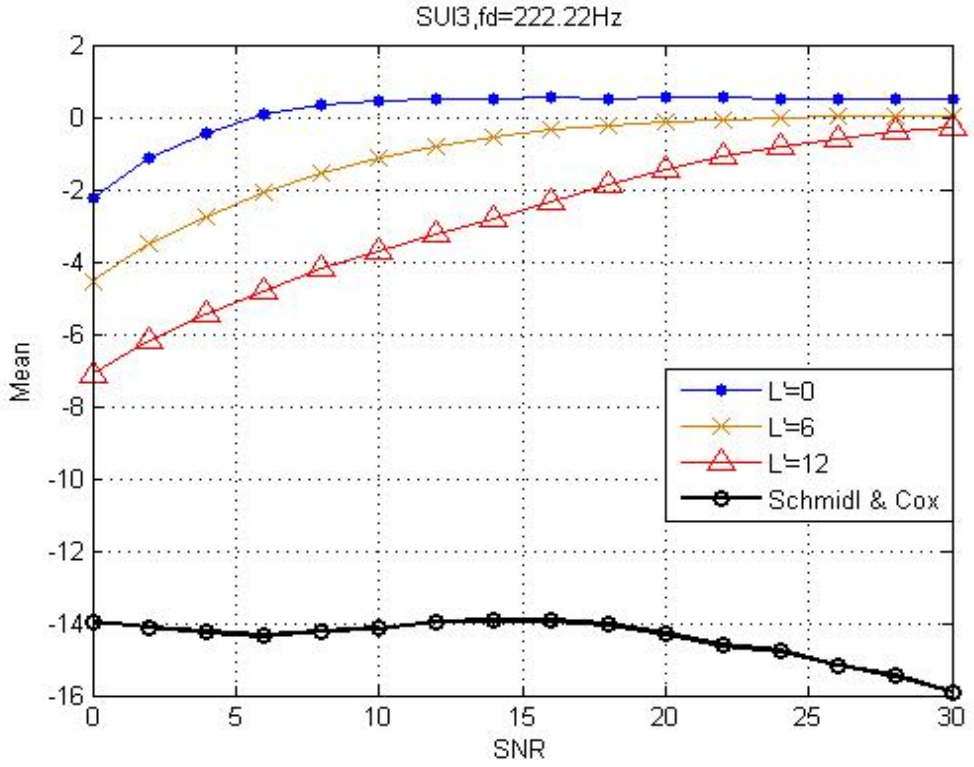

Figure 4.4.1-5 (a) Mean comparison in mobile SUI3 with f_d=222.22Hz in downlink mode

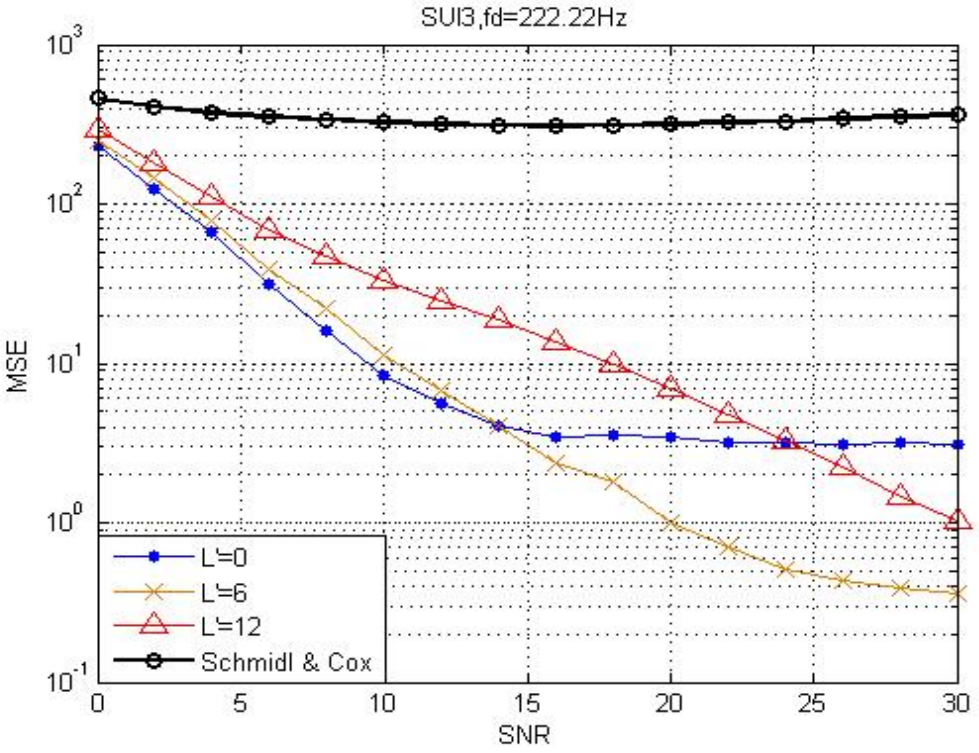

Figure 4.4.1-5 (b) Mean comparison in mobile SUI3 with f_d=222.22Hz in downlink mode

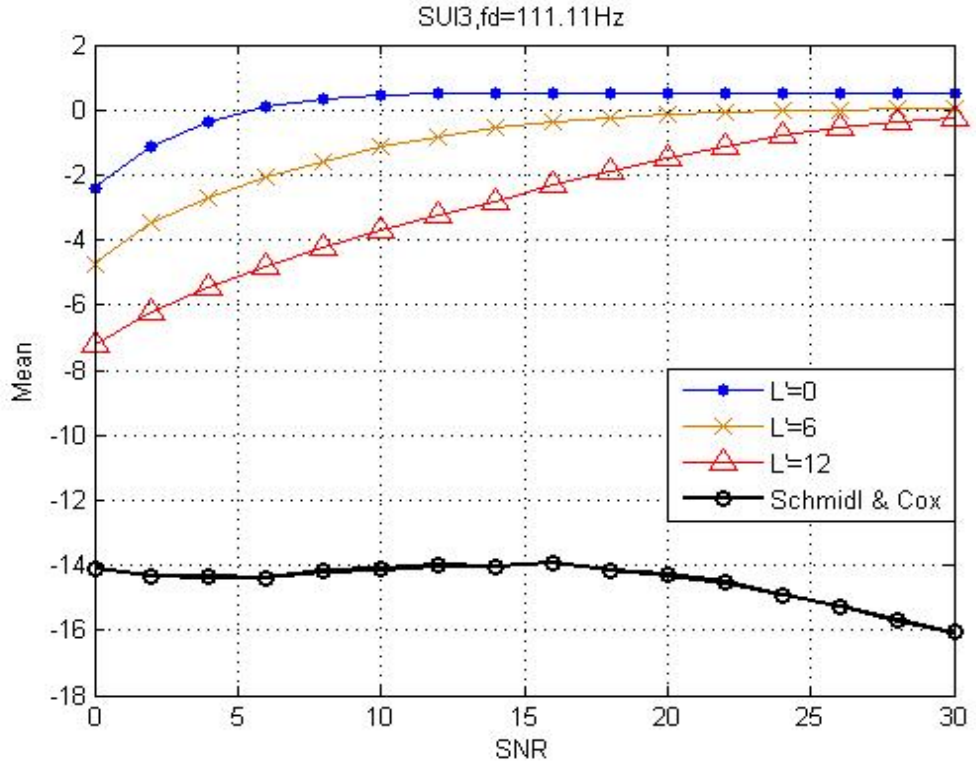

Figure 4.4.1-6 (a) Mean comparison in mobile SUI3 with f_d=111.11Hz in downlink mode

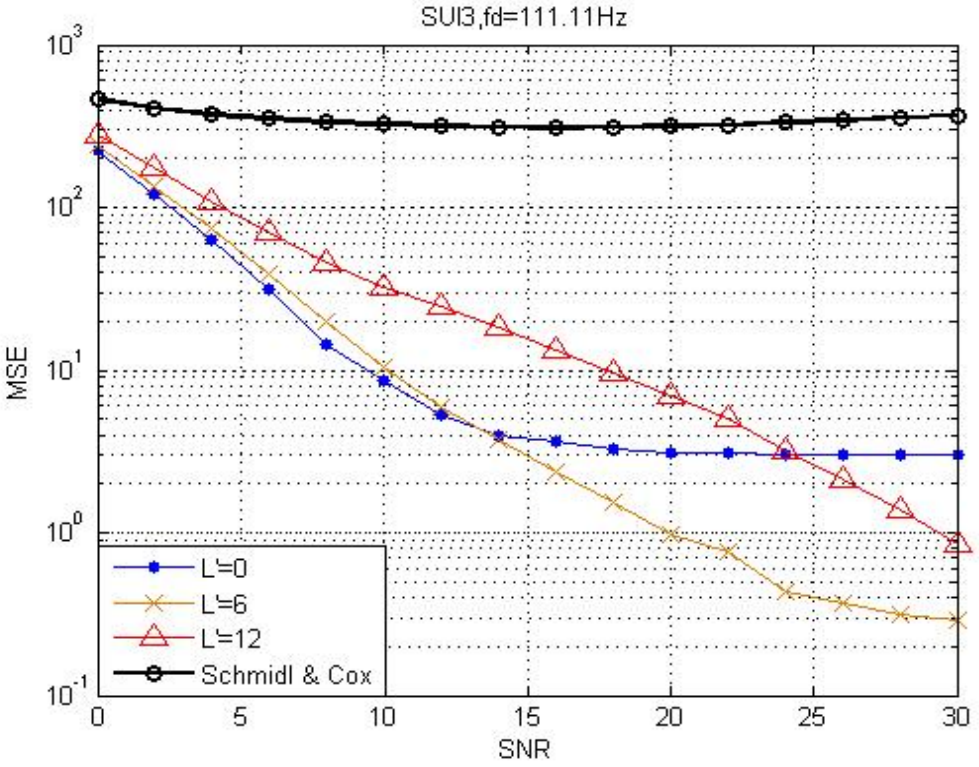

Figure 4.4.1-6 (b) MSE comparison in mobile SUI3 with f_d=111.11Hz in downlink mode

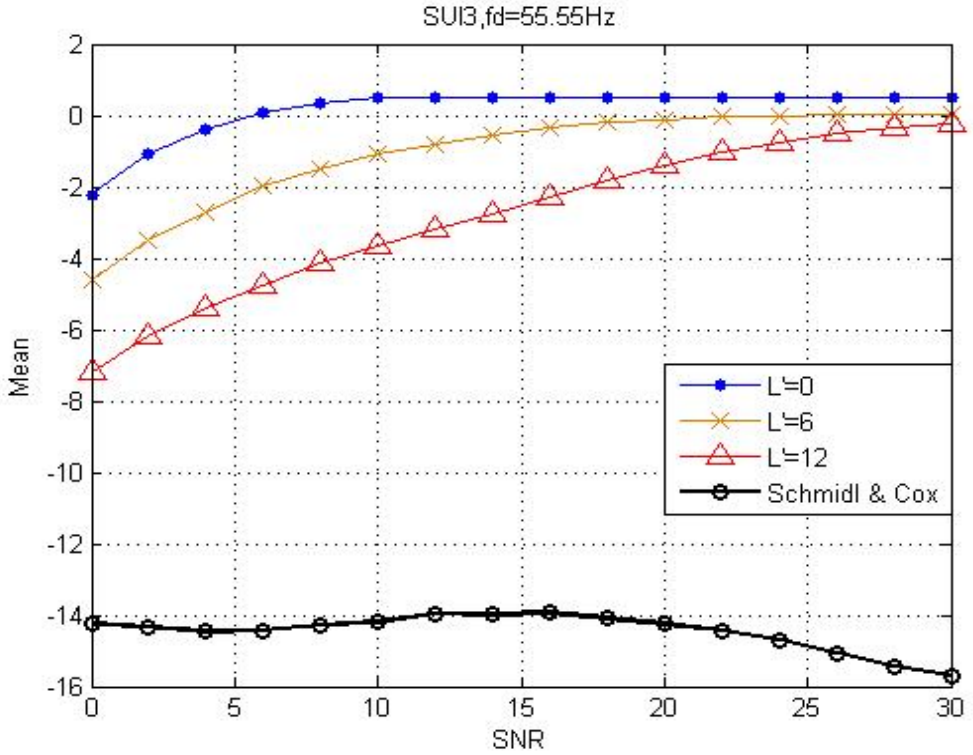

Figure 4.4.1-7 (a) Mean comparison in mobile SUI3 with f_d=55.55Hz in downlink mode

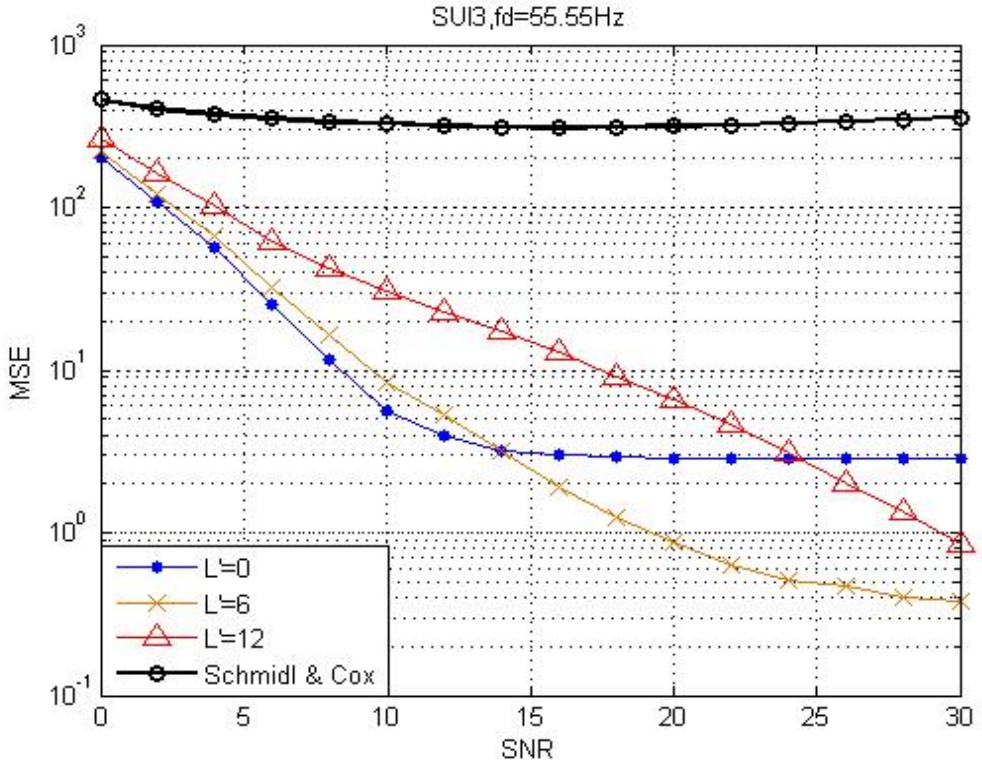

Figure 4.4.1-7 (b) MSE comparison in mobile SUI3 with f_d=55.55Hz in downlink mode

4.4.2 Preamble Structure in Uplink Mode

Section 3.2.9 illustrates TDD and FDD frame structure. For TDD frame structure , downlink subframe has a Tx/Rx transition gap (TTG) in time between uplink subframe. Hence,there is no damage within CP of long preamble in the uplink mode if TTG is larger than CP time. For FDD uplink subframe structure ,if Rx/Tx transition gap (RTG) is larger than CP time of long preamble, there is also no damage within CP.

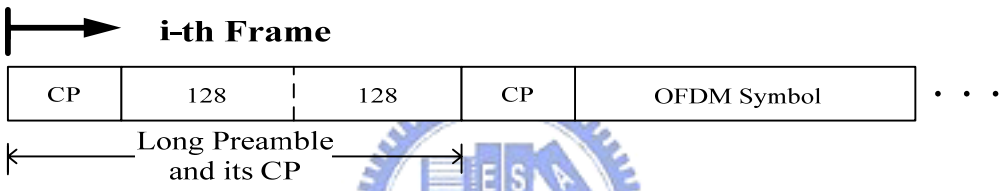

Figure 4.4.2-1 The simulation frame structure in the uplink mode

Figure 4.4.2-2 (a)&(b), 4.4.2-3 (a)&(b), 4.4.2-4 (a)&(b) show the performance when received side has the different velocities 120,60 and 30 km/hr, under SUI-2 channel.

Figure 4.4.2-5 (a)&(b), 4.4.2-6 (a)&(b), 4.4.2-7 (a)&(b) show the performance when received side has the different velocities 120,60 and 30 km/hr ,under SUI-3 channel.

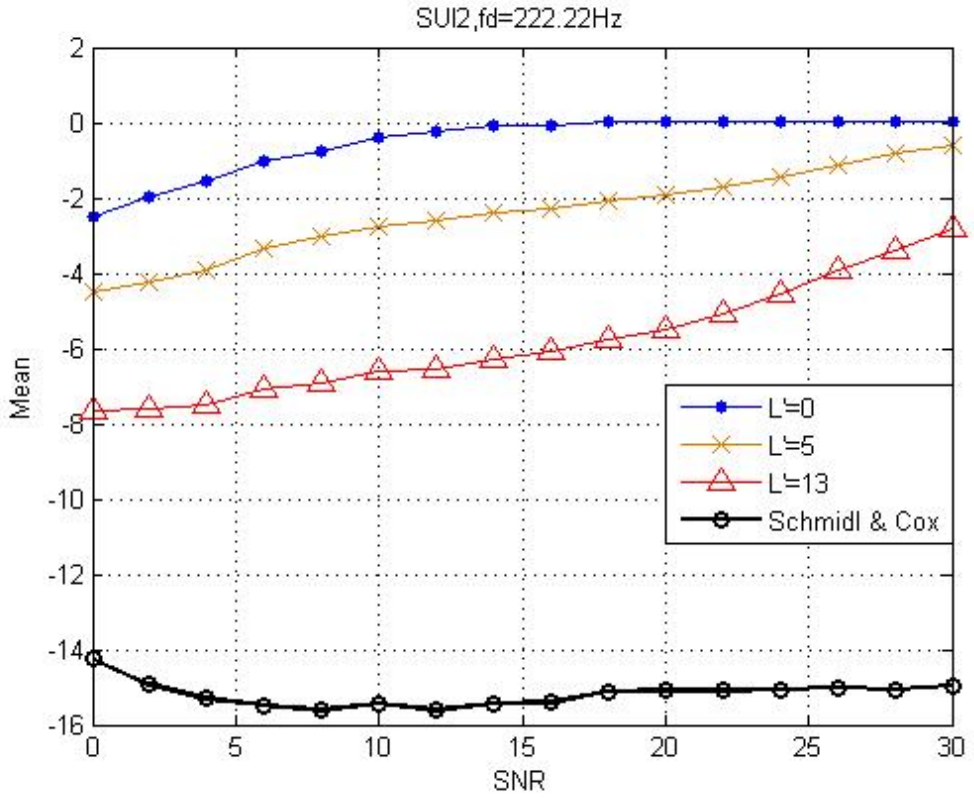

Figure 4.4.2-2 (a) Mean comparison in mobile SUI2 with f_d=222.22Hz in uplink mode

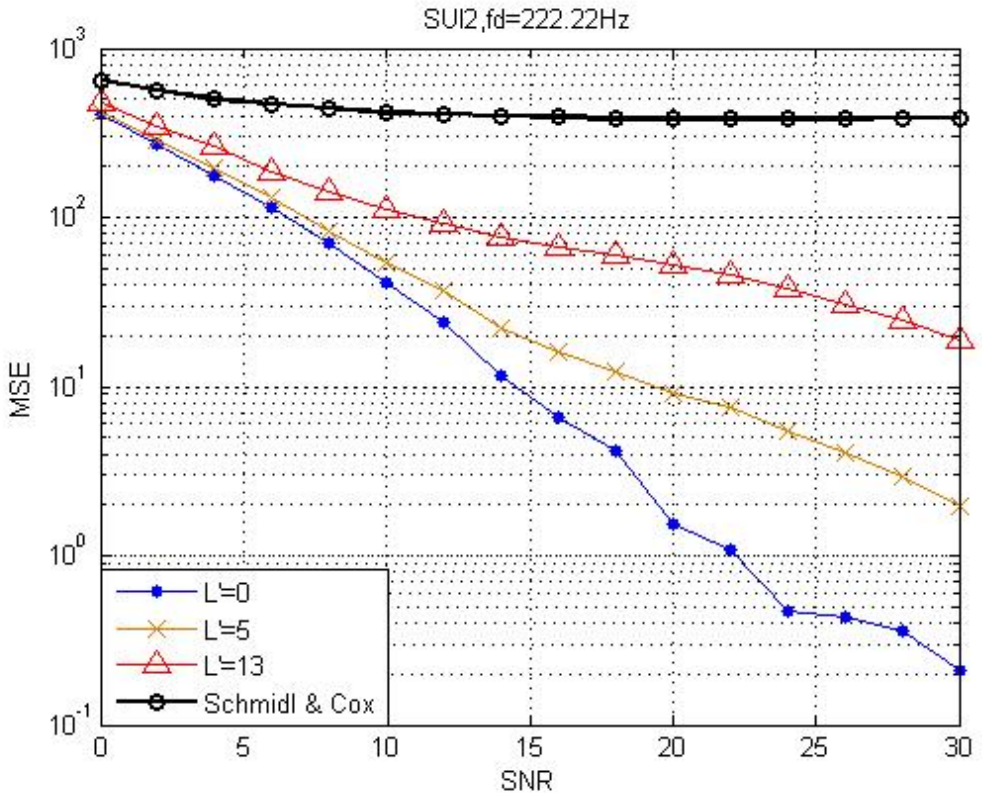

Figure 4.4.2-2 (b) MSE comparison in mobile SUI2 with f_d=222.22Hz in uplink mode

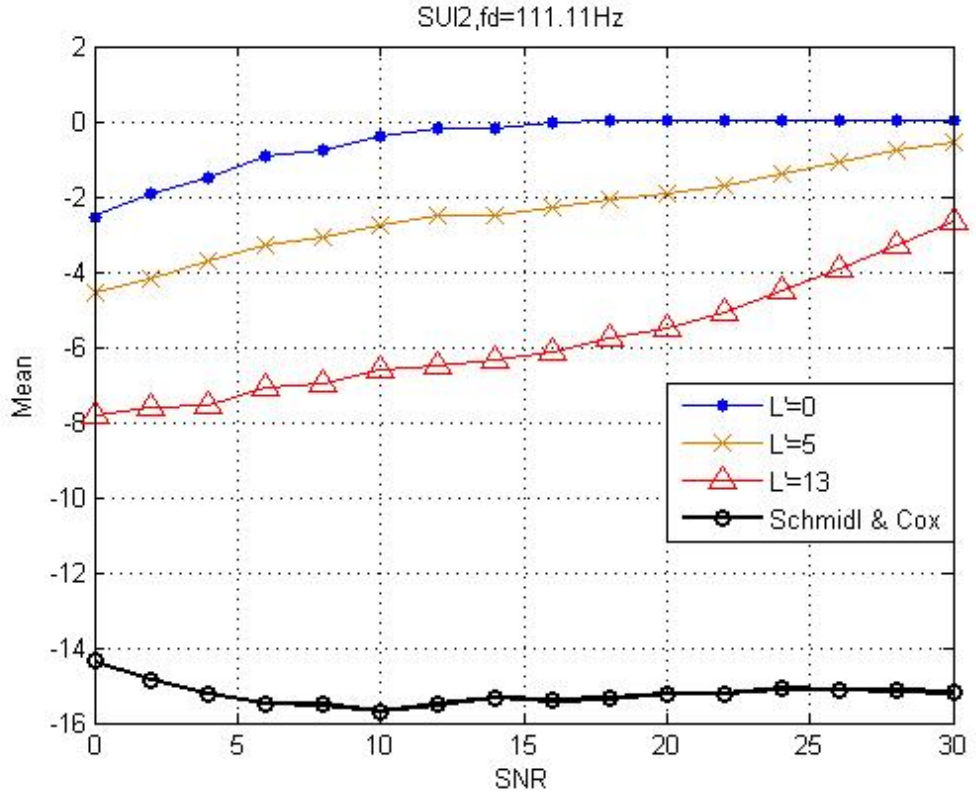

Figure 4.4.2-3 (a) Mean comparison in mobile SUI2 with f_d=111.11Hz in uplink mode

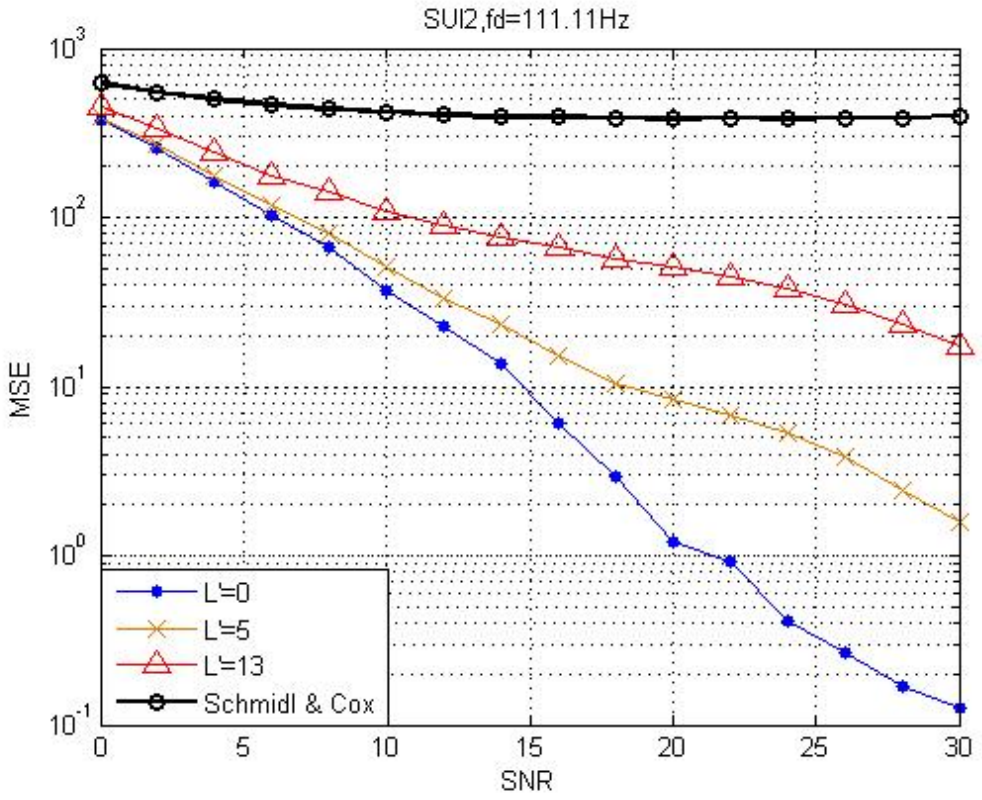

Figure 4.4.2-3 (b) MSE comparison in mobile SUI2 with f_d=111.11Hz in uplink mode

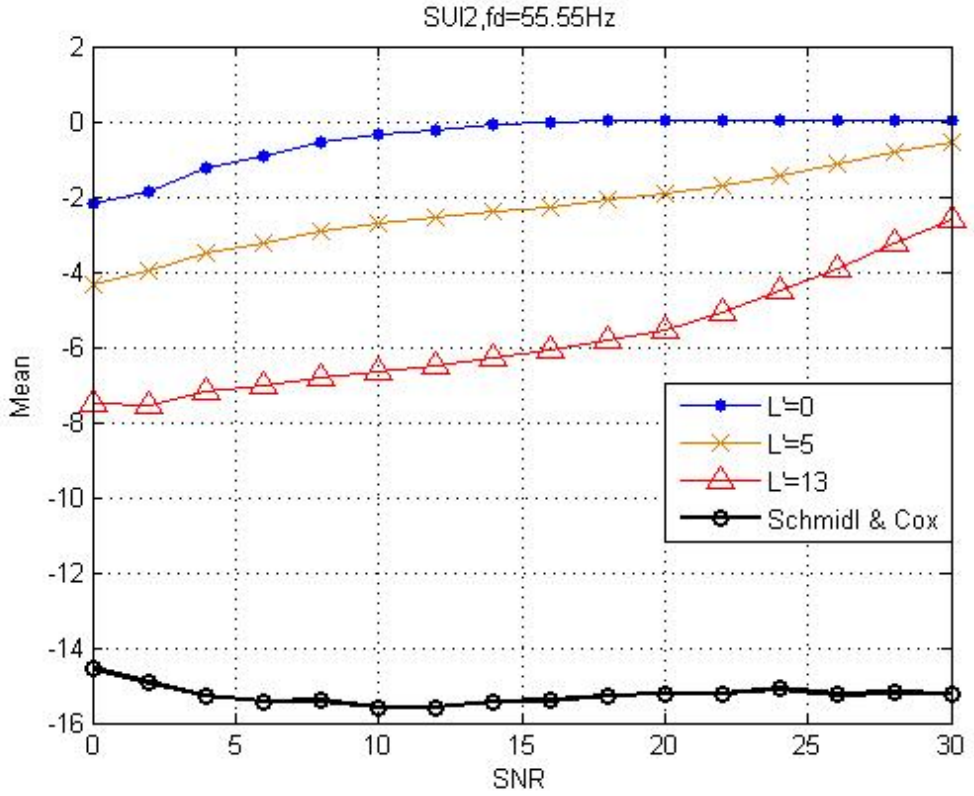

Figure 4.4.2-4 (a) Mean comparison in mobile SUI2 with f_d=55.55Hz in uplink mode

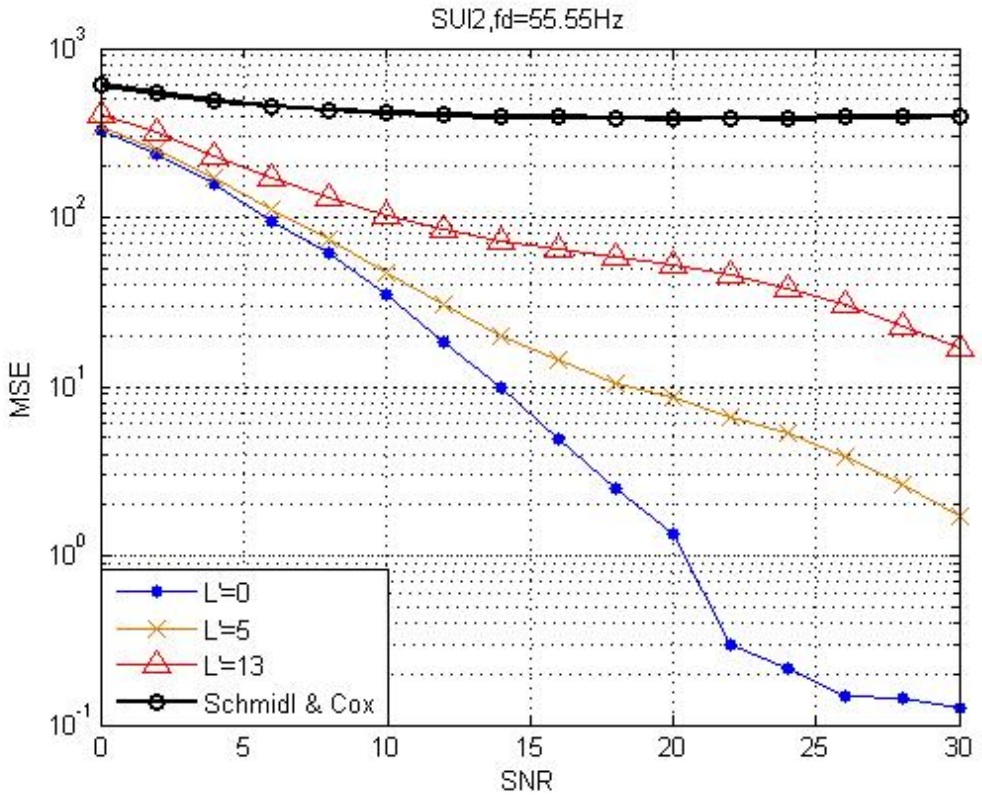

Figure 4.4.2-4 (b) MSE comparison in mobile SUI2 with f_d=55.55Hz in uplink mode

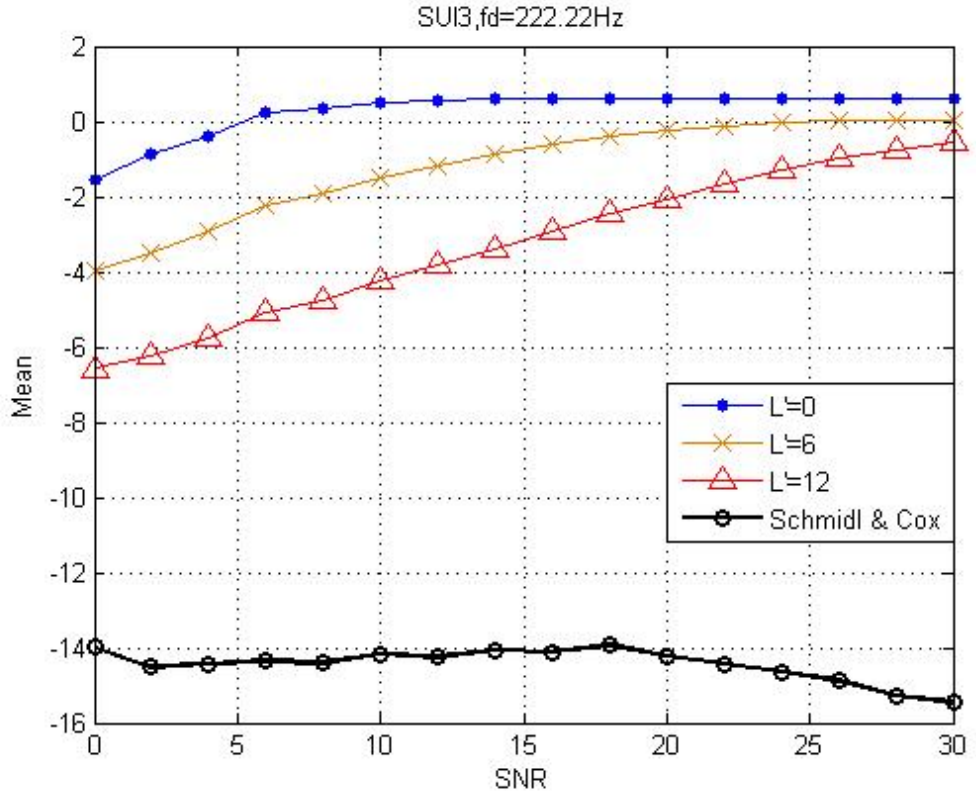

Figure 4.4.2-5 (a) Mean comparison in mobile SUI3 with f_d=222.22Hz in uplink mode

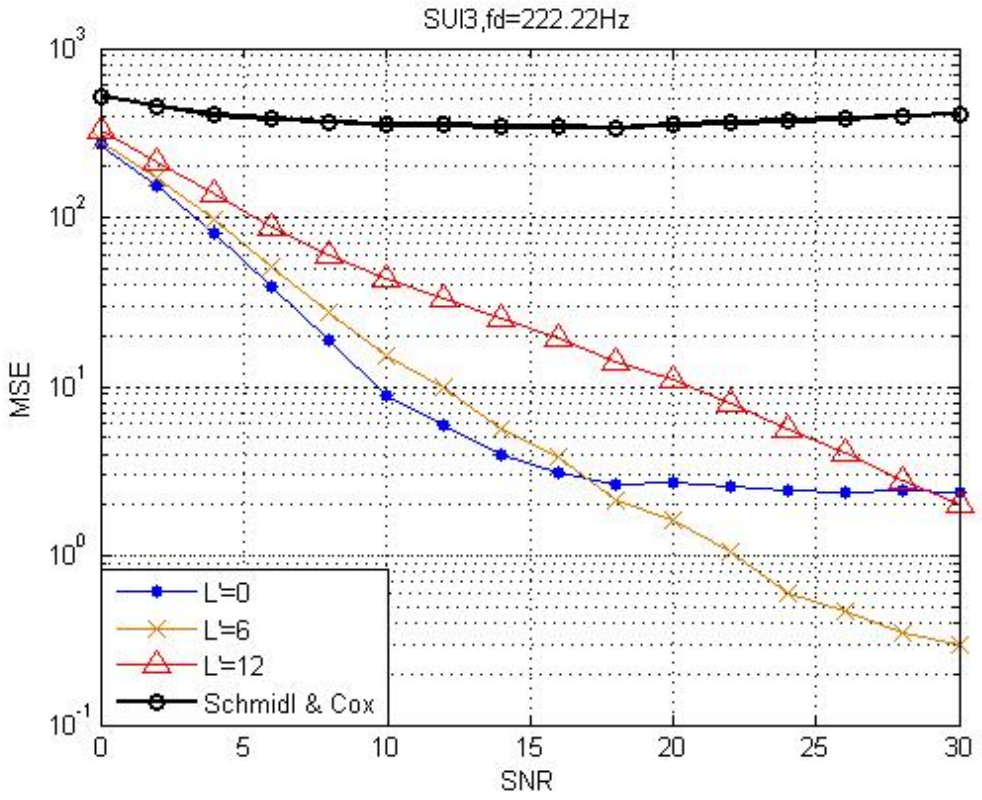

Figure 4.4.2-5 (b) MSE comparison in mobile SUI3 with f_d=222.22Hz in uplink mode

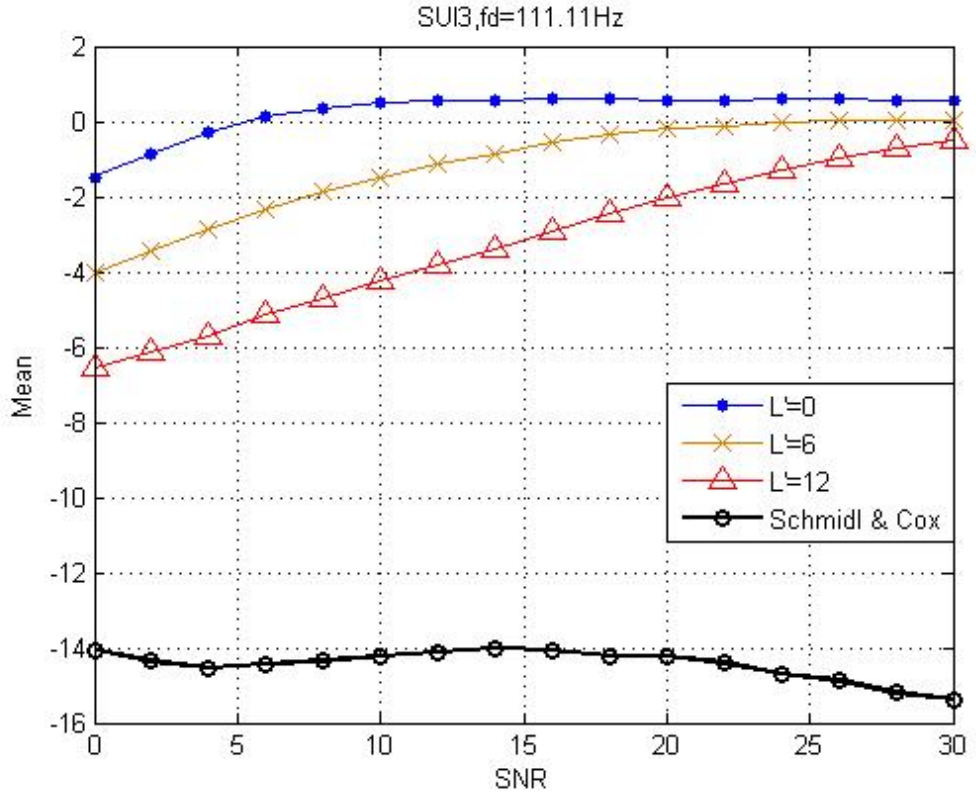

Figure 4.4.2-6 (a) Mean comparison in mobile SUI3 with f_d=111.11Hz in uplink mode

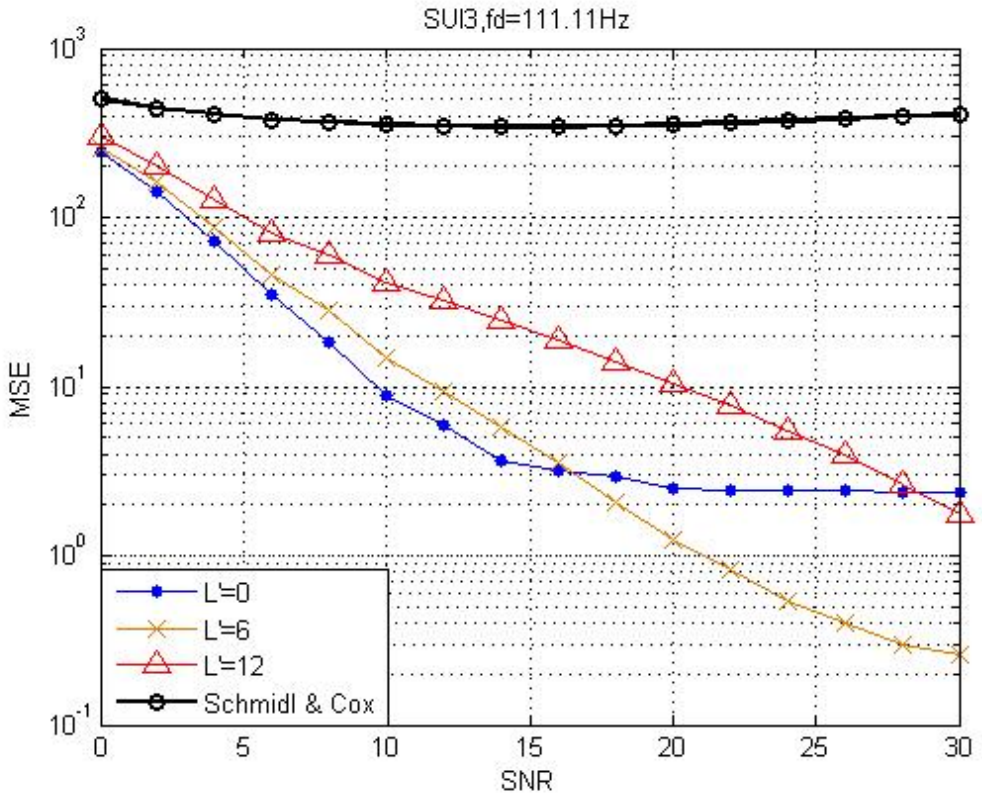

Figure 4.4.2-6 (b) MSE comparison in mobile SUI3 with f_d=111.11Hz in uplink mode

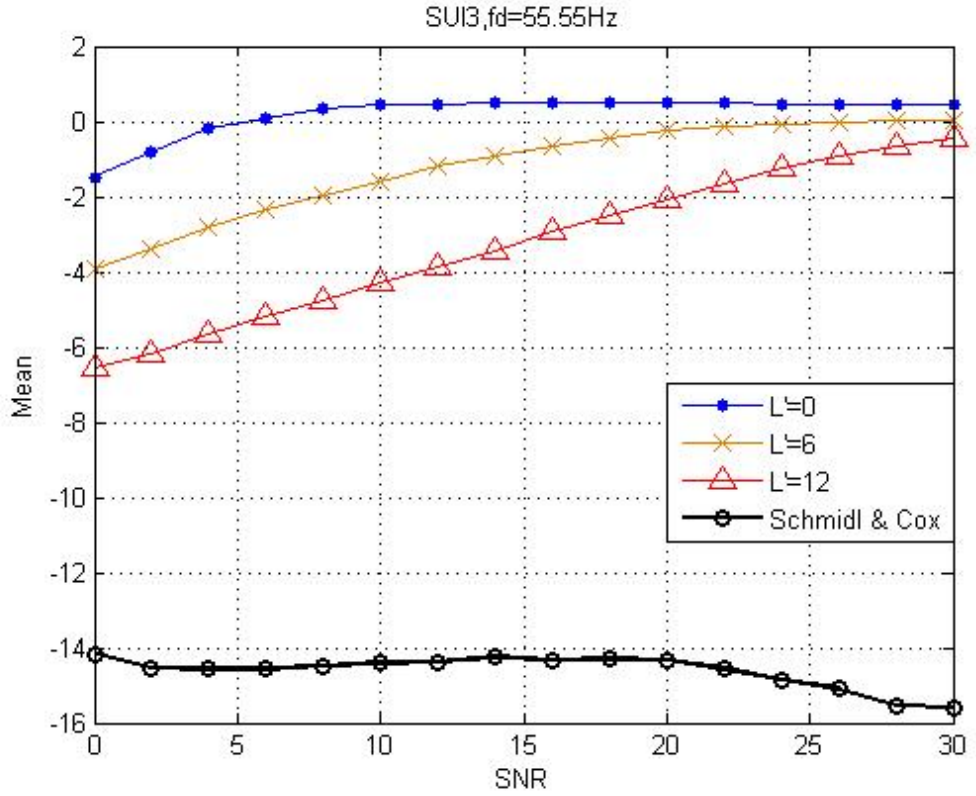

Figure 4.4.2-7 (a) Mean comparison in mobile SUI3 with f_d=55.55Hz in uplink mode

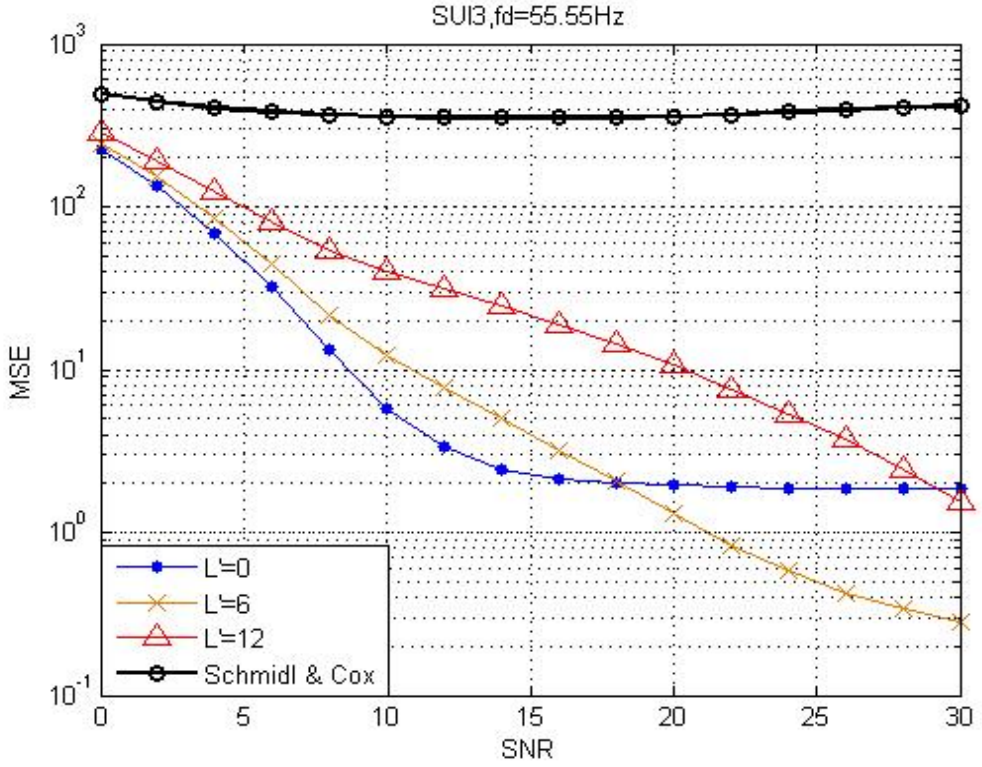

Figure 4.4.2-7 (b) Mean comparison in mobile SUI3 with f_d=55.55Hz in uplink mode

Chapter 5 Conclusion

In this thesis,a low-complexity algorithm for frame boundary estimation is presented.A test environment is built to analyze the performance of the Schmidl & Cox method and our proposed method.From computer simulation ,we find that the proposed method's performance is better than that of Schmidl & Cox method over the mobile SUI3 & SUI2 channels.

In the proposed method, it is effective when ISI effect is serious and the window length L' need to be chosen properly according to the channel condition,such as the length of channel impulse response and then result in the best performance.But sometimes it may be difficult to decide which L' should be chosen.From empirical data (from simulation), case $L'=160, d=1$, may be a good selection,because we don't need spend any resource to measure the channel condition,although it has a slight ISI effect and larger MSE in the simulation,but still be acceptable compared with the performance of Schmidl & Cox method. This also satisfies the request which is with mobility system including " NLOS Channel with Vehicular speed 120 Km/hr " by WiMax IEEE 802.16e.

References：

[1]Richard Van Nee and Ramjee Prasad,OFDM for Wireless Multimedia Communications,Artech House ,2000

[2]Jan-Jaap van de Beek , Magnus Sandell ,Per Ola Borjession, “ML estimation of time and frequency offset in OFDM system” IEEE Trans. Signal Processing , vol. 45, no.7 , pp.1800-1805,July 1997

[3] P. H. Moose “A technique for orthogonal frequency division multiplexing frequency offset corrections”，IEEE Trans. Commun., vol.2,pp.2908-2914,Oct.1994

[4] Timothy M. Schmidl, Donald C. Cox, “Robust frequency and timing synchronization for OFDM”, IEEE Trans.Comm., vol. 45, pp.1613-1621, Dec.1997.

[5] Sun-Ting Lin , Regular Member and Che-Ho Wei,Nonmember,”Precusor ISI-Free Frame Synchronization for DMT VDSL System”, IEICE TRANS. COMMUN., VOL .E85-B , NO.8 AUGUST 2002

[6]Kenkichi Takahashi and Takahiko Saba “A Novel Symbol Synchronization Algorithm with Reduced Influence of ISI for OFDM Systems” 2001 IEEE

[7] Meng Wu, Wei-Ping Zhu,”A preamble-aided symbol and frequency synchronization scheme for OFDM systems” IEEE, pp. 2627-2630

[8] http://www.itri.org.tw/chi/services/transferable/itri_show.jsp?idx=1698

[9] IEEE Standard for Local and Metropolitan Area Networks Part 16: Air Interface for Fixed Broadband Wireless Access Systems
IEEE Std 802.16-2004 (Revision of IEEE Std 802.16-2001)
2004 Page(s):0_1 - 857

[10] IEEE Standard for Local and metropolitan area networks Part 16: Air Interface for Fixed and Mobile Broadband Wireless Access Systems Amendment 2: Physical and Medium Access Control Layers for Combined Fixed and Mobile Operation in Licensed Bands and Corrigendum 1
IEEE Std 802.16e-2005 and IEEE Std 802.16-2004/Cor 1-2005 (Amendment and Corrigendum to IEEE Std 802.16-2004)
2006 Page(s):0_1 - 822

[11]Dent,P; Bottomley,G.E.;Croft, T. “Jakes Fading Model Revisited”,Electronics Letters,Vol.29,No.13,24 June 1993,pp. 1162-1163.

[12] Jakes ,William C. Microwave Mobile Communication. New York,Wiley,1974.

[13]Bernard Sklar” Digital Communications ,Fundamentals and Applications”,Second Endition,Prentice-Hall International,Inc.2001

作者簡歷

鍾國洋，民國 69 年 8 月 31 日生。高中就讀於台北市立和平高級中學，隨後進入華梵大學電子工程學系，於民國 92 年 6 月畢業。原定 92 年 9 月進入中正電機所碩士班就讀，因母親身體微恙而放棄。而在民國 93 年進入 9 月進入交通大學電子工程研究所碩士班，民國 95 年 6 月取得碩士學位。從事無線通訊領域相關研究，碩士論文題目為：”符合 IEEE802.16e 都會區域網路傳輸框同步技術研究”。研究興趣包括：通訊系統、信號處理。